# Master Thesis

# Design study of the MONIKA-ORC-Turbine and comparison with experimental results

**Cristian Leonardo Niño Avella**

**Advisors**

**Prof. Dr.-Ing. Thomas Schulenberg**

**Prof. Dr.-Ing. Andreas Class**

**Dipl.-Ing. Hans-Joachim Wiemer**

**Institute for Thermal Energy Technology and Safety (ITES)**

**Karlsruher Institut für Technologie (KIT)**

**October 2022 – March 2023**

# Declaration by Author

I truthfully affirm to have written the thesis independently, to have indicated all used aids completely and accurately, and to have marked everything taken from the works of others unchanged or with modifications, as well as to have observed the KIT Statutes for Safeguarding Good Scientific Practice in the currently valid version.

Ich versichere wahrheitsgemäß, die Arbeit selbstständig verfasst, alle benutzten Hilfsmittel vollständig und genau angegeben und alles kenntlich gemacht zu haben, was aus Arbeiten anderer unverändert oder mit Abänderungen entnommen wurde sowie die Satzung des KIT zur Sicherung guter wissenschaftlicher Praxis in der jeweils gültigen Fassung beachtet zu haben.

Date 31.03.2023 Signature

# Acknowledgement

I would like to express my gratitude to all the people who accompanied me during this process of learning and personal growth. It has been a challenging yet rewarding journey, and I couldn't have done it without their constant support and motivation.

I feel particularly fortunate to have had the opportunity to carry out my master's thesis under the guidance of Prof. Dr.-Ing. Thomas Schulenberg and Hans-Joachim Wiemer, who dedicated their time and expertise to mentor me through this project. Their mentorship and support have been essential in achieving my goals.

I would also like to acknowledge the significant contribution of Dr. Cecilia Smoglie and Dr. Ferdinand Schmidt, who gave me with the opportunity to be here.

Last but not least, I want to express my gratitude to my family and friends, who have always been by my side, providing me with their unconditional support. I cannot express how grateful I am for everything they have done for me.

# Abstract

The main objective of the project is to develop, verify, and validate a MATLAB code which implements a mean-line analysis for the ORC-Turbine located in the MONIKA facility. The mean-line analysis method is a useful tool to design turbomachines. In this study it was used to simulate and analyze the performance and properties into the turbine, under different operating conditions by analyzing its properties in a mean radius for each one of the inside inlet and outlet cross sections of the stages. It was taken into consideration different loss correlations in order to achieve a better result.

For the implementation of the mean-line analysis, the geometry and design properties for the ORC-Turbine were used, along with the experimental data obtained from the MONIKA facility in previous works. These data were used for the verification and validation process, ensuring that it accurately represents the behavior of the turbine under different scenarios.

The MATLAB code was designed to implement the mean-line analysis method, which can simulate the performance of the ORC-Turbine under various operating conditions, such as different mass flow rates, inlet and outlet temperatures, and pressures.

The results of the mean-line analysis showed that the developed code can accurately predict the performance and the properties of the ORC-Turbine, within a reasonable level of accuracy. The code can also be used to evaluate the impact of different design modifications, such as changes in the inlet and outlet thermodynamic properties of the fluid, on the turbine's performance.

# Kurzzusammenfassung

Das Ziel der Arbeit ist die Entwicklung, Verifizierung und Validierung eines MATLAB-Codes, der die „*Mittenschnittsrechnung*“ für die ORC-Turbine in der MONIKA-Anlage durchführt. Die Methode der „*Mittenschnittsrechnung*“ ist ein übliches Werkzeug zur Auslegung von Turbomaschinen. In dieser Arbeit wird diese Methode zur Simulation und Analyse der Leistung und der Eigenschaften der Turbine unter verschiedenen Betriebsbedingungen verwendet. Dazu werden die Eigenschaften in einem mittleren Radius der Beschaufelung für jeden des Eintritts und Austritts Querschnitte der Stufen analysiert. Es werden verschiedene Verlustkorrelationen in Betracht gezogen, um ein besseres Ergebnis zu erzielen.

Für die Implementierung der „*Mean-Line-Analyse*“ werden die Geometrie und die Gestaltungsparameter der ORC-Turbine zusammen mit den experimentellen Daten von früheren Arbeiten der MONIKA-Anlage verwendet. Durch diese Daten kann das erstellte Simulationsprogramm verifiziert und validiert werden. Damit ist sichergestellt, dass das Verhalten der Turbine unter verschiedenen Szenarien genau beschrieben werden kann.

Der MATLAB-Code wurde entwickelt, um die Methode der „*Mean-Line-Analyse*“ zu implementieren. Somit kann die Leistung der ORC-Turbine unter verschiedenen Betriebsbedingungen simuliert werden, wie z. B. bei unterschiedlichen Massendurchsätzen, Eintritts- und Austrittstemperaturen und Drücken.

Die Ergebnisse der „*Mean-Line-Analyse*" zeigen, dass der entwickelte MATLAB-Code die Leistung und die Eigenschaften der ORC-Turbine mit einer angemessenen Genauigkeit vorhersagen kann. Das entwickelte Programm kann auch die Leistung der Turbine z.B. unter Änderungen der thermodynamischen Eigenschaften des Fluids am Ein- und Auslass bewerten.

# Table of content

# List of Latin Symbols

| Description | Symbol | Unit |
|---|---|---|
| Work | $A$ | $J$ |
| Area of cross section | $An$ | $m^2$ |
| Throat area of vanes | $At$ | $m^2$ |
| Nitrogen concentration | $CN_2$ | - |
| Vane/Blade chord length | $ca$ | $m$ |
| Diameter of the pipe | $d$ | $m$ |
| Specific turbine work | $dA$ | $m^2/s^2$ |
| Specific pressure drop | $\frac{dP}{dL}$ | $Pa/m$ |
| Latent heat of evaporation | $dHv$ | $J/kg$ |
| Diameter of Labyrinth tips | $DL$ | $m$ |
| Relative mass flow error | $dM$ | $kg/s$ |
| Pressure correction | $dP$ | $kPa$ |
| Specific energy losses | $dq$ | $m^2/s^2$ |
| Expansion factor | $ef$ | - |
| Fraction of aperture in the partial admission | $F$ | - |
| Frequency | $f$ | $Rps$ |
| Relaxation factor | $FR$ | - |
| Enthalpy | $h$ | $J/kg$ |
| Blade height | $hb$ | $m$ |
| Open clearance of Labyrinth tips | $HL$ | $m$ |
| Length of the pipe | $L$ | $m$ |
| Mass flow | $M$ | $kg/s$ |
| Specific mass velocity | $m$ | $kg/m^2\,s$ |
| Mach Number | $Ma$ | - |
| Mass flow loss (Labyrinth) | $Ml$ | $kg/s$ |
| Mass flow vanes | $Mv$ | $kg/s$ |
| Number of cross sections | $ncs$ | - |
| Number of open vane passages | $ovp$ | - |
| Pressure | $P$ | $kPa$ |
| Critical pressure | $Pcrit$ | $kPa$ |
| Power of the turbine | $Pturb$ | $W$ |
| Ventilation Power | $PV$ | $W$ |
| Heat flux | $q$ | $W/m^2$ |
| Specific energy by Filling/emptying process | $qFE$ | $J/kg$ |
| Specific energy by Ventilation | $qV$ | $J/kg$ |
| Outer Radius | $R_e$ | $m$ |
| Inner Radius | $R_i$ | $m$ |
| Mean Radius | $R_m$ | $m$ |
| Reynolds number | $Re$ | - |
| Reaction factor | $RF$ | - |
| Entropy | $s$ | $J/kg\,K$ |
| Stages of the turbine | $Stages$ | - |
| Temperature | $T$ | $K$ |

| | | |
|---|---|---|
| Throat of vane passages | $tvp$ | - |
| Blade velocity | $U$ | $m/s$ |
| Absolute velocity | $V$ | $m/s$ |
| Relative velocity | $W$ | $m/s$ |
| Fluid quality | $X$ | - |
| Number of Labyrinth tips | $z1$ | - |

# List of Greek symbols

| Description | Symbol | Unit |
|---|---|---|
| Angular velocity | $\omega$ | $Rad/s$ |
| Aperture angle | $\Omega$ | $deg$ |
| Deflection angle | $\varepsilon$ | $Rad$ |
| Density | $\rho$ | $kg/m^3$ |
| Dynamic viscosity | $\nu$ | $kg/ms$ |
| Efficiency of the turbine | $\eta_{turb}$ | - |
| Friction factor | $\xi$ | - |
| Loss coefficient | $\zeta'$ | - |
| Outlet angle of blades | $\beta$ | $Rad$ |
| Outlet angle of vanes | $\alpha$ | $Rad$ |
| Soderberg loss coefficient | $\zeta$ | - |

# List of subscripts

| Description | Symbol |
|---|---|
| Axial component | $ax$ |
| Circumferential component | $u$ |
| Gas | $g$ |
| Inlet properties for cross section 0 | $0$ |
| Isentropic process | $s$ |
| Liquid | $l$ |
| Number of cross section | $n$ |
| Number of stage | $m$ |
| Outlet of the turbine | $8$ |

# 1. Introduction

The growing global demand for energy and the need to reduce the environmental impact associated with energy production and use of it, have driven the search for alternative energy sources and more efficient production processes. In this sense, the use of waste and renewable heat sources has taken on relevance in the generation of energy. These sources include thermal energy from geothermal reservoirs, residual heat from engines, turbines and industrial processes, biomass combustion and concentrated solar energy.

An emerging technology that has come as a solution to harnessing these heat sources is the organic Rankine cycle ORC. These use organic fluids as the working fluid instead of water vapor, allowing energy to be generated from low-temperature heat sources. In addition, these cycles offer good efficiency and an economically viable solution for generating plants.

Generation plants using ORC cycles have great flexibility in terms of capacity and temperature levels, making them ideal for use in conjunction with cogeneration systems. In addition, these plants can be used in a variety of applications such as generating electricity from biomass, generating energy from geothermal sources and generating energy from industrial and process waste.

The global installed capacity of ORC plants in renewable energy and waste heat installations has been growing rapidly over the last few years, with it being estimated that there are now around 2000 MW of installed capacity in plants using ORC cycles. This growing interest in ORC cycles is due to their high efficiency, low environmental impact and flexibility of application in different industries. [1]

The focus of this thesis is on the turbine of the project called MONIKA (Modular Low Temperature Cycle Karlsruhe), which is a facility of the Institute of Thermal Energy and Technology and Safety (ITES) of the Karlsruhe Institute of Technology (KIT). Said canning is on Campus Nord.

The MONIKA plant consists of a supercritical ORC cycle which uses propane as the working fluid, and is designed to take as heat source geothermal energy, however, MONIKA is a test plant, so its heat source is hot water which simulates the temperatures that would be reached with geothermal energy.

The work is focused on the study of the MONIKA ORC-Turbine, which is the main element of the installation, since it is in charge of transforming, through an expansion process, the enthalpy of the fluid into mechanical energy.

## 1.1. Motivation

The Organic Rankine Cycles (ORC) are a thermodynamic cycle that use organic fluids instead of steam of water, such as hydrocarbons, to generate power. It is similar to the classical steam Rankine cycle but is typically used for lower-temperature applications where water cycles are not suitable. Therefore, the Organic Rankine Cycles are used with the purpose of recover and utilize heat energy with a low temperature, which can be provided by different types of industrial processes, solar thermal energy and geothermal energy [2].

In an ORC, the organic fluid is heated by an external heat source to create vapor that drives a turbine, in order to generate electricity. The vapor is then cooled and condensed back into a liquid using a cooling medium, such as air or water, and then the cycle is closed.

The organic fluid propane used in this cycle has a lower critical temperature and pressure than the water cycle, which allow to compress with less effort to the supercritical pressure. The advantage of the process of heating for supercritical ORC [3], is that it has a better match for the exchange of energy between the heat source and the work fluid because it reduces the logarithmic mean temperature difference and therefore reducing efficiency losses.  Another advantage of this cycle process is that it can be used in decentralized application in medium and small scale [4].

The MONIKA ORC facility is a power plant located in the KIT Campus Nord, Karlsruhe. It uses a supercritical organic cycle that uses propane as a working fluid. The facility was set in order to optimize low temperature geothermal cycles to increase the efficiency during its power generation [5].

In order to analyze the behavior of the MONIKA ORC-Turbine, this thesis presents as focus the determination of the diverse properties of the turbine in each one of its expansion stages by the theorical calculation of it in steady state operation. The results obtained are based on the properties provided by the manufacturer and the experimental data from previous works [6], which shows the behavior of the turbine under different scenarios. This analysis is carried out in order to be able to predict the behavior of the turbine under different operating conditions, varying properties such as pressure or temperature at the inlet and the pressure at the outlet of the turbine, as well as to study the influence of the working fluid used.

## 1.2. Objective

The objective of the thesis is to create a MATLAB code based on a mean line analysis which can be used to simulate the thermodynamic behavior of the turbine being able to calculate the different properties of the fluid in all of the stages of the turbomachine.

## 1.3. Scope

The scope of this work is to program a MATLAB code using the theorical equations and correlations of a mean line analysis, which can predict the thermodynamic properties, power and efficiency of a turbine using as input data the geometry of the turbomachine, inlet and outlet properties and validate the results of it with the measured data of the turbine used in the MONIKA facility from the KIT.

The geometric characteristics such as cross sections, outlet angle of the blades and vanes and labyrinth tips have been measured using the CAD data provided by the manufacturer of the turbine.

The calculation results obtained under different boundary conditions, as well as the entrance of the turbine, will be stored in an Excel file to make it easier to interpret the data.

# 2. Basic principles

## 2.1. Supercritical Rankine Organic cycle

A supercritical Rankine cycle refers to a cycle in which the working fluid is heated after its compression stage to pressures and temperatures above the critical point (CP) of the working substance. The main difference from superheated cycles is the heat exchange stage, where this cycle aims to smoothly transition from subcooled liquid to superheated vapor across the critical point. In this stage, heat exchange is gradual and all properties vary continuously during the heating process. In organic Rankine cycles, the working fluids used have critical pressures and temperatures lower than those presented by water, making it easier to reach this state for these types of fluids.

As a result, better performance in the heating process can be achieved, which is especially useful when the temperature of the heat source is limited. It's worth noting that by properly selecting the working fluid, it's possible to find a heating curve (2) to (3) that matches the red heat source curve in Figure 2.1, reducing the logarithmic temperature difference and therefore reducing efficiency losses. [7]

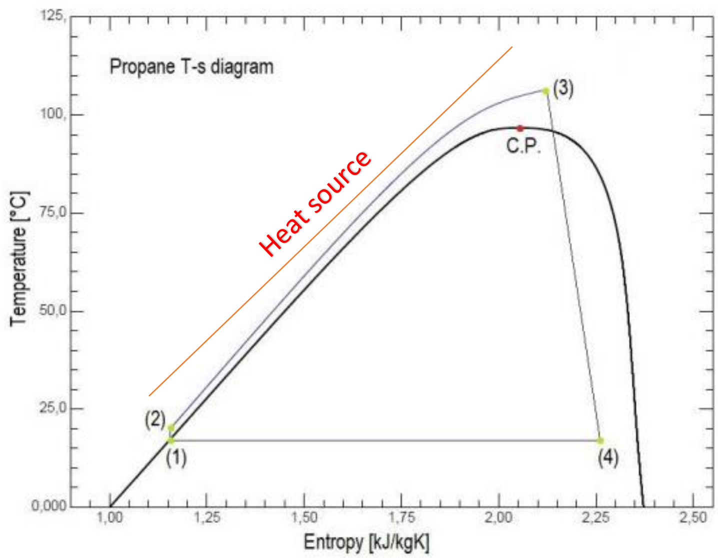


*Figure 2.1 – Supercritical organic cycle of propane*

## 2.2. MONIKA facility

The Modular Low Temperature Cycle Karlsruhe is the acronym for MONIKA is a facility located in the Karlsruhe Institute of Technology Campus Nord. This facility consists of a generic power plant circuit of a geothermal power plant. This cycle is modular, mobile and offers unique opportunities for the study of geothermal power generation and low-temperature electricity generation.

The main goal of this installation is to study the different components in order to increase the efficiency for the power generation from low enthalpy geothermal sources.

The power plant is connected to a boiler as a heat source, which works instead of the water cycle that should possess in a geothermic facility. The boiler simulates the behavior of the heat exchanger. In this way, temperature and mass flow can be varied within wide limits. The Figure 2.2 shows the MONIKA power plant facility [5].

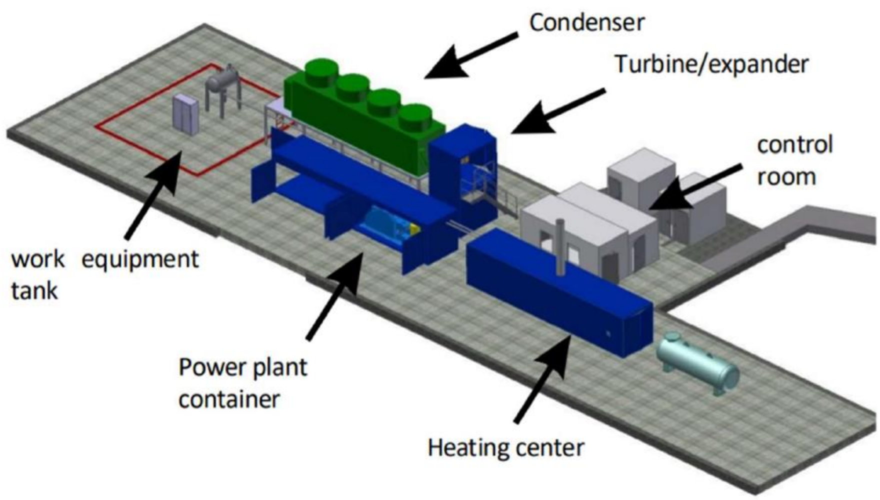


*Figure 2.2 – MONIKA power plant Facility [5]*

The different components of the facility are presented in the Figure 2.3. The red line represents the cycle when the turbine is running under normal operation conditions. The major components of the power plant are:

- Turbine
- Propane Tank
- Pumps
- Heat exchanger
- Condenser

The turbine was manufactured by M+M Turbinen-Technik GmbH and is positioned between the heat exchanger and the condenser. According to the design requirements, the turbine can handle maximum inlet parameters of 6.3 MPa and 130°C for pressure and temperature, respectively. This means that it should generate a simulated power output of 139 kW. It will be described better in the Chapter 2.4 [8].

The propane tank is located after the condenser, and its function is to store propane to be sent to the system's pumps later on.

The condenser is positioned in between the turbine's exit and the propane tank. It is designed with heat exchange surfaces that are arranged in a "V" shape, and there are three separate sections for exchanging heat between the propane and the air. Each motor has a power consumption limit of 13 kW at 322 RPM, and they can handle a maximum volume flow rate of 44 $m^3/s$ each.

To achieve supercritical conditions, two pumps work together to provide sufficient pressure. The first pump, a LEWA triplex M514US G3G, is a piston pump that has a maximum power output of

75 kW and can handle a maximum mass flow of 3.6 kg/s. It is designed to operate under a pressure of 6.5 MPa. To prevent cavitation from occurring within the main pump, a second centrifugal pump is installed. This one is made by Grundfos (CRN20-04 E-FGJ-G-E) and has a maximum power output of 5.5 kW.

GESMEX has provided a heat exchanger that replaces the geothermal heat source. This new heat exchanger is versatile and can operate in both subcritical and supercritical cycles. Its design allows it to generate a thermal power of 1000 kW when it is fully operational. In order to simulate the thermal source, water is used as the working fluid with a parameter range of 0.7-1 MPa and 40-160°C. On the propane side of the heat exchanger, pressures can range between 4.2 and 6.3 MPa, while temperatures can range from 20 to 130°C. During the previous experiment, it was able to achieve a maximum temperature of 113°C [6].

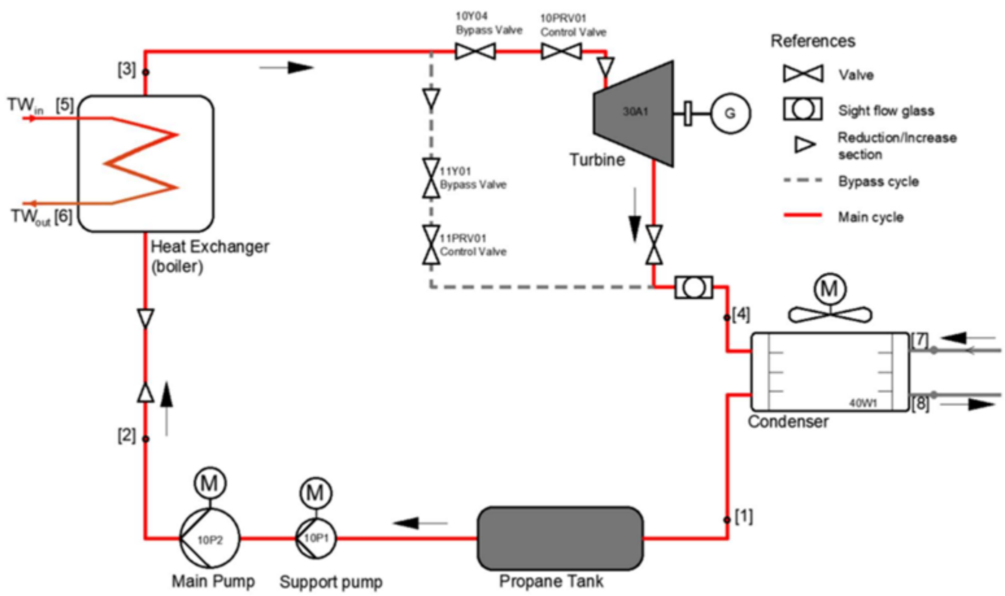


*Figure 2.3 – Modular diagram of the components in the MONIKA power plant facility [6]*

## 2.3. Axial turbomachines

A turbomachine is a machine in which there is energy exchange based on flow generated forces. It works by transferring these forces to the rotating components of the machine, it can happen in both directions. There are mainly two configurations that depend on the construction characteristics: axial turbomachines and radial turbomachines.

In an axial turbomachine the fluid flows mainly in the axial direction of the machine unlike the radial machine in which the fluid goes in radial direction as its name says.

In order to distribute the enthalpy drop over the stages, there are different ways to compound the pressure drop.

An impulse turbine is a turbomachine with no pressure drop in the rotor. The entire pressure drop and the compounding enthalpy drop are used in the stator to produce kinetic energy. The rotor work is produced only by the momentum (impulse) which has been made available by the nozzle. The reaction factor for these turbines is around *RF=0*. [9]

A reaction turbine produces a pressure drop also in the rotor, usually the reaction factor is *RF=0.5*.

Machines with the slowest degree of reaction produce the largest work per stage but the efficiency is lower. There is not a specific optimum reaction ratio, but it is around 0.5. A consequence of using this reaction factor is that it will need more stages. In the Equation 2.1, the reaction factor is determined as a function of the enthalpy h [10].

$$RF = \frac{h_2 - h_3}{h_1 - h_3} \tag{2.1}$$

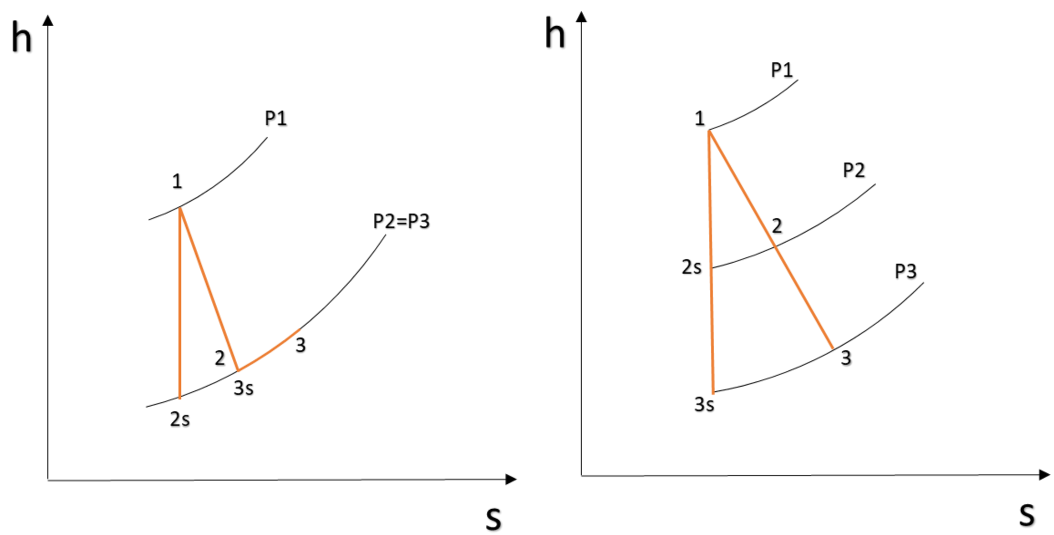


*Figure 2.4 - Diagram h-s of a stage of an impulse turbine RF≈0 at left and a stage of a reaction turbine RF=0.5 at right*

| Item | Axial Turbine | |
|---|---|---|
| | Impulse Turbine | Reaction Turbine |
| Reaction Factor | Aprox. 0 | 0.5 |
| Internal efficiency | Lower | Higher |
| Work Coef. | Higher | Lower |
| Number of stages | Less | More |
| Wheel Friction losses | Lower | Higher |
| Leakage | Lower | Higher |
| Total efficiency | depends on the machine | depends on the machine |

*Table 2.1 – Impulse and reaction turbines comparison*

## 2.4. Description of MONIKA Steam ORC Turbine

The turbine used in the MONIKA facility is an ORC steam impulse turbine with propane as working substance.

The model is GT 120 – 4 manufactured by M + M Turbinen-Technik GmbH. The design parameters are presented in Table 2.2. However, the design parameters may be different from the measured data for the tested states due to some nitrogen in the work fluid. A great aspect to highlight is that the turbine possesses the same radius through all the turbine as presented in Figure 2.5, and the vane rows are only partially open, called a partial admission.

| GT 120 – 4 design parameters – MONIKA ORC steam turbine | |
|---|---|
| Steam mass flow | 2.9 kg/s |
| Rotor speed | 9960 rpm |
| Turbine inlet pressure of steam (abs) | 5.5 MPa |
| Turbine outlet pressure of steam (abs) | 1.1 MPa |
| Turbine inlet temperature | 117 °C (390 K) |
| Power (Calculated) | 139 kW |

*Table 2.2 – Design properties of MONIKA ORC-Turbine at the KIT*

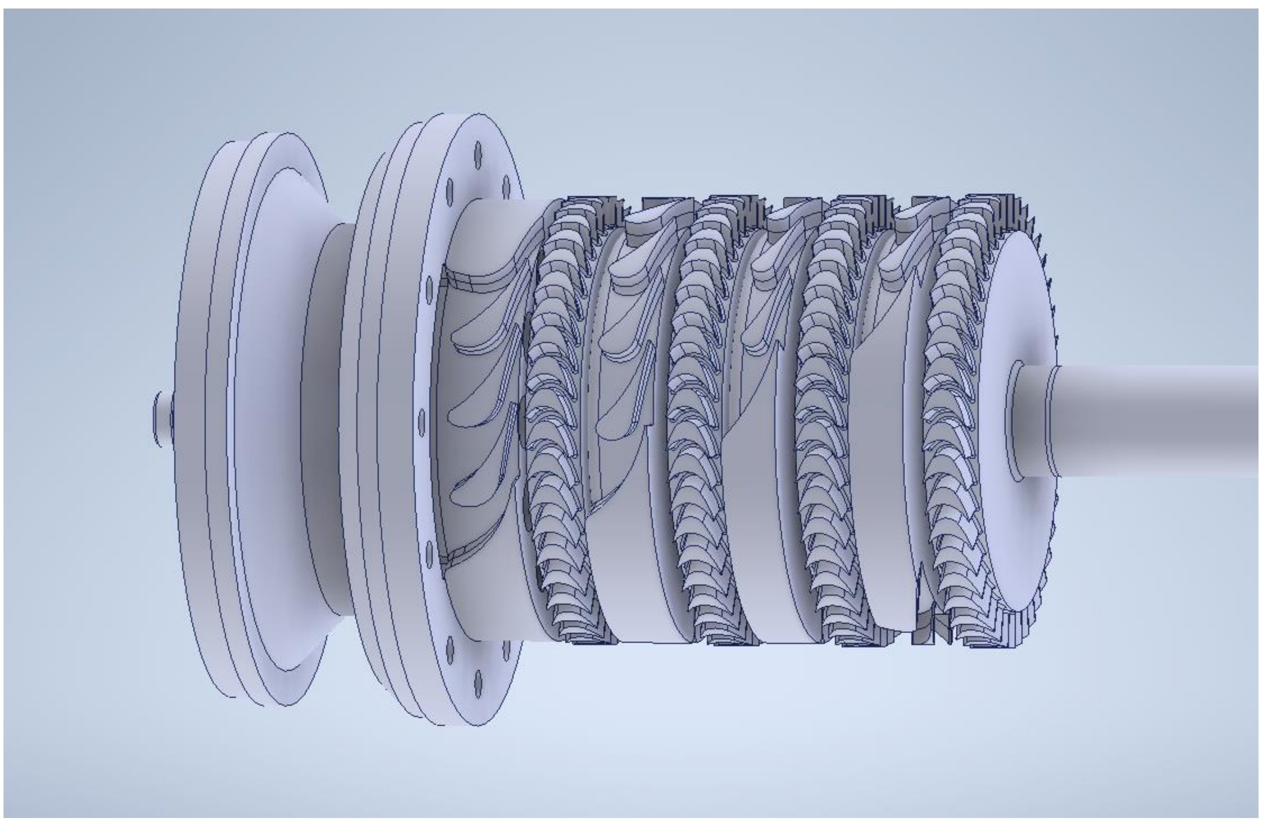

*Figure 2.5 – MONIKA ORC-Turbine configuration*

The turbine is made by a static housing with four stages, one solid rotor and a changing area between stages, that limits the flow through the stage as presented in Figure 2.6. For operation, nitrogen is used as a sealing gas, which prevents propane leakage through the casing, as a consequence, there will be a remaining amount of $N_2$ inside the work fluid during operation, the effect of this will be studied in the next chapters.

The following Figure 2.6 shows the rotor and blades of the turbine. The image shows, there are three Labyrinth tips inside the vane stages 2 to 4, the influence of it will be considered in the calculation of the leakage mass flow.

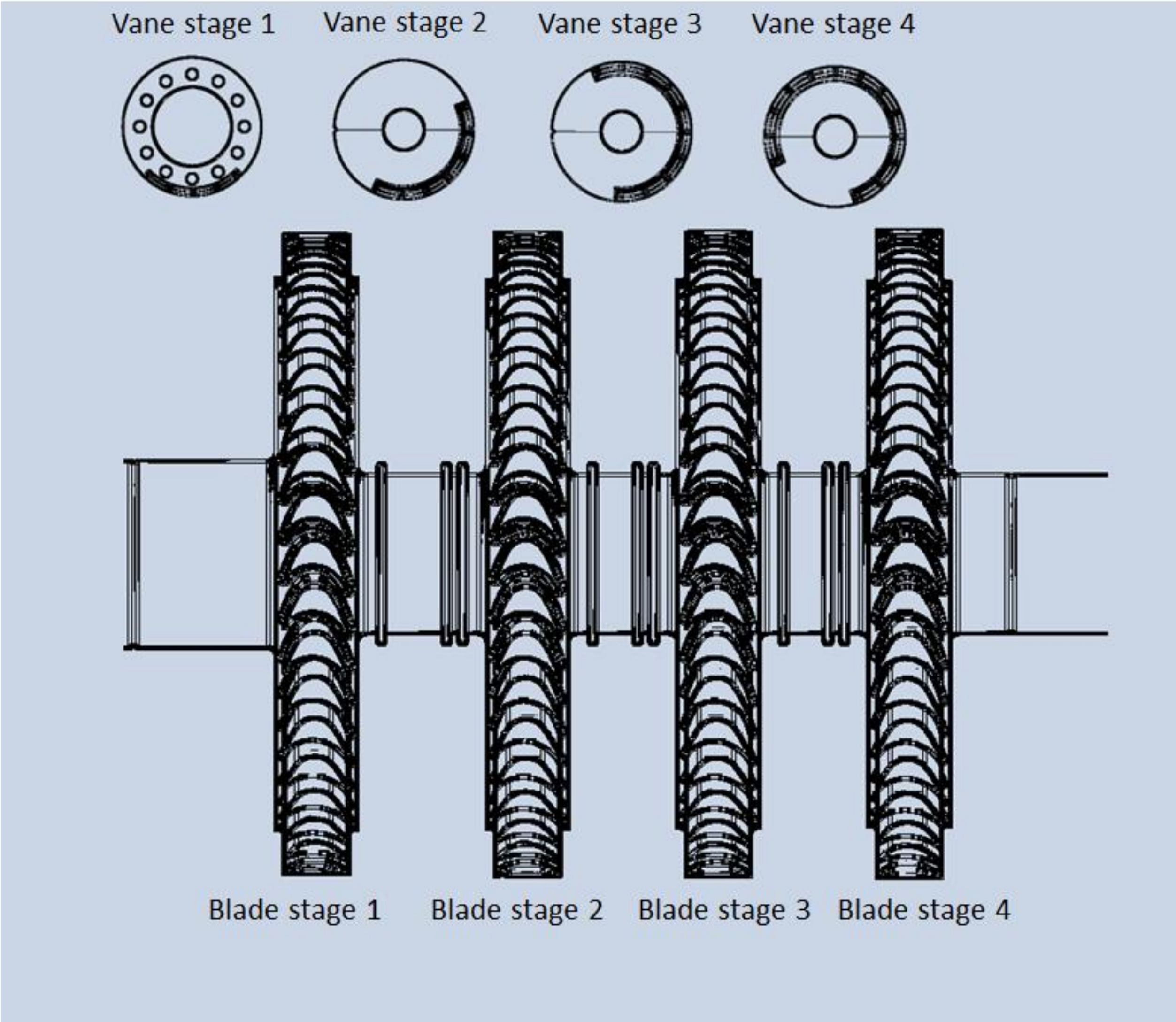


*Figure 2.6 – Rotor design and area changes in the vane stages*

In order to get the geometry characteristics of the turbine, I used the CAD files provided by the manufacturer to measure them.

It is essential to calculate as precisely as possible the outlet angle of the vanes of the turbine. To achieve this, the method used relates the cross-section area to the throat area at each vanes stage. Figure 2.7 shows how the throat passage is determined. The procedure I followed is to set a cylinder in the mean radius of the vane centered at the pressure side trailing edge to measure with it the distance to the next vane that corresponds to the radius $tvp$ of this cylinder [11, p. 271].

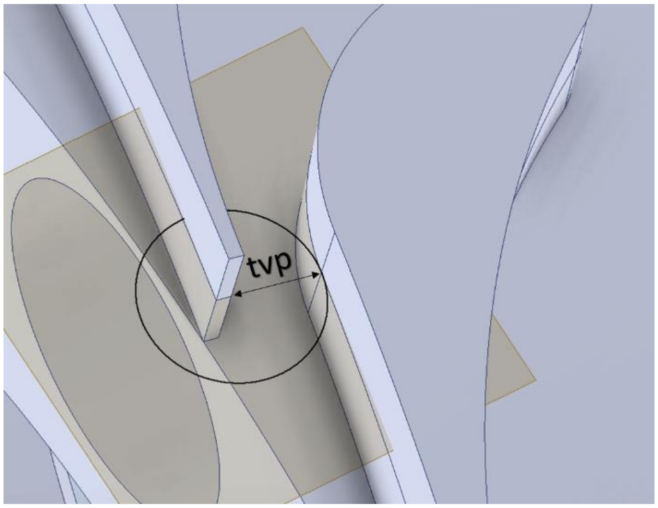


*Figure 2.7 – Measurement of the throat of the vane passage*

Equation 2.2 presents the relation between the throat area $At$ and the cross-section area $An$ with the outlet angle of the vane α. Here, $hb$ is the vane height, $ovp$ is the number of open vane passages, $R_e$ is the outer radius of the vane, $R_i$ is the inner radius of the vane and $\Omega$ the aperture angle of the vane cross section to determine the value of the outlet angle $\alpha$ for the vanes.

$$\sin(\alpha) = \frac{At}{An} = \frac{2 * tvp * hb * ovp}{\Omega({R_e}^2 - {R_i}^2)} \tag{2.2}$$

The blade outlet angle is measured directly at the mean radius, by extending the pressure side of the blade.

The chord length *ca* was taken instead of the axial width as measured as presented in Figure 2.8 for vanes at the left and blades at the right, this will increase the Soderberg losses. This is a conservative approach.

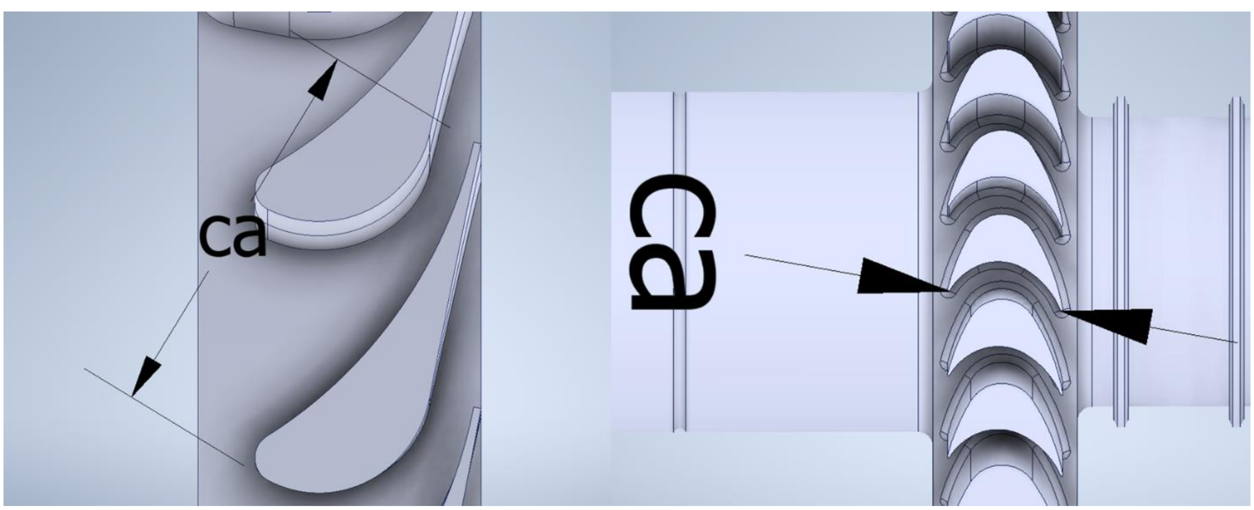


*Figure 2.8 – Measurement of the chord length for vanes and blades*

The geometric characteristics that are used for the calculation of the MONIKA ORC-Turbine are presented in the Table 2.3.

| Cross Section | Omega (Aperture Angle) [deg] | Fraction of aperture, partial admission | Ri (Inner radius) [mm] | Re (Outer radius) [mm] | ca (Chord length) [mm] | hb (Vane/Blade height) [mm] | Outlet angle of Vanes and Blades [deg] | Outlet angle of Vanes and Blades [rad] | DL (Diameter of Labyrinth tips)[mm] | HL (Open clearance of Labyrinth tips) [mm] |
|---|---|---|---|---|---|---|---|---|---|---|
| 0 | 90.00 | 0.25 | 70.50 | 81.50 | 0.00 | 0.00 | 90.00 | 1.57 | 45.60 | 0.00 |
| 1 | 90.00 | 0.25 | 70.50 | 81.50 | 39.36 | 9.00 | 8.00 | 0.14 | 45.60 | 0.00 |
| 2 | 135.00 | 0.38 | 70.50 | 81.50 | 15.64 | 11.02 | 161.00 | 2.81 | 45.60 | 0.10 |
| 3 | 135.00 | 0.38 | 70.50 | 81.50 | 39.05 | 10.00 | 8.62 | 0.15 | 45.60 | 0.10 |
| 4 | 202.50 | 0.56 | 70.50 | 81.50 | 15.64 | 11.02 | 161.00 | 2.81 | 45.60 | 0.10 |
| 5 | 202.50 | 0.56 | 70.50 | 81.50 | 34.40 | 10.10 | 8.89 | 0.16 | 45.60 | 0.10 |
| 6 | 270.00 | 0.75 | 70.50 | 81.50 | 15.64 | 11.02 | 161.00 | 2.81 | 45.60 | 0.10 |
| 7 | 270.00 | 0.75 | 70.50 | 81.50 | 32.31 | 11.00 | 9.79 | 0.17 | 45.60 | 0.10 |
| 8 | 270.00 | 0.75 | 70.50 | 81.50 | 15.64 | 11.02 | 161.00 | 2.81 | 45.60 | 0.00 |

*Table 2.3 – Geometric characteristic of the MONIKA ORC-Turbine*

# 3. Measured data

## 3.1. Inlet and outlet properties

The facility is equipped with different sensors of pressure and temperature located at the inlet and outlet of the turbine as shown in Figure 3.1. The mass flow sensor can be found behind the pump of the plant. These sensors transmit a continuous signal to the control plant; therefore, the average of the data will be considered.

| Facility code | Magnitude | Accuracy | max Abs. error | Location | Model | Manufacturer |
|---|---|---|---|---|---|---|
| PS 10-02 | Pressure | 0.2% Full range | 0.2 bar | Upstream Turbine | VEGABAR 81 | VEGA |
| TS 10-02 | Temperature | ±0.15+0.002*\|T\| | 0.4 K | Upstream Turbine | TR34 Class A | WIKA |
| PI 10-03 | Pressure | 0.2% Full range | 0.2 bar | Upstream Turbine | VEGABAR 81 | VEGA |
| PI 10-12 | Pressure | 0.1% Full range | 0.1 bar | Downstream Turbine | VEGABAR 82 | VEGA |
| FI 10-01 | Mass Flow | ±[0.1+90.0025/m)] * (m/100) | 0.005 kg/s | Downstream Turbine | PROMASS 83F | Endress + Hauser |

*Table 3.1 – Description of equipment used [6]*

In order to get consistent results, the inlet data chosen fulfill the condition of steady state, in which the bypass valve is completely closed. These measured data were taken from the previous work of Joaquin Mardon Perez [6], in which we find the pressure, temperature and mass flow of the fluid as well as the power produced under different conditions.

Figure 3.1 shows the configuration of the MONIKA layout, with the position of the different sensors and the definition of the measuring points 2p, 1p, 0p and 4.

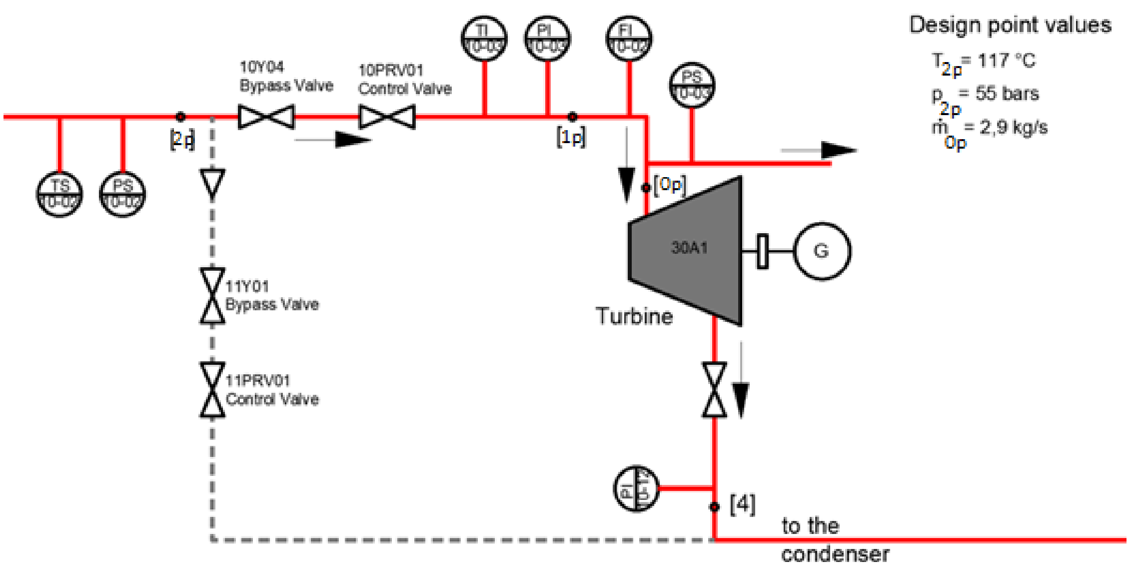


*Figure 3.1 – MONIKA ORC-Turbine facility configuration [6]*

| Day | Time | | Mass Flow [kg/s] | Temperature [$K$] | | Pressure [$kPa$] | | | Power Turb. [$kW$] | Enthalpy [$J/kg$] | |
|---|---|---|---|---|---|---|---|---|---|---|---|
| | | | 0p | 2p | 1p | 2p | 1p | 4 | 0p-4 | 2p | 1p |
| | | Min. of Running | Turbine | TS10-02 | TI10-03 | PS10-02 | PI10-03 | PI10-12 | Power Turb. | H | H-Hloss |
| 08.11.21 | 4th Running | Average | 2.2 | 381.3 | 369.7 | 5189.7 | 4321.1 | 1035.2 | 96.0 | 579683.3 | 579533.5 |
| | 6th Running | Average | 1.9 | 383.1 | 364.6 | 5190.4 | 3916.6 | 1039.7 | 83.7 | 601921.6 | 601744.9 |
| 09.11.21 | 3rd Running | Average | 2.6 | 383.6 | 375.3 | 5627.1 | 4818.5 | 1115.6 | 102.2 | 563768.7 | 566776.3 |
| | 4th Running | Average | 2.6 | 382.5 | 375.4 | 5499.3 | 4824.4 | 1117.0 | 102.6 | 561934.0 | 565111.2 |
| | 5th Running | Average | 2.6 | 382.1 | 375.7 | 5427.7 | 4837.4 | 1120.0 | 103.4 | 562537.7 | 565905.1 |
| | 6th Running | Average | 2.6 | 380.8 | 375.6 | 5295.3 | 4830.9 | 1121.5 | 103.1 | 559167.3 | 562724.6 |
| | 7th Running | Average | 2.6 | 379.9 | 375.9 | 5196.9 | 4851.6 | 1123.7 | 103.8 | 558031.3 | 561852.5 |
| | 8th Running | Average | 2.6 | 379.2 | 375.8 | 5131.0 | 4849.5 | 1124.4 | 103.6 | 555033.2 | 558908.9 |
| | 9th Running | Average | 2.7 | 379.9 | 376.7 | 5219.9 | 4935.0 | 1128.6 | 104.4 | 555982.3 | 559603.7 |

***Table 3.2 – Measured data [6]***

## 3.2. Reference data base for thermodynamic and Transport Properties

In order to calculate the MONIKA turbine, it is crucial to accurately determine the thermodynamic properties of both pure propane and propane-nitrogen mixtures. This can be achieved by using specialized software programs such as COOLPROP or REFPROP, which rely on models to calculate the required properties. These programs allow the user to define the desired mixture type and search for the required thermodynamic property based on other fluid properties. Additionally, they can be seamlessly integrated into the calculation software MATLAB, which was used in this study.

The data base used during this work is REFPROP. This software has been developed by the National Institute of Standards and Technology (USA). REFPROP calculates the thermodynamic properties for the propane-nitrogen mixture using Kunz and Wagner model for hydrocarbon mixtures. [12]

The command used in MATLAB to find the properties of the mixture using REFPROP is presented below:

*result=refpropm(required property, input value1, value1, input value2, value2, substance1, substance2,mass concentration).*

## 3.3. Nitrogen Concentration

The remaining nitrogen present in the mixture is due to the sealing process, to determine the percentage of it, the pressure and the temperature in the time measured after the outlet of the turbine by the sensors PI 10-04 and TI 10-04 were used. MATLAB was used for the calculation of the Nitrogen concentration $CN_2$ and as an initial guess of 2% of Nitrogen in the mixture as mixture 1 $CN_{2,mix\ 1}$ and 3% of Nitrogen in the mixture as mixture 2 $CN_{2,mix\ 2}$. The results of the MATLAB simulation are presented in the Figure 3.2. From the saturation pressures

$$P' = P(T, mixture\ 1) \qquad [Pa]$$

$$P'' = P(T, mixture\ 2) \qquad [Pa]$$

We get the nitrogen concentration as:

$$CN_2 = CN_{2,mix\ 1} + \frac{P_{measured} - P'}{P'' - P'}(CN_{2,mix\ 2} - CN_{2,mix\ 1}) \qquad - \qquad (3.1)$$

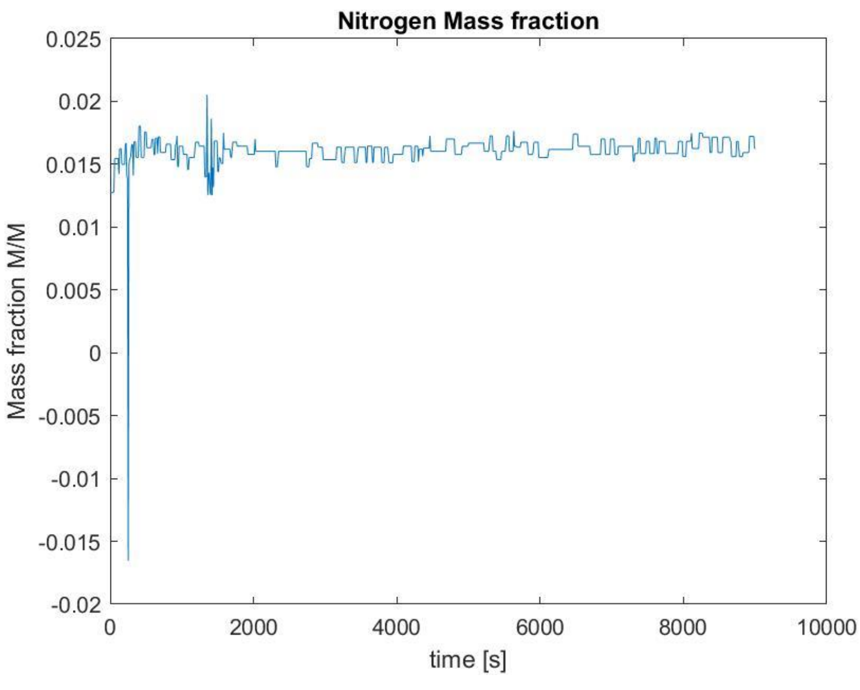


*Figure 3.2 – Nitrogen mass fraction in time in function with measured pressure in PI 10-04*

From the results, I took the average to determine the amount of Nitrogen in the mixture. This value corresponds to 1.6% mass of nitrogen content and will be used in following step to specify the thermodynamic properties.

# 4. Entrance of the turbine

The turbine entrance has a pressure drop between the measured values in 2p and 1p up to the inlet of the turbine, due to heat exchange, friction losses and change of geometry. These differences will change not only the pressure but also the enthalpy and temperature of the fluid and therefore the power produced and the efficiency of the turbine in the expansion process.

The calculation of the inlet conditions for the turbomachine was made using a MATLAB code, presented in the Appendix 11.2.1, using the measured data in PI 10-02, TI 10-02 and PI 10-03. The procedure used for this purpose is presented below.

## 4.1. Critical Properties

As it was mentioned before, the turbine was designed to perform under supercritical conditions, therefore it is necessary to determine the critical pressure and temperature in order to take them as a reference on the state of the fluid at the entrance of the turbomachine as well as in all the stages of it.

REFPROP was used to get these properties depending on the nitrogen concentration which has a great impact in these properties, as well as in the two-phase zone of the fluid.

## 4.2. Calculation of fluid properties in the measured points

Once the critical properties have been determined the enthalpy *h*, entropy *s* and density *ρ* are calculated for 2p. The value of enthalpy for 1p is determined using the enthalpy loss and the enthalpy for the previous point as below:

$$h_{1p} = h_{2p} - h_{1loss} \qquad [J/kg] \qquad (4.1)$$

Then using the measured pressure in 1p and the calculated enthalpy for this point, it is possible to define other the mixture properties.

## 4.3. Calculation of the fluid properties at the entrance of the turbine

Once I have got the properties for the fluid in 1p, I proceeded to calculate the pressure drop between 1p and 0p. For this, it is necessary to calculate the velocity, as a consideration, the density *ρ* will remain constant at first in these two points, this value will be corrected by iteration. It is considered in this step, that there is no heat exchange with the environment therefore it will be isenthalpic $h_{0p} = h_{1p}$.

The geometry data of the pipe between these points are presented in the Table 4.1.

| | | |
|---|---|---|
| Pipe length [$m$] | $L$ | 0.6 |
| Pipe diameter 1p [$m$] | $d$ | 0.05 |
| Pipe diameter 0p [$m$] | $d$ | 0.04 |

*Table 4.1 – Geometric data of the inlet pipe*

The pressure drop calculation depends on the quality of the fluid $X$. In case it is a single-phase fluid, the Bernoulli Equation 4.2 is used where *V* is the velocity of the fluid, $\xi$ is the friction factor of the pipe and $ef$ is the expansion factor for the change of section in the pipe.

$$Pressure\ drop = \frac{\rho V^2(\frac{\xi L}{d} + ef)}{2} \qquad [Pa] \qquad (4.2)$$

In the case of two-phase flow, the pressure drop will be calculated using the Reynolds number for both states of the fluid as in Equation 4.5 [13]. This method represents the total pressure drop as a function of the pressure drop in each phase (liquid and gas).

It is necessary to calculate the friction factor $\xi$ for each phase, and depending on the Reynolds number $Re$ as presented in Equation 4.3. The specific mass velocity $m$ and the dynamic viscosity $\nu$ are used for the calculation.

$$\xi_l = \frac{64}{Re_l};\ \xi_g = \frac{64}{Re_g}\ for\ Re_l, Re_g \le 1187 \qquad - \qquad (4.3)$$

$$\xi_l = \frac{0.3164}{{Re_l}^{1/4}};\ \xi_g = \frac{0.3164}{{Re_g}^{1/4}}\ for\ Re_l, Re_g > 1187 \qquad - \qquad (4.4)$$

$$Re_l = \frac{md}{\nu_l};\ Re_g = \frac{md}{\nu_g} \qquad - \qquad (4.5)$$

The parameters *A* and *B* used in the pressure drop, represents the losses in the pressure for each phase of the flow, being *A* for liquid phase and *B* for gas phase.

$$\left(\frac{dP}{dL}\right)_{f,l} = \xi_l \frac{m^2}{2\rho_l d} = A \qquad [Pa/m] \qquad (4.6)$$
$$\left(\frac{dP}{dL}\right)_{f,g} = \xi_g \frac{m^2}{2\rho_g d} = B$$

The energy balance is used to find the quality of the fluid at the end of the pressure drop, which is necessary to determine the pressure drop. Equation 4.7 uses the heat flux $q$ through the walls of the pipe, the length of the pipe $L$, the specific mass velocity, the diameter of the pipe and the latent heat of evaporation $dHv$ to calculate the exit flow quality of the fluid $X_{out}$.

$$X_{out} = X + \frac{4qL}{md.\,dHv} \qquad - \qquad (4.7)$$

Having A and B, it is possible now to calculate G (A, B), that represents the linear increase of the pressure drop for increasing quality of $X$ < 0.7. To cover the full range 0< $X$ <1 the previous expressions for A and B with the expression for G are superimposed and then integrated.

$$G = A + 2(B - A)X \qquad - \qquad (4.8)$$

$$Pressure\ drop = \int_0^L \frac{dP}{dL} dL = \left\{ -\frac{3}{4}(1-x)^{\frac{4}{3}}[A + 2(B - A)X] + \frac{1}{4}BX - \frac{9}{14}(B - A)(1 - X)^{7/3} \right\}_{X_{in}}^{X_{out}} L \qquad [Pa] \qquad (4.9)$$

Once the pressure drop has been determined, I calculated the value of the pressure for point 0p.

$$P_{0p} = P_{1p} - Pressure\ drop * 0.001 \qquad [kPa] \qquad (4.10)$$

With the enthalpy and pressure in 0p, it was possible to find the values for temperature, density and entropy. Now, the density found in 0p is used as input for the next iteration and the procedure will be repeated until the values converge.

At the entrance of the turbine, upstream the first vane, there is a change of cross section that must be considered and the velocity of the flow will change for this reason. The density is constant at this point as an assumption $\rho_{0p} = \rho_0$.

$$V_0 = \frac{M}{\rho_0 An_0} \qquad [m/s] \qquad (4.11)$$

$$An_0 = (R_e - R_i)R_m\Omega \qquad [m^2] \qquad (4.12)$$

The method described is used to calculate the inlet properties of the turbine for the different measured data in order to use the values founded as input for the calculation of the turbine.

# 5. Turbine Mean line Analysis

The focus I used to calculate the different stages in the MONIKA-ORC impulse turbine is a mean line analysis.

The mean line analysis is a fundamental analysis applied to machines with periodicity in the circumferential direction. This method considers the average values in the tangential direction. Despite the fact that the flow in a turbomachine is unsteady due to the movement of the rotor, at a constant speed of rotation, the average flow is steady and can be described using steady flow equations. This approximation is considered acceptable if the circumferential flow variations are minimal.

For axial turbomachines can be considered that the streamlines of the average flow do not have a radial velocity component. Therefore, the flow becomes one-dimensional in the sense that it only considers the axial variation. However, the flow remains multidimensional because its velocity possesses axial and tangential components. The relations used on a mean streamline of the average flow are representative of the entire machine [9].

In the one-dimensional representation of the flow, it is assumed that the flow is uniform in the cross sections perpendicular to the axis, and that the flow only varies in the axial direction. For the stationary flow, the basic equations used by the mean line analysis are the conservation of mass Equation 5.1, the Euler equation 5.2 (shown here for blade one) and the conservation of energy Equation 5.3. Here $M$ is the mass flow, $An$ is the cross section, $W$ is the velocity in the rotating system, $U$ is the rotor speed, d$A$ is the specific turbine work and $dq$ are energy losses [11].

$$M = \rho A n V_{ax} = constant \tag{5.1}$$

$$dA = \frac{{U_1}^2 - {U_2}^2}{2} + \frac{{V_1}^2 - {V_2}^2}{2} - \frac{{W_1}^2 - {W_2}^2}{2} \tag{5.2}$$

$$d\left(h + \frac{1}{2}V^2\right) = dA + dq \tag{5.3}$$

In order to develop the analysis of the MONIKA ORC-Turbine, the study was carried out on each cross section. The index *n* represents the cross section in which the calculation is being made as presented in Figure 5.1.

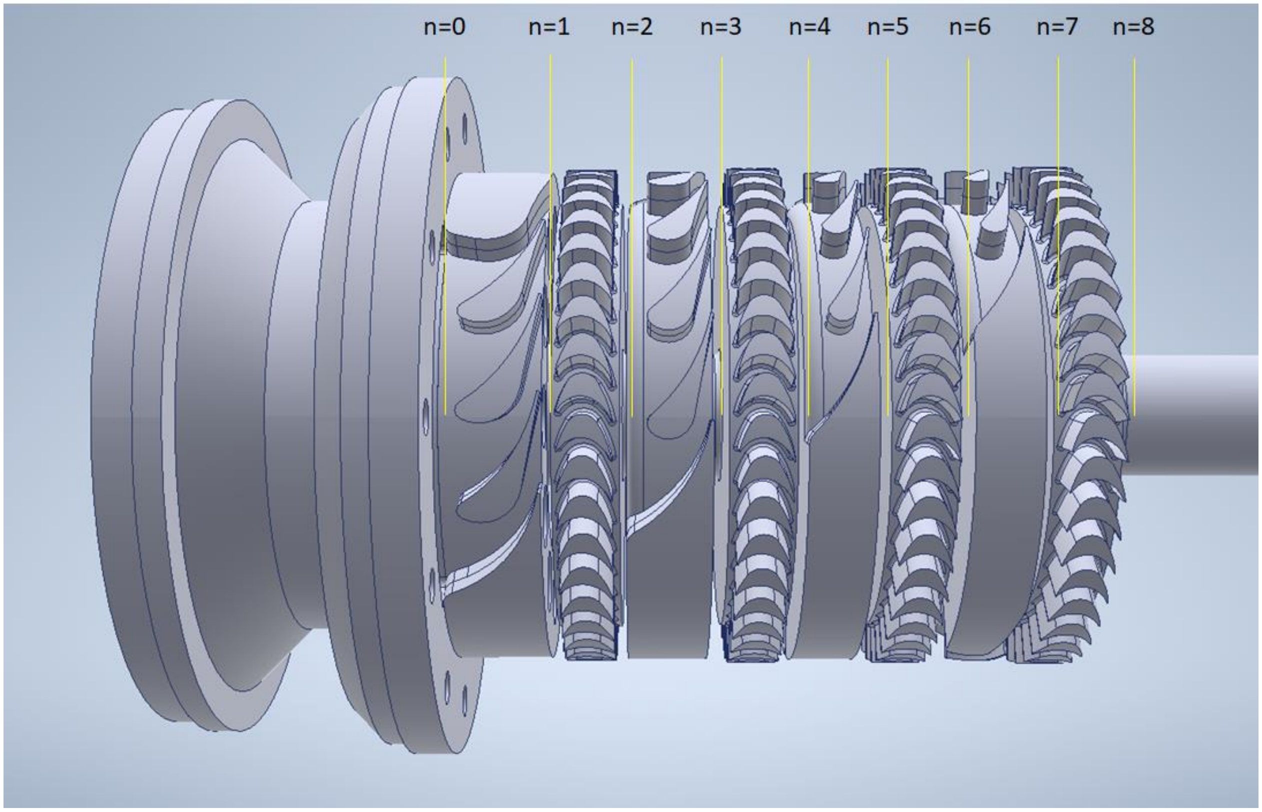


*Figure 5.1 – Stage distribution into the MONIKA ORC Turbine*

As can be seen in the Figure 5.1, the outlets of the vanes are represented by the odd numbers of *n*, the outlets of the blades for the even numbers and the inlet section by 0. This nomenclature is used in the mean line analysis in order to go through the different cross sections of the turbine.

As it was mentioned before, the geometry and the fluid properties at the entrance of the turbine were given as input as well as the outlet pressure of the turbine. The approach taken to develop the analysis, unlike conventional methods, is to use the outlet pressure as input, and use these pressures to give an initial estimate pressure distribution inside the turbine, then use this distribution to calculate the fluid properties, power produced, and mass flow per stage, and then use these results and take them as feedback to calculate the turbine again.

This method iterates the pressure distribution inside the turbine until the mass flow in each stage converges, once the value does not change more than a set error, the calculation is finished [14].

The mass flow was measured in previous works [6] as well as the total mechanical power produced, therefore it is possible to compare these values with the experimental data, and evaluate how good the results are.

The procedure is based on the mean line analysis presented in the book Thermische Turbomaschinen of Walter Traupel [11].

It should be noted that the empirical correlations used to determine losses within the turbine have been derived only for gases or steam. If the fluid enters the turbine with a high liquid content, bubbles and therefore cavitation will occur in the first stage of the vanes, like in a pump. Therefore, the fluid would be far from the range of application of the correlations to be used. Quality values greater than $X > 0.8$ are considered to be correct.

## 5.1. Initial pressure distribution

It is necessary to set an initial pressure distribution for the different cross section between stages. For this, the inlet pressure and outlet pressure were used to fit an approximate pressure drop between the stages. This distribution is used as an initial input to determine fluid properties. The index $m$ corresponds to each one of the four stages of the turbine and its value will represent in which it is being calculated.

If the total pressure ratio $PR$ is given as in Equation 5.4, each stage will have the same pressure ratio as an initial assumption.

$$m = 1, \dots 4$$

$$PR = \frac{P_0}{P_8} \qquad [kPa] \qquad (5.4)$$

$$P_{2m-1} = \frac{P_{2m-2}}{PR^{1/4}} \qquad [kPa] \qquad (5.5)$$

For the case of an ideal impulse turbine:

$$P_{2m} = P_{2m-1} \qquad [kPa] \qquad (5.6)$$

As the MONIKA turbine is an impulse turbine, in the initial distribution, I supposed that the pressure at the outlet of the vanes is the same as the pressure at the outlet of the blades for the same stage.

## 5.1. Velocity of the blades

The MONIKA turbine has been designed as an axial impulse turbine, this means that the fluid moves in the axial direction, and the blades move only in the circumferential direction, which means that their velocity $U$ will depend only on the angular velocity $\omega$ and the mean radius $R_m$ of the blade as presented in the Equation 5.9. As it was mentioned before, the mean radius of the blades and vanes remains constant and therefore the circumferential velocity $U_u$ of the blades remains constant through all the turbine.

With the angular velocity, I get the axial (ax) and circumferential (u) components of the blade velocity.

$$\omega = 2\pi f \qquad [rad/s] \qquad (5.7)$$

$$U_{ax,n} = 0 \qquad [m/s] \qquad (5.8)$$

$$U_{u,n} = R_{m,n}\omega \qquad [m/s] \qquad (5.9)$$

## 5.2. Calculation for the vane stage

The calculation for the vane part of the stages, the values for n are 1,3,5,7. This means, that the procedure presented below is repeated for each outlet of the vanes.

The first step, is find the isentropic enthalpy $h_{s,n}$ using the entropy $s_{n-1}$ for the previous step and the given pressure $P_n$ for this step. In the case in which n=1, the entropy used corresponds to the inlet entropy $s_0$ of the turbine.

$$h_{s,n} = h(P_n, s_{n-1}) \qquad [J/kg]$$

Once the isentropic enthalpy has been determined, I used the Soderberg's correlation to find the loss coefficient $\zeta_n{}'$, here, $\varepsilon_n$ is the vane deflection angle, which is the difference between the inlet $\alpha_{n-1}$ and outlet angle $\alpha_n$. Once the loss coefficient has been calculated as in Equation 5.10, it is used together with the chord length $ca_n$ and the vane height $hb_n$ to get and overall losses for each vane stage $\zeta_n$ as in Equation 5.12 [10, p. 97].

$$\zeta_n{}' = 0.04 + 0.06 * \left(\frac{\varepsilon_n}{100}\right)^2 \qquad - \qquad (5.10)$$

$$\varepsilon_n = \alpha_n - \alpha_{n-1} \qquad [rad] \qquad (5.11)$$

$$\zeta_n = (1 + \zeta_n{}') * \left(0.993 + 0.021 * \frac{ca_n}{hb_n}\right) - 1 \qquad (5.12)$$

The efficiency $\eta$ of the vane stage can be expressed as function of the losses, therefore [11, p. 164]:

$$\eta_n = 1 - \zeta_n \qquad (5.13)$$

Once the efficiency of the stage has been defined, I proceeded to find the value for the real enthalpy after the vanes stage $h_n$ in Equation 5.14.

$$h_n = h_{n-1} - \eta_n(h_{n-1} - h_{s,n}) \qquad [kPa] \qquad (5.14)$$

Now, having enthalpy and pressure in the cross-section n, it was possible to find the properties of the fluid. Using REFPROP, I get:

$$s_n = s(h_n, P_n) \qquad [J/kg\,K]$$

$$\rho_n = \rho(h_n, P_n) \qquad [kg/m^3]$$

$$T_n = T(h_n, P_n) \qquad [K]$$

$$X_n = X(h_n, P_n)$$

From the energy balance, it is possible to write the change of enthalpy in function with the change in kinetic energy, as presented in Equation 5.15 where $V$ is the absolute velocity at the inlet (n-1) and outlet (n) of the vane.

$$\frac{{V_n}^2}{2} - \frac{{V_{n-1}}^2}{2} = h_{n-1} - h_n \quad [J/kg] \qquad (5.15)$$

The mass flow $Mv_n$ through the vane passages is directly related with the velocity and the density of the fluid as presented in Equation 5.16:

$$\frac{{V_n}^2}{2} = \frac{Mv_n}{\rho_n An_n sin\alpha_n} and \ \frac{{V_{n-1}}^2}{2} = \frac{Mv_n}{\rho_{n-1} An_{n-1} sin\alpha_{n-1}} \quad [J/kg] \qquad (5.16)$$

Being the mass flow constant at the inlet and outlet of the vane, I can write it by the relation between enthalpy and velocity for the vane stage as in Equation 5.17.

$$Mv_n = \sqrt{2 * (h_{n-1} - h_n) * (\frac{1}{(\rho_n An_n sin\alpha_n)^2} - \frac{1}{(\rho_{n-1} An_{n-1} sin\alpha_{n-1})^2})} \quad [kg/s] \qquad (5.17)$$

Having determined the mass flow through the vanes, now I proceeded to calculate the velocity $V$ in the absolute system.

$$V_{ax,n} = \frac{Mv_n}{\rho_n An_n} and \ V_{u,n} = \frac{V_{ax,n}}{tan \ \alpha_n} \quad [m/s] \qquad (5.18)$$

$$|V_n| = \sqrt{{V_{ax,n}}^2 + {V_{u,n}}^2} \quad [m/s] \qquad (5.19)$$

As mentioned, the mass flow $Mv$ corresponds only to amount of fluid flowing through the vanes. In order find a more precise estimation, the leakage mass flow through the labyrinth tips is consider as $Ml$. It depends on the geometry configuration of the labyrinth, the density of the fluid, the number of labyrinth tips $z1$ and the pressure difference before and after the labyrinth tips [15].

With the tips diameter $DL$ of the labyrinth and the clearance $HL$ above the tips, we get:

$$Ml1_n = 0.8 * \pi * DL * HL * \sqrt{\rho_{n-1} P_{n-1}} \quad [kg/s] \qquad (5.20)$$

$$Ml_n = ML1_n * \sqrt{\frac{1 - \left(\frac{P_n}{P_{n-1}}\right)^2}{z1 + \ln\left(\frac{P_{n-1}}{P_n}\right)}} \quad [kg/s] \qquad (5.21)$$

Finally, the total mass flow $M$ estimation for the vane stage is:

$$M_n = Mv_n + Ml_n \qquad [kg/s] \qquad (5.22)$$

## 5.3. Calculation for the blade stage

Once the mass flow has been determined for the vane, it is possible to continue the calculation for the blades meaning the value of n=2,4,6,8.

The first consideration that I used for the inlet of the blades, is the density remains constant as a first approximation, being:

$$\rho_n = \rho_{n-1} \qquad [kg/m^3] \qquad (5.23)$$

This value for the density is calculated again in function of enthalpy and pressure and then it will be given as inlet value and calculated over and over again until it converges. In order to make this, it is necessary to find the enthalpy and pressure after the blade stage.

The relative velocity $W$ at the inlet of the blades can be calculated as:

$$\vec{W}_{n-1} = \vec{V}_{n-1} - \vec{U}_{n-1} \qquad [m/s] \qquad (5.24)$$

The mass flow is considered constant as a second consideration.

$$M_n = M_{n-1} \qquad [kg/s] \qquad (5.25)$$

In order to determine the losses in the blade, the Soderberg's correlation has been used again. The expression in the case of the blades is slightly different to the one used for the vanes [10], being:

$$\beta_{n-1} = \operatorname{atan}\left(\frac{W_{ax,n-1}}{W_{u,n-1}}\right) \; and \; \beta_n(measured) \qquad [rad] \qquad (5.26)$$

$$\zeta_n' = 0.04 + 0.06 * \left(\frac{\varepsilon_n}{100}\right)^2 \qquad - \qquad (5.27)$$

The blade deflection angle $\varepsilon_n$ is determined from the inlet and outlet angles $\beta_{n-1}$ and $\beta_n$ of the blades as:

$$\varepsilon_n = \beta_n - \beta_{n-1} \qquad [rad] \qquad (5.28)$$

$$\zeta_n = (1 + \zeta_n') * \left(0.975 + 0.075 * \frac{ca_n}{hb_n}\right) - 1 \qquad - \qquad (5.29)$$

Now with the Soderberg's loss coefficient, I determined the efficiency for the blade as in Equation 5.30 [11, p. 164].

$$\eta_n = 1 - \zeta_n \qquad - \qquad (5.30)$$

$$W_{ax,n} = \frac{M_n}{\rho_n An_{n-1}} \; and \; W_{u,n} = \frac{W_{ax,n}}{tan\,\beta_n} \qquad [m/s] \qquad (5.31)$$

Having determined the velocity $W_n$ in the rotating system, I get the velocity $V_n$ in the absolute system at the outlet of the blade which will be used to calculate the next vane.

$$\vec{V}_n = \vec{W}_n + \vec{U}_n \qquad [m/s] \qquad (5.32)$$

The change of cross section between the outlet of the blade, and the inlet in the next vane must be considered. Due to this the velocity of the fluid will change. For this purpose, I considered the density constant during this step, therefore, the velocity will change depending only on the expansion of the area.

$$\vec{V}_n = \vec{V}_n * \frac{An_{n-1}}{An_n} \qquad [m/s] \qquad (5.33)$$

From this, I get the inlet angle $\alpha_n$ of the vane as:

$$\alpha_n = \operatorname{atan}\left(\frac{V_{ax,n}}{V_{u,n}}\right) \qquad [rad] \qquad (5.34)$$

$$|W_n| = \sqrt{{W_{ax,n}}^2 + {W_{u,n}}^2} \qquad [m/s] \qquad (5.35)$$

$$|W_{n-1}| = \sqrt{{W_{ax,n-1}}^2 + {W_{u,n-1}}^2} \qquad [m/s] \qquad (5.36)$$

$$|V_n| = \sqrt{{V_{ax,n}}^2 + {V_{u,n}}^2} \qquad [m/s] \qquad (5.37)$$

With the velocities fully determined and the efficiency of the blade, now I proceed to calculate the isentropic enthalpy for the outlet in this stage according to Equation 5.38 [11, p. 165].

$$h_{s,n} = h_{n-1} - \left(\frac{|W_n|^2}{2\eta_n}\right) + \frac{1}{2}(|W_{n-1}|^2 - |U_{n-1}|^2 + |U_n|^2) \qquad [J/kg] \qquad (5.38)$$

For turbines with partial admission, i.e., partially open vane passages, ventilation losses have been considered in the calculation; these losses may be defined as an energy dissipation process due to the unsteady flow process when the blades are not receiving a flow from the upstream vanes but they are running through stagnant fluid instead. The ventilation power $PV$ can be represented with sufficient accuracy as in Equation 5.39 [11, p. 420].

$$PV_n = \pi C_n (1 - F_{n-1}) \rho_n 2 R_{m,n} hb * {U_{u,n}}^3 \qquad [W] \qquad (5.39)$$

The ventilation coefficient $C$ depends on the structural arrangement and whether the turbine rotates forward or backward. For the MONIKA turbine the expression for wreath wrapped, forward flow is:

$$C_n = 0.0095 + 0.55 * \left(0.125 + \frac{hb_n}{2R_m}\right)^2 \qquad - \qquad (5.40)$$

With the ventilation power and the mass flow, it is possible now to find the energy losses $qV$ due to the ventilation process

$$qV_n = \frac{PV_n}{M_n} \qquad [J/kg] \qquad (5.41)$$

Additionally, the losses produced by the partial admission will be considered too during this calculation, which are caused near to the edges of the active arcs due to the flow from the admitted into the blocked section, which is known as emptying, and from the rotor leaving the blocked section (filling). These emptying and filling losses are proportional to the circumferential blade velocity $U_{u,n}$ [16].

This method was developed for partial admission in a steam turbine. However, it was not designed for partial admission of all stages, which could lead to deviations in the results.

$$qFE_n = \frac{0.21ca_n U_{u.n}\sqrt{h_{n-1} - h_{s,n}}}{F_{n-1}2R_{m,n}} \qquad [J/kg] \qquad (5.42)$$

The real enthalpy at the outlet of the blade stage, was calculated using the values of the relative velocity, circumferential velocity of the blade and previous enthalpy as presented in Equation 5.43 [11].

$$h_n = h_{n-1} - \frac{(|W_n|^2 - |W_{n-1}|^2 + |U_{n-1}|^2 - |U_n|^2)}{2} \qquad [J/kg] \qquad (5.43)$$

The ventilation losses and filling and emptying losses must be added to the calculated value of real enthalpy.

$$h_n = h_n + qV_n + qFE_n \qquad [J/kg] \qquad (5.44)$$

As the enthalpy increases, the power produced by each blade stage decreases, therefore the ventilation losses and the filling and emptying losses reduce the power of the turbine.

In order to find all the fluid properties at the outlet of this stage, it is still missing the pressure at this point. To determine this value, it will be used the isentropic enthalpy and the previous calculated entropy. Using these two values and a secant method along with REFPROP, I determined the output pressure [17].

$$P_n = P(s_{n-1}, h_{s,n}) \qquad [kPa] \qquad (5.45)$$

With the enthalpy and the pressure, it is now possible to determine the fluid properties with direct functions in REFPROP.

$$s_n = s(h_n, P_n) \qquad [J/kg\,K]$$

$$\rho_n = \rho(h_n, P_n) \qquad [kg/m^3]$$

$$T_n = T(h_n, P_n) \qquad [K]$$

$$X_n = X(h_n, P_n)$$

This density value found is used as inlet for the next iteration until the calculation of the blade converges.

## 5.4. Convergence of the method

The procedure described for the vane stage and the blade stage is repeated for all the stages of the turbine to calculate the fluid properties of each cross section.

The calculation approach I have chosen, as already mentioned, is to iterate the mass flow and to specify as input a pressure distribution for each cross-section. In the previous steps, the mass flow was determined for each stage, then a pressure correction must be made depending on the relative difference in the mass flow for each cross-section, which means that a pressure array from n=1 to n=8 is created. The relative mass flow errors are presented by:

$$dM_n = \frac{M_n}{M_0} - 1 \qquad [kg/s] \qquad (5.46)$$

$$M_0 = M_1 \qquad [kg/s] \qquad (5.47)$$

The pressure correction $dP$ is calculated based on the relative mass flow error $dM$ for the next vane stage, with the exception of the outlet pressure which has been measured. Then the correction is made just for the first three stages, leaving unchanged the pressure values for the cross sections 7 and 8.

$$dP_n = -P_n * dM_{n+2} \ \ where \qquad [kPa] \qquad (5.48)$$

$dM_{n+2}$ *is the mass flow error of the next vane*

Then the new pressure distribution is:

$$P_n = P_n + dP_n * FR \qquad [kPa] \qquad (5.49)$$

The relaxation factor $FR$ has to be considered in the calculation in order to avoid negative values for the pressure and therefore complex values for enthalpy. Once the new pressure distribution has been set, the next iteration must be done for all the turbine cross sections once again.

The iteration process is controlled by the mass error (*Merror*) which is the maximum value of the array $dM$. Once this mass error is lower than a previously defined error, it was assumed that the turbine's state points were found.

With the convergence of all values, the total power of the turbine $Pturb$, the total efficiency $\eta_{turb}$ and the mass flow can be calculated.

The mass flow *M* corresponds with the converged mass flow from above.

$$Pturb = M(h_0 - h_8) \qquad [W] \qquad (5.50)$$

To calculate the global efficiency of the turbine, the specific power produce by the turbine is divided by the isentropic change of enthalpy between the inlet and outlet of the turbomachine.

$$h_{s,outlet} = h(P_8, s_0) \qquad [W]$$

$$\eta_{turb} = \frac{h_0 - h_o}{h_0 - h_{s,8}} \qquad - \qquad (5.51)$$

At the end of the calculation, the fluid velocity must be compared with the local sound velocity of the fluid in order to analyze if the supersonic flow is reached in the different cross sections. When this happens, it could be said that the cascade is “choked”. This choking limit is relevant for the mass flow, because it limits the mass flow of the turbine [18].

$$if\ Ma \geq 1\ Supersonic\ flux$$

$$else\ Ma < 1\ Subsonic\ flux$$

The results obtained with the previous procedure, must fulfil a verification and validation based on the design parameters and on the measured data.

# 6. Verification under design conditions

The evaluation of the results is an important part of the project and must be carried out to determine if the calculation method used leads to good predictions both in the calculation of the thermodynamic properties of the fluid and in obtaining the power and efficiency of the turbine. This verification process comes to check if the properties calculated match with the specifications provided by the manufacturer.

To carry out this process, the calculation of the different stages of the turbine was made under the design conditions previously described. It is important to highlight that, as these are ideal conditions, I considered that the working fluid is pure propane, this means that the critical properties, the two-phase zone among the other thermodynamic properties will differ for the case in which the fluid has a concentration of nitrogen in it. The critical properties for pure propane are presented in Table 6.1.

| Critical Properties of Propane | |
|---|---|
| Temperature $[K]$ | 369.8 |
| Pressure $[kPa]$ | 4251.2 |

*Table 6.1 – Critical Properties for pure Propane*

According to the design point, the inlet conditions are supercritical and the outlet pressure for this calculation was set on 1100 kPa.

Once the calculation is done, the results obtained will be compared with the information provided by the manufacturer. For the calculation it was set a value for the relaxation factor $FR = 0.5$. The results under the described precious conditions are presented in Table 6.2

| Cross Section | Enthalpy $[J/kg]$ | Entropy $[J/kgK]$ | Pressure $[kPa]$ | Density $[kg/m^3]$ | Specific Volume $[m^3/kg]$ | Quality | Performance | Mass Flow $[kg/s]$ | Temperature $[K]$ |
|---|---|---|---|---|---|---|---|---|---|
| 0 | 640520.17 | 2259.49 | 5500.00 | 175.00 | 0.005 | 1 | 0 | 0 | 390.60 |
| 1 | 627527.77 | 2267.03 | 3410.57 | 96.24 | 0.01 | 1.01 | 0.82 | 2.84 | 358.14 |
| 2 | 629496.31 | 2271.77 | 3436.45 | 96.28 | 0.01 | 1.03 | 0.73 | 2.84 | 358.97 |
| 3 | 616912.32 | 2277.52 | 2339.31 | 58.59 | 0.02 | 0.95 | 0.86 | 2.84 | 338.07 |
| 4 | 617880.03 | 2281.91 | 2309.43 | 57.39 | 0.02 | 0.95 | 0.74 | 2.84 | 337.43 |
| 5 | 604903.82 | 2288.10 | 1608.98 | 37.75 | 0.03 | 0.95 | 0.86 | 2.84 | 320.29 |
| 6 | 605642.94 | 2292.21 | 1587.46 | 37.04 | 0.03 | 0.95 | 0.74 | 2.84 | 319.68 |
| 7 | 591737.30 | 2298.82 | 1100.00 | 24.98 | 0.04 | 0.95 | 0.87 | 2.84 | 303.94 |
| 8 | 592048.88 | 2303.78 | 1070.65 | 24.19 | 0.04 | 0.96 | 0.74 | 2.84 | 302.84 |

*Table 6.2 – Calculated properties of the MONIKA turbine under design conditions*

From these results, the outlet pressure is slightly lower than the outlet pressure under the design conditions. It is important to mention, that the calculated pressure corresponds directly to the outlet of the blade stage, which means that after the last stage there will be a pressure increase through the outlet diffuser. However, the calculation for this part was not performed in the present work.

Figure 6.1 shows the enthalpy-entropy (h-s) diagram. As expected for an impulse turbine, the enthalpy drops in the vane stages and it has a slight increment in the blades. It is possible to see that after the first blade stage the turbine works in the two-phase zone with high quality in each cross section.

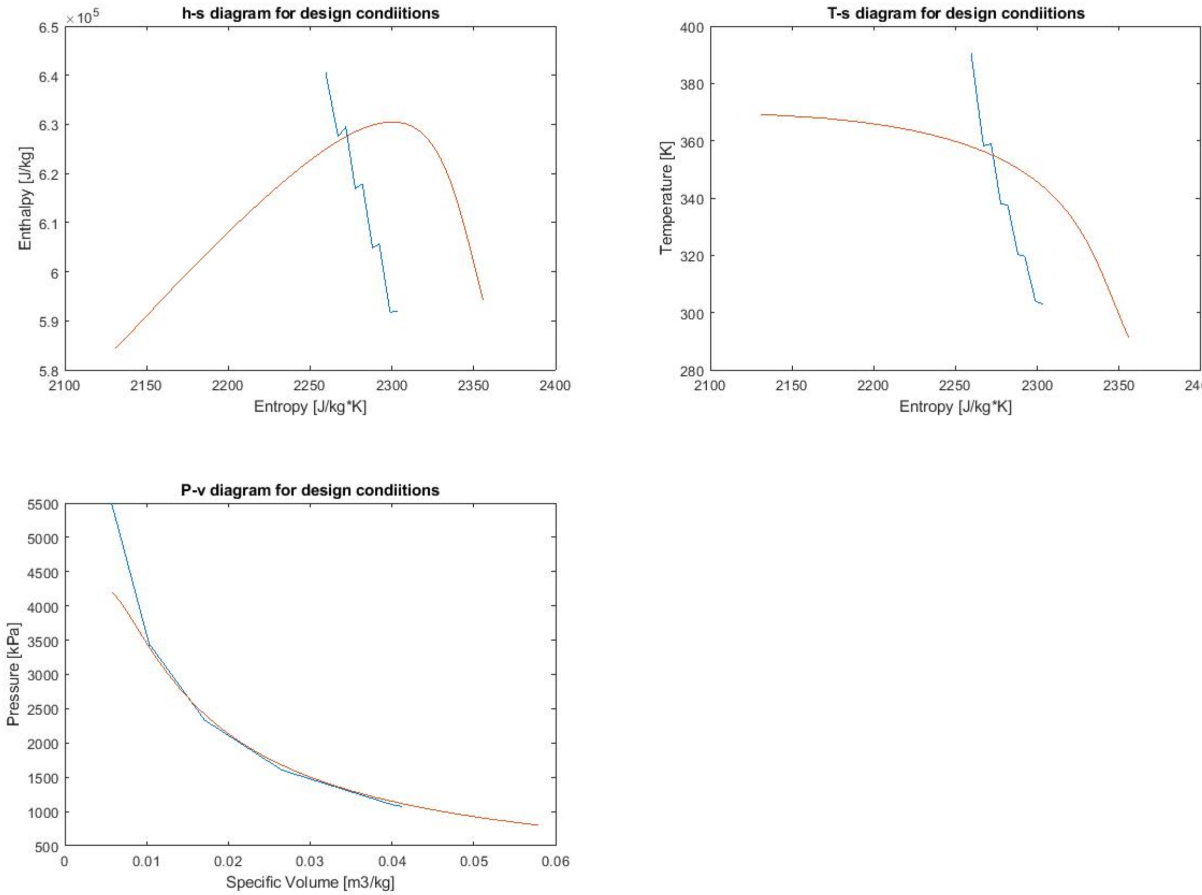


*Figure 6.1 – Diagrams h-s T-s and P-v for calculation of turbine stages under design conditions*

The total turbine power has been calculated according with (5.50) as well as the total efficiency of the turbine with (5.51). From the calculated data now, I proceeded to find the error for these quantities.

| **Item** | **Unit** | **Design** | **Calculated** | **Error** |
|---|---|---|---|---|
| Total turbine power | W | 139000 | 137834 | 1% |
| Total turbine efficiency | % | - | 78 | - |
| Mass flow | kg/s | 2.9 | 2.84 | 2% |

*Table 6.3 – Comparison between calculated power and mass flow with design values*

According to Table 6.3, a small deviation in the results obtained regarding the design data can be observed. This difference may be due to the methods used to determine the losses in the turbine, as well as which losses were included. The losses considered were the efficiency of the blades and vanes through the Soderberg's correlation, ventilation losses, filling and emptying losses, and the labyrinth losses which consider the mass flow lost through the seals.

It must be noticed that the turbine has a design in which the mean radius remains constant, and there is partial admission of all the stages. To calculate this, as mentioned earlier, the filling and emptying losses were used, which were designed for admission to the turbine. This could also bring differences in the results.

As it was mentioned before, the velocity of the fluid must be below the sound speed of the fluid, In the Figure 6.2 is shown that the velocity always stays below the sound speed, having its maximum value at the end of the first vane stage. It is important to mention that the sound velocity has been taken from REFPROP, in which the sound velocity for two phase regions is not available. Therefore, for these cases, it was taken the sound velocity for saturated steam at the pressure of the cross section.

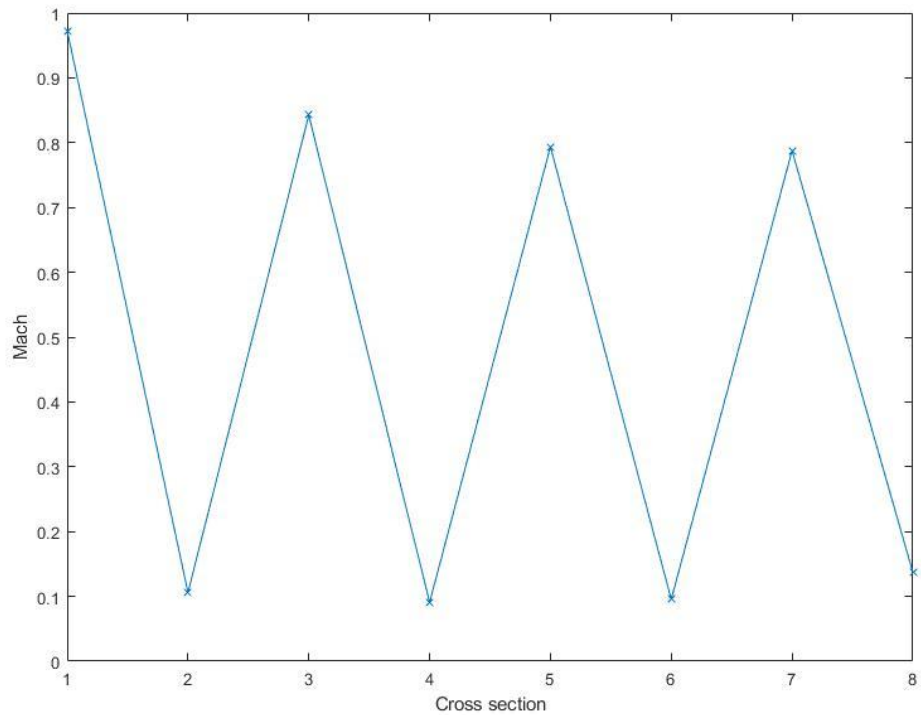


*Figure 6.2 – Mach number for the cross sections of the turbine for design values*

Although there is a deviation in the results obtained regarding the design data, this difference is in the order of 1%, so it can be considered that the correlations and calculation methods used are sufficiently close to those used by the manufacturer. Therefore, I consider that the calculation method can be used to determine the properties of the turbine under experimental conditions and to predict its behavior.

# 7. Validation with measured data

Once the calculation method has been verified, the code must be validated. This procedure consists on check if the results obtained from the method used fit with the intended purpose of it, which is to calculate the properties of the MONIKA ORC-Turbine. For this it is necessary to evaluate the method under measured real conditions and compare these with the properties obtained through the mean line analysis described above.

As in the verification, the quantities to be compared will be the total power generated by the turbine and the mass flow of the turbine, having as input variables the pressures at the inlet and outlet of the turbine, as well as the inlet temperature of it. Since these are experimental data, it is necessary to consider the amount of nitrogen present in the fluid, so according to the calculation in Chapter 3.3, the mass concentration of nitrogen in the propane corresponds to 1.6%. The critical properties obtained from REFPROP for this concentration of nitrogen are presented in Table 7.1.

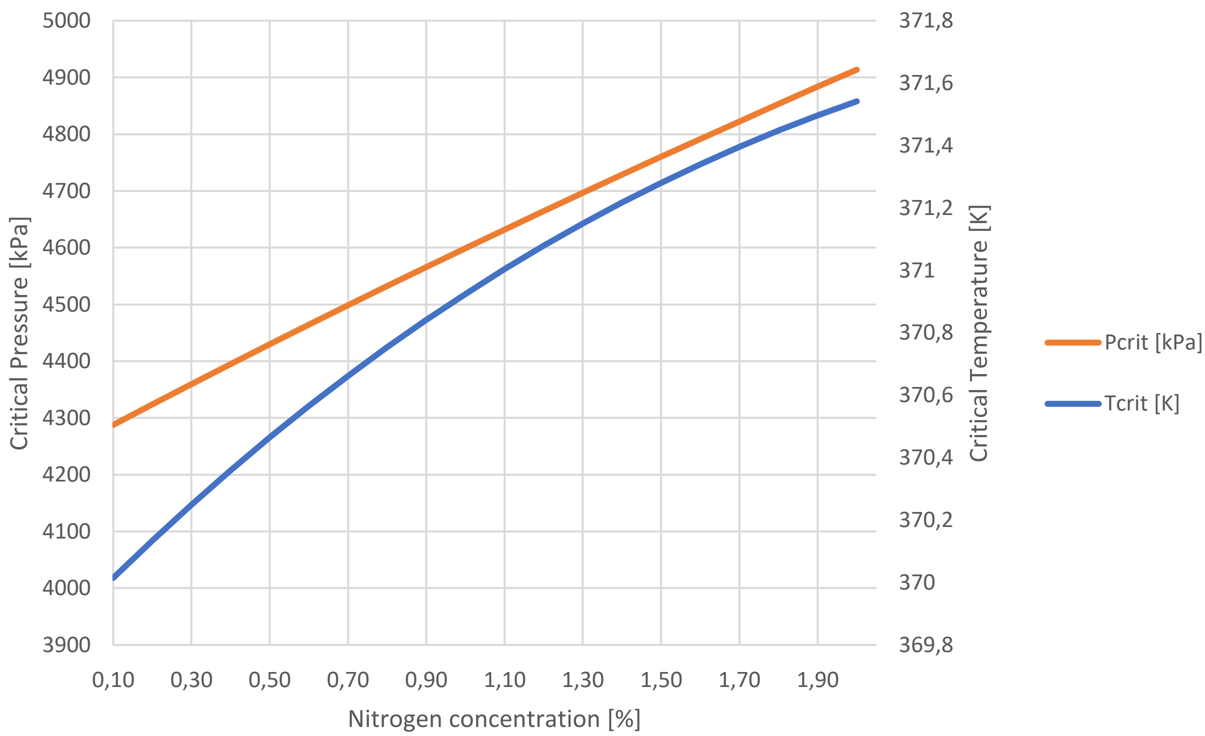


*Figure 7.1 – Critical Properties for different concentration of Nitrogen*

| Critical Properties of 98.4 % Propane and 1.6 % Nitrogen | |
|---|---|
| Temperature $[K]$ | 371.34 |
| Pressure $[kPa]$ | 4791.4 |

*Table 7.1 – Critical Properties for 98.4 % Propane and 1.6 % Nitrogen*

The calculation of the turbine of the MONIKA plant under the measured experimental conditions will be divided into two parts, the first part corresponds to the turbine inlet and the second part corresponds to the mean line analysis.

## 7.1. Inlet properties of the turbine

The method described in Chapter 4 was used to determine the properties at the turbine inlet, using as input data those presented in Table 3.2. The results obtained are presented below in Table 7.2. It should be remembered that the data correspond to the average of the steady state measurements on the days when the turbine was working with the bypass valve completely closed.

| Date | Running | Enthalpy $[J/kg]$ | Entropy $[J/kgK]$ | Pressure $[kPa]$ | Velocity $[m/s]$ | Density $[kg/m^3]$ | Temperature $[K]$ |
|---|---|---|---|---|---|---|---|
| 08.11.21 | 4th Running | 623159.90 | 2322.47 | 4288.47 | 13.20 | 126.85 | 369.22 |
| | 6th Running | 634859.46 | 2364.15 | 3876.54 | 16.20 | 103.39 | 365.07 |
| 09.11.21 | 3rd Running | 606420.84 | 2268.01 | 4793.05 | 10.27 | 162.98 | 374.31 |
| | 4th Running | 608484.08 | 2273.43 | 4798.66 | 10.39 | 161.22 | 374.60 |
| | 5th Running | 611477.69 | 2281.20 | 4811.32 | 10.54 | 158.93 | 375.10 |
| | 6th Running | 612920.59 | 2285.16 | 4804.55 | 10.65 | 157.29 | 375.17 |
| | 7th Running | 615636.20 | 2292.04 | 4825.04 | 10.75 | 155.70 | 375.77 |
| | 8th Running | 615677.55 | 2292.19 | 4822.86 | 10.76 | 155.57 | 375.74 |
| | 9th Running | 612825.98 | 2283.16 | 4909.43 | 10.34 | 161.92 | 376.53 |

*Table 7.2 – Calculated inlet properties of the turbine*

It can be observed from the results obtained that on 08.11.21 the fluid entered the turbine superheated, while on 09.11.21 it was slightly above the critical properties.

## 7.2. Turbine stages calculation by mean line analysis

Using the results obtained above, I proceeded to calculate the properties for each of the cross sections of the turbine using the method described in Chapter 5. For this, as previously described, the PI 10-12 pressure measurement at the turbine outlet was also used as a starting value to determine the preliminary pressure distribution for each case and to perform the iterations on this basis.

To perform this calculation, a relaxation factor of $FR = 0.5$ was taken. The results obtained for each of the simulations are detailed in Tables 11.4 – 11.12 of the Appendix. In the next figures, the graphs for enthalpy-entropy (h-s), temperature-entropy (T-s) and pressure-specific (P-v) volume are shown.

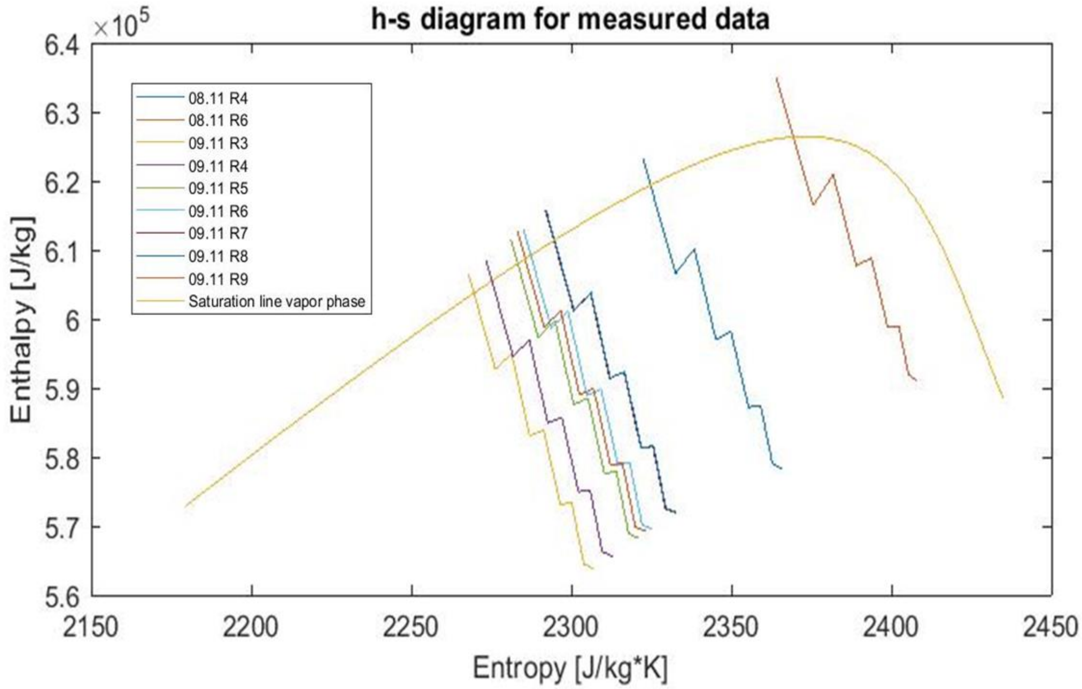


*Figure 7.2 - Diagram h-s calculated for measured data*

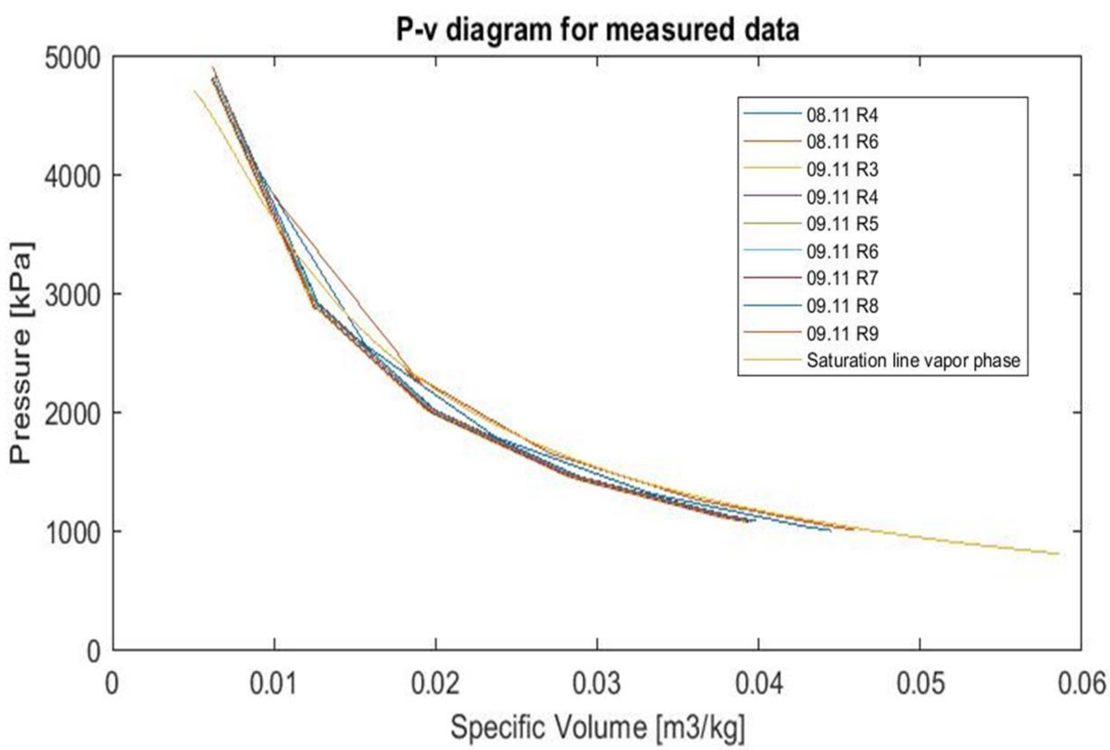


*Figure 7.3– Diagram P-v calculated for measured data*

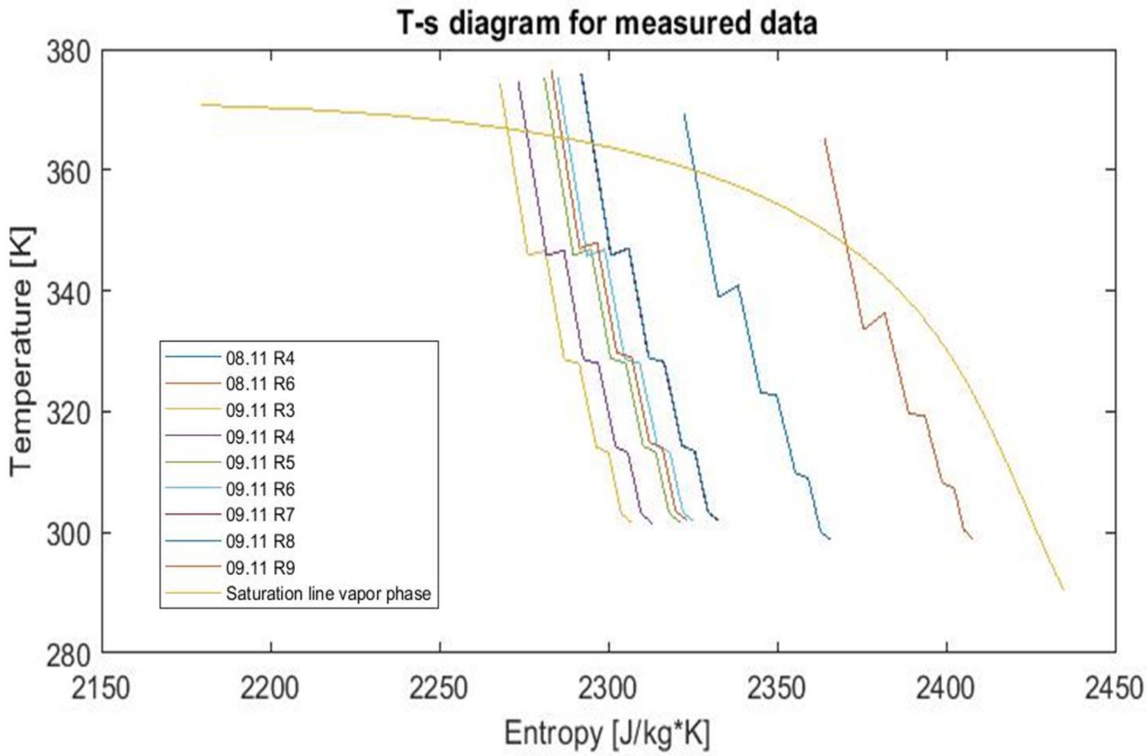


*Figure 7.4 – Diagram T-s calculated for measured data*

The above diagrams show the evolution of the thermodynamic properties of the working fluid in the different stages of the turbine. It is also noticeable that the behavior of the enthalpy is consistent with an impulse turbine, where the enthalpy drop occurs in the vanes and slightly increases in the rotor blades. Similarly, the pressure in the rotating stages of the turbine remains constant.

In all cases, the fluid is in the two-phase zone shortly after entering the first stage of the vanes, and the quality of the fluid remains above 0.85.

The comparison between the velocity of the fluid and the velocity of sound is presented Figure 7.5. It can be seen, all the values are below Mach number one, therefore the fluid does not reach the supersonic condition in any of the cross sections.

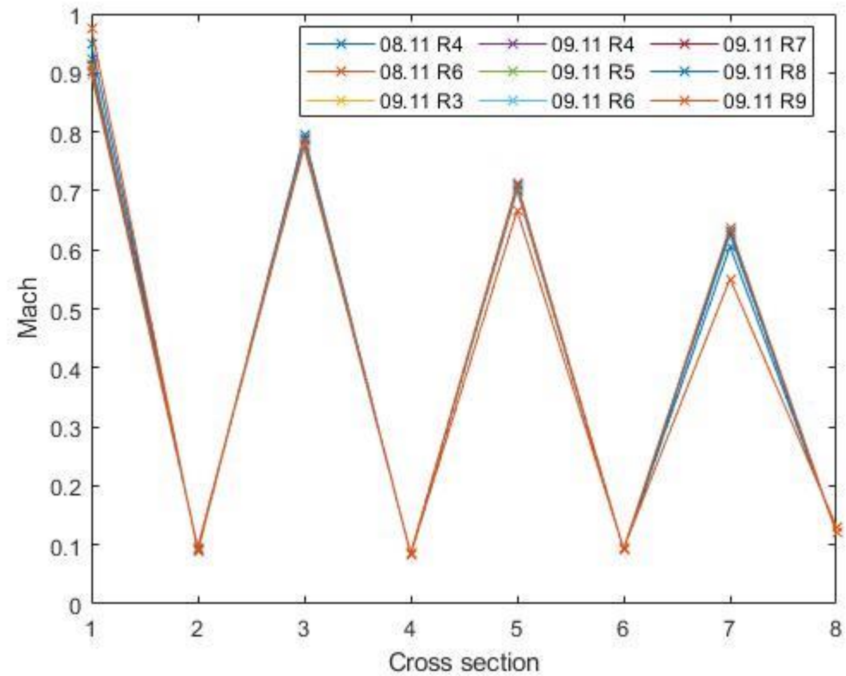


*Figure 7.5 - Mach number for the cross sections of the turbine for measured data*

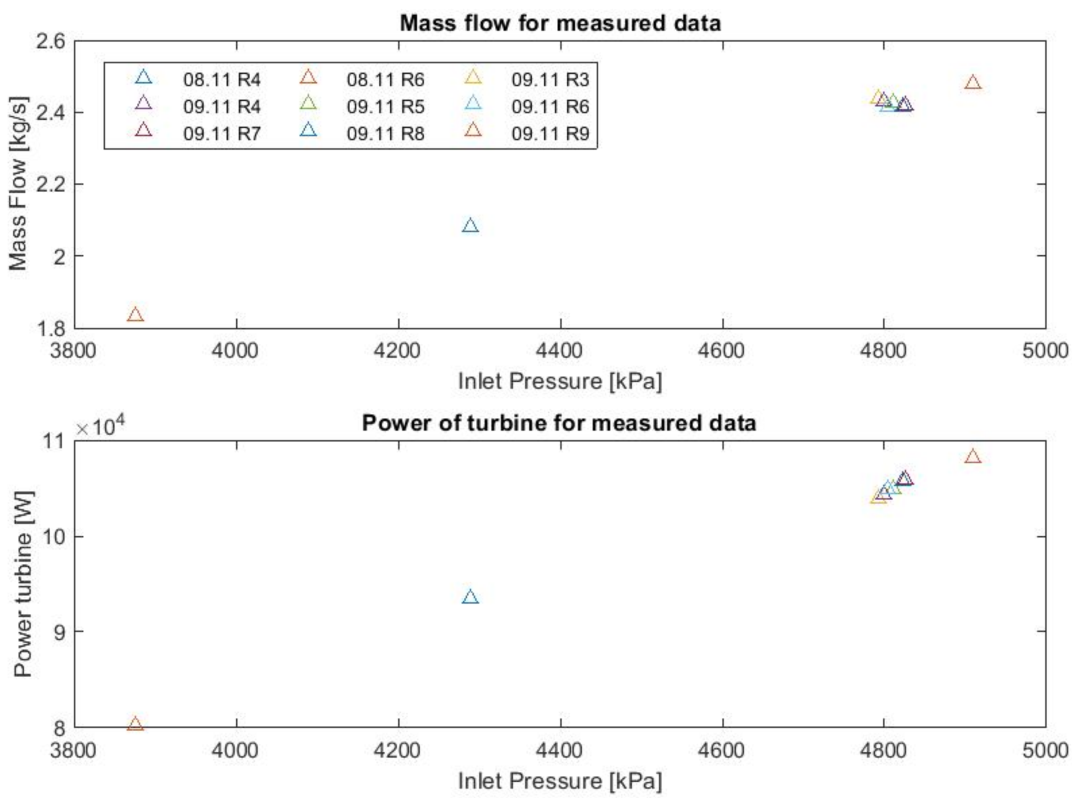


*Figure 7.6 – Mass flow and power calculated for measured data*

The Figure 7.6 shows the impact on both power and mass flow from the fact that the input properties are not at supercritical levels as showed for the day 08.11.21, in which the inlet properties did not reach this state, reducing the amount of power produced by up to 20 kW.

Table 7.3 shows the comparison in the mass flow, power produced and efficiency calculated.

| Date | Running | Calculated | | | Measured | |
|---|---|---|---|---|---|---|
| | | Mass Flow $[kg/s]$ | Power $[W]$ | Efficiency | Mass Flow $[kg/s]$ | Power $[W]$ |
| 08.11.21 | 4th Running | 2.08 | 93420.57 | 0.77 | 2.19 | 96023.51 |
| | 6th Running | 1.83 | 80174.33 | 0.77 | 1.89 | 83658.79 |
| 09.11.21 | 3rd Running | 2.43 | 103812.66 | 0.78 | 2.59 | 102159.94 |
| | 4th Running | 2.43 | 104228.21 | 0.78 | 2.60 | 102626.09 |
| | 5th Running | 2.42 | 104922.88 | 0.78 | 2.60 | 103436.72 |
| | 6th Running | 2.41 | 104802.35 | 0.78 | 2.60 | 103068.79 |
| | 7th Running | 2.41 | 105819.96 | 0.78 | 2.60 | 103811.72 |
| | 8th Running | 2.41 | 105698.38 | 0.78 | 2.59 | 103623.18 |
| | 9th Running | 2.47 | 108138.24 | 0.78 | 2.68 | 104401.82 |

*Table 7.3 – Calculated vs Measured Mass Flow, Power and efficiency.*

It is evident that the inlet pressure and temperature with which the fluid enters the turbine have a great impact on the power produced, being this lower for the day on which the fluid does not reach the supercritical conditions at the turbine inlet. Although these values are lower than for the case of design conditions, the total efficiency of the turbine is not greatly altered, since this reduction in the generated power is directly related to the reduction of the mass flow and the drop in enthalpy of the different stages of the turbine is similar for all cases.

| Date | Running | Error | |
|---|---|---|---|
| | | Mass Flow | Power |
| 08.11.21 | 4th Running | 5% | 3% |
| | 6th Running | 4% | 4% |
| 09.11.21 | 3rd Running | 6% | -2% |
| | 4th Running | 7% | -2% |
| | 5th Running | 7% | -1% |
| | 6th Running | 7% | -2% |
| | 7th Running | 7% | -2% |
| | 8th Running | 7% | -2% |
| | 9th Running | 8% | -4% |

*Table 7.4 – Percentage of error in each variable between measured and calculated properties*

The efficiency calculated in previous studies [6] was not considered because it was based on a nitrogen concentration in the fluid of 0.2%, which may differ considerably from the current study.

As shown in Table 7.4, the results exhibit differences compared to the measured data. These deviations could be attributed to inaccuracies in the manufacturing of the turbine, since small changes in the exit angles at different vane and blade stages can significantly impact the turbine's performance. Additionally, inaccuracies in the calculation of the lost flow through the seals may also contribute to the observed deviations. Furthermore, the accuracy of the measuring equipment implies a degree of uncertainty in the measured results.

Taking all of the above into account, it can be concluded that the deviations in the results obtained through the implemented calculation method, compared to the measured data, are in the range of 4% to -4% in the power produced, and 4% to 8% in the mass flow. Therefore, they can be considered accurate enough to be validated and used to predict the turbine's operation under different operating conditions.

# 8. Sensitivity analysis

To conclude the study on the behavior of the calculation method, a sensitivity analysis was carried out in order to observe the change of the properties found in the cross sections of the turbine, when varying the input properties and their impact on the power produced, mass flow, and total efficiency of the turbomachine.

During this analysis, pure propane was considered as the working fluid, since these are the ideal design conditions. Accordingly, the critical pressure is 4251 kPa and the temperature is 369.8 K.

Two different variables were varied while keeping the other fixed, these being the inlet pressure and the inlet temperature, with the outlet pressure fixed at 1000 kPa for all cases.

## 8.1. Sensitivity analysis for inlet pressure

First of all, a sensitivity analysis was made for the pressure. This consisted of varying the inlet pressure from Pmax = 5500 kPa, which corresponds to the design pressure, to Pmin = 4603 kPa, which corresponds to the lowest pressure measured on 08.11.21 in the running. The lowest pressure calculated from the measured properties at the inlet of the turbine was 3876.53 kPa, which corresponds to the lowest pressure among the analyzed cases.

As mentioned in Chapter 5, once the calculations have been made, it is important to verify that the fluid quality is within the range of validity of the loss correlations used. As can be seen in Figure 8.1, the fluid quality values are above 0.8 for all cases in all cross sections of the turbine, therefore it can be considered that the results are correct.

Qualities greater than 1 indicate that the substance is in a vapor state, while values below 0 indicate that the substance is in a liquid state.

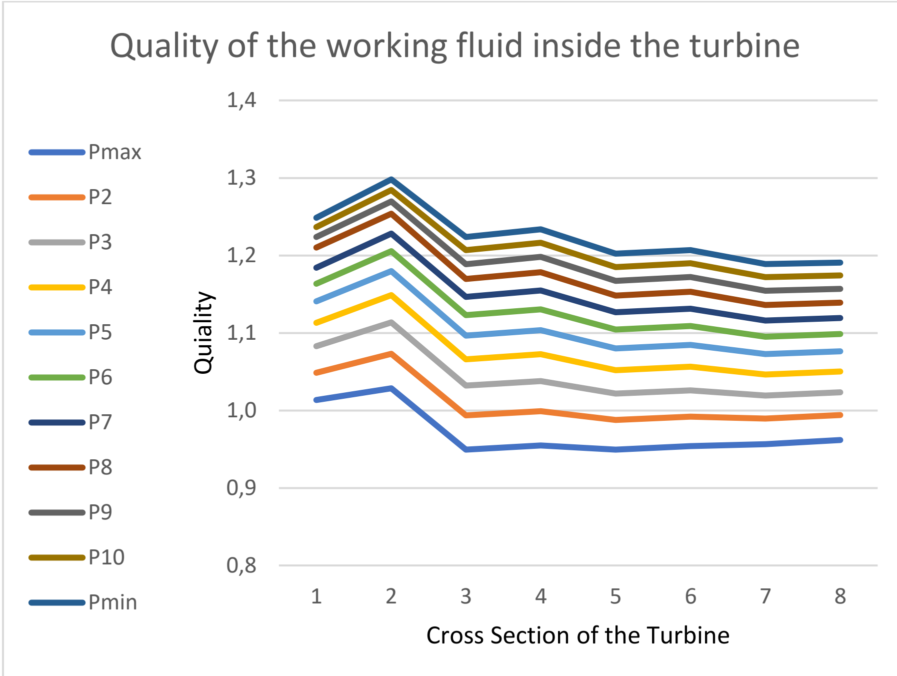


*Figure 8.1 – Quality distribution per cross section of the turbine for pressure sensitivity analysis*

In Figure 8.2, it can be observed that as the inlet pressure decreases, the enthalpy distribution in the different stages shifts from the supercritical zone to the superheated fluid zone, and at the same time, entropy increases, moving away from the saturated vapor line.

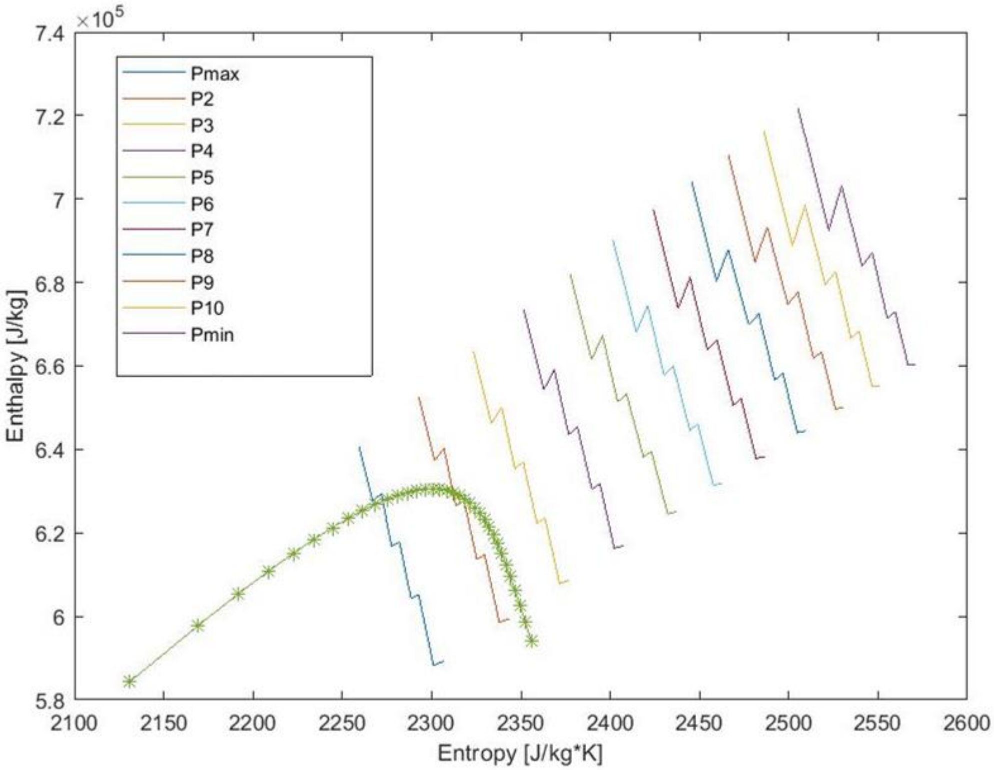


*Figure 8.2 – Diagram h-s from sensitivity analysis for inlet pressure*

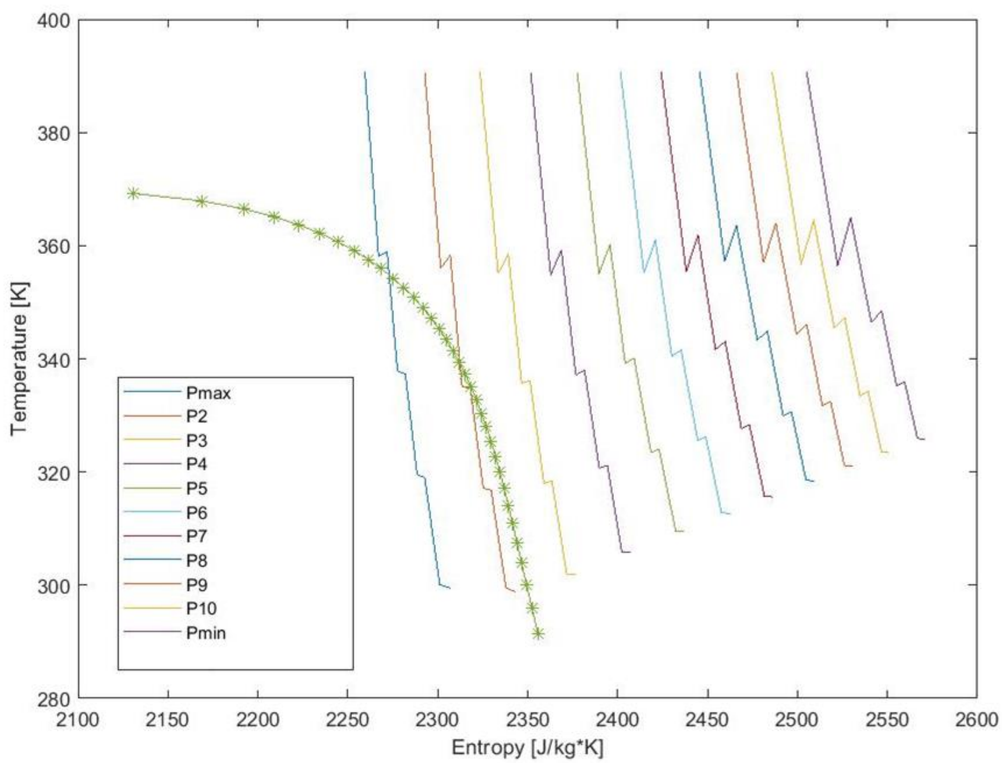


*Figure 8.3 – Diagram T-s from sensitivity analysis for inlet pressure*

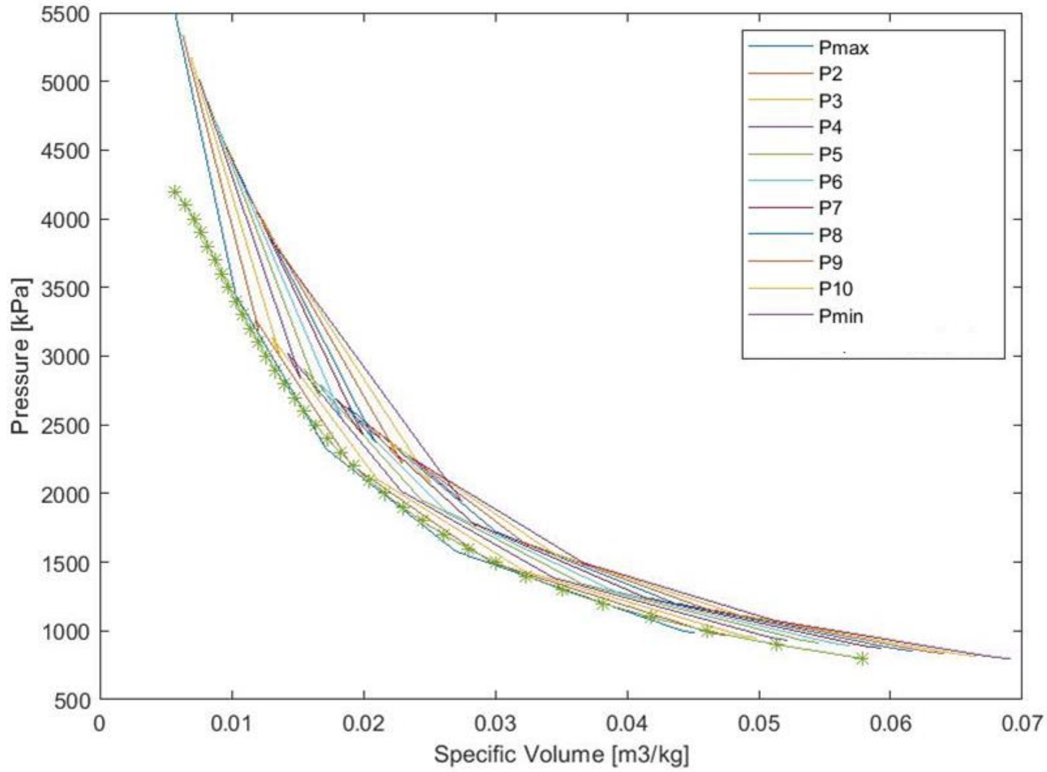


*Figure 8.4 – Diagram P-v from sensitivity analysis for inlet pressure*

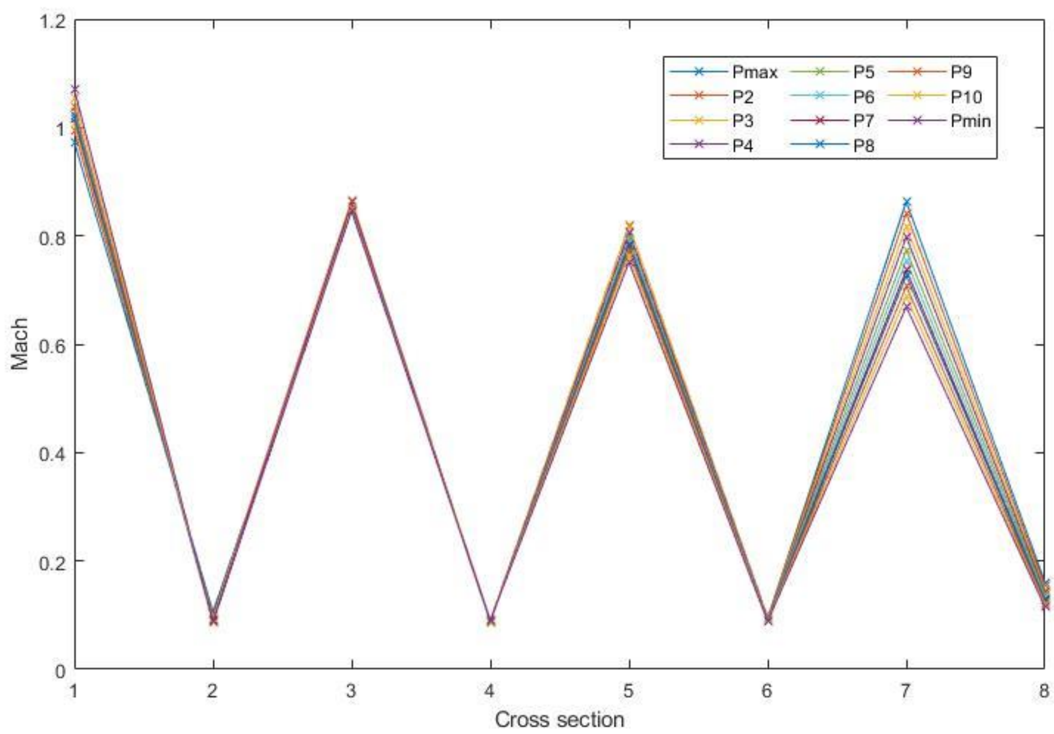


*Figure 8.5 - Mach number for the cross sections of the turbine for pressure sensitivity analysis*

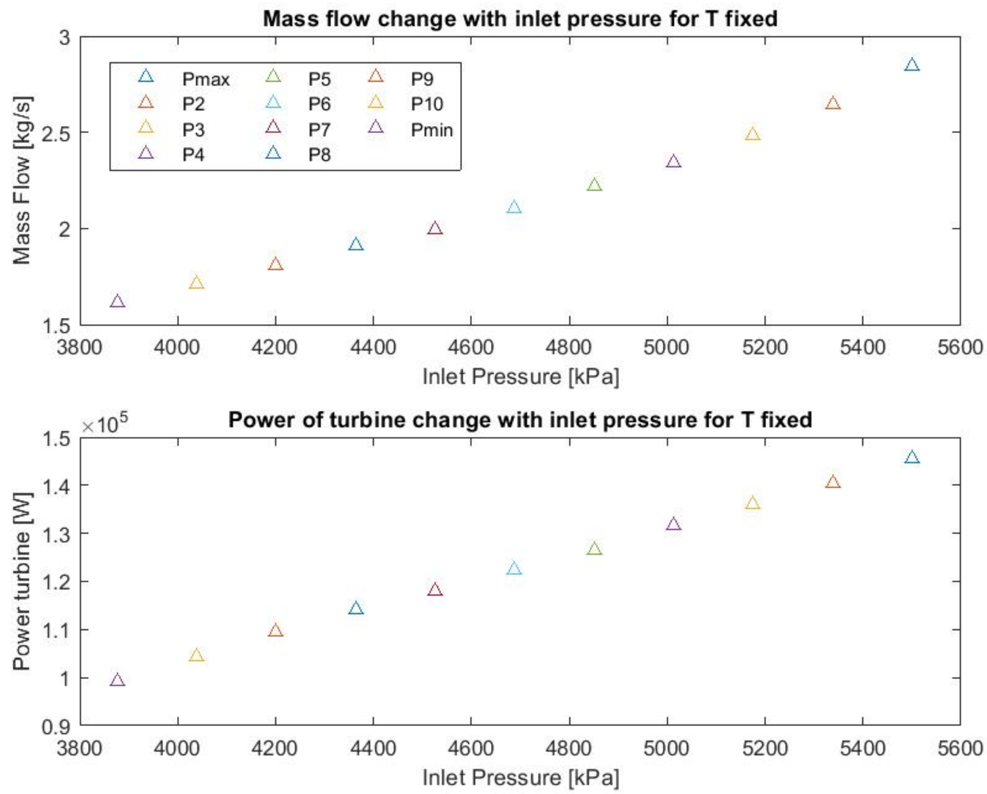


*Figure 8.6 – Power produced and mass flow from sensitivity analysis*

Figure 8.6 illustrates the correlation between power production and mass flow as a function of inlet pressure. It is important to note that the outlet pressure remains fixed at 1000 kPa. As the inlet pressure into the turbine increases, more mass flow passes through it, resulting in higher power production. However, this flow can only increase until the maximum speed inside the turbine reaches the speed of sound, in the Figure 8.5 is presented the comparison between the fluid velocity and the sound of the speed for the different cross sections. It can be noticed that for the inlet pressure of 5013 kPa until 3876 kPa the velocity of the fluid is slightly higher than the sound speed, therefore it is not possible to fulfil the requirement of subsonic flow.

On the other hand, it is observed that the turbine generation efficiency is not significantly affected by changes in the inlet pressure.

By keeping the inlet temperature constant and only decreasing the pressure, the fluid's density decreases and its state shifts from the supercritical phase to the superheated zone. Only in the initial stages, where the initial pressure is higher, does the fluid enter the turbomachine in the two-phase zone with a high value for the quality. Based on the above, the correlations used to calculate the losses are valid, and the results can be considered reasonable.

All calculated values for each of the turbine cross-sections for the inlet pressure sensitivity analysis are detailed in Tables 11.13 - 11.23 of the Appendix.

## 8.2. Sensitivity analysis for inlet Temperature

As a second part of the sensitivity analysis, the pressure value is set and the temperature of the fluid inlet to the turbine is varied, starting from the design temperature of Tmax = 390.6 K to the temperature of Tmin = 365.0 K, which corresponds to the minimum temperature calculated from data measured for the day 08.11.2021.

As in the previous case, it is important to check the quality of the fluid for the different inlet temperatures. In Figure 8.6, it can be observed that only the two cases with the highest temperature present a quality above X>0.8, thus fulfilling the hypotheses of the loss correlations. The case of the third temperature is close to this quality, so it could be considered that its results may be correct. However, from the fourth inlet temperature, the quality values are much lower and even from the sixth case, the fluid at the turbine inlet is in a liquid state, therefore, the loss correlations for these conditions are not valid.

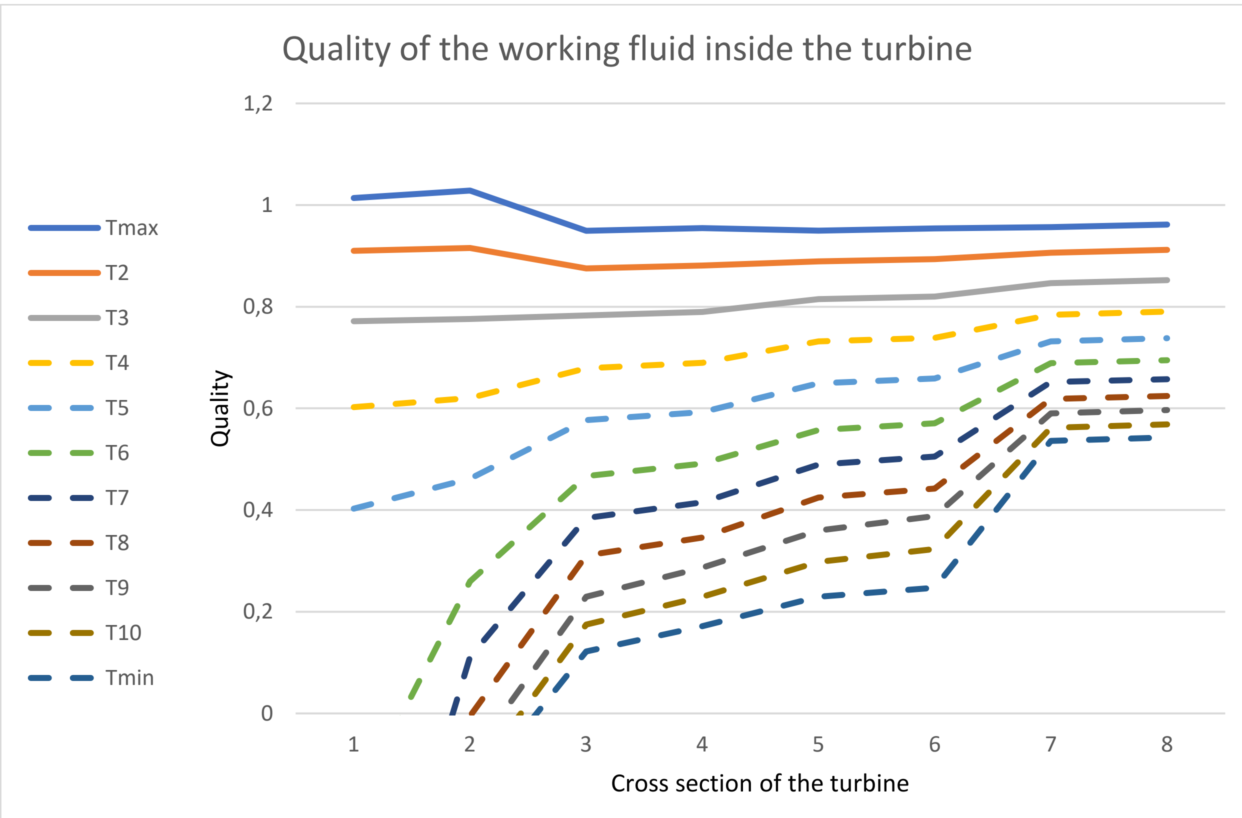


***Figure 8.7 - Quality distribution per cross section of the turbine for Temperature sensitivity analysis. Values below X<0.8 are presented as dashed lines.***

In Figure 8.8 and Figure 8.9, it can be seen that, although the inlet temperature decreases, in the first instance, the inlet conditions to the initial stage of the turbine are closer to the critical point of the fluid. From the second stage, the two-phase zone is reached, but contrary to the calculations for the high values of the inlet temperature, these have a higher liquid content, resulting in lower qualities. If the temperature continues to drop, the first stage reaches the liquid phase due to the high pressure at which it operates.

Although the correlations for grades below 0.8 are not valid and the calculated results may not correctly represent the turbine behavior, it can be observed in simulations close to the liquid phase that, as might be expected for these cases, expansion occurs mainly in the final stages of the turbine, where there is a higher percentage of steam. This shows that the calculation method is robust and can yield results even under these conditions, and can converge with reasonable results.

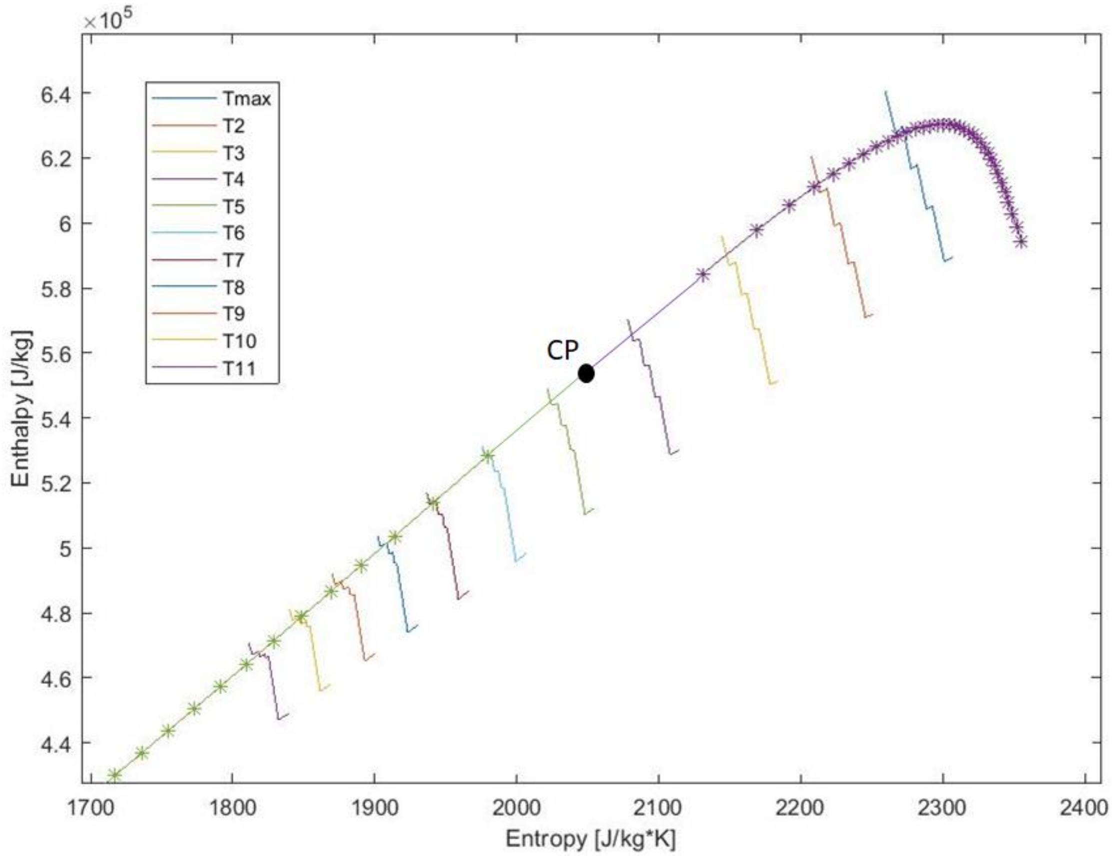


*Figure 8.8 - Diagram h-s from sensitivity analysis for inlet Temperature*

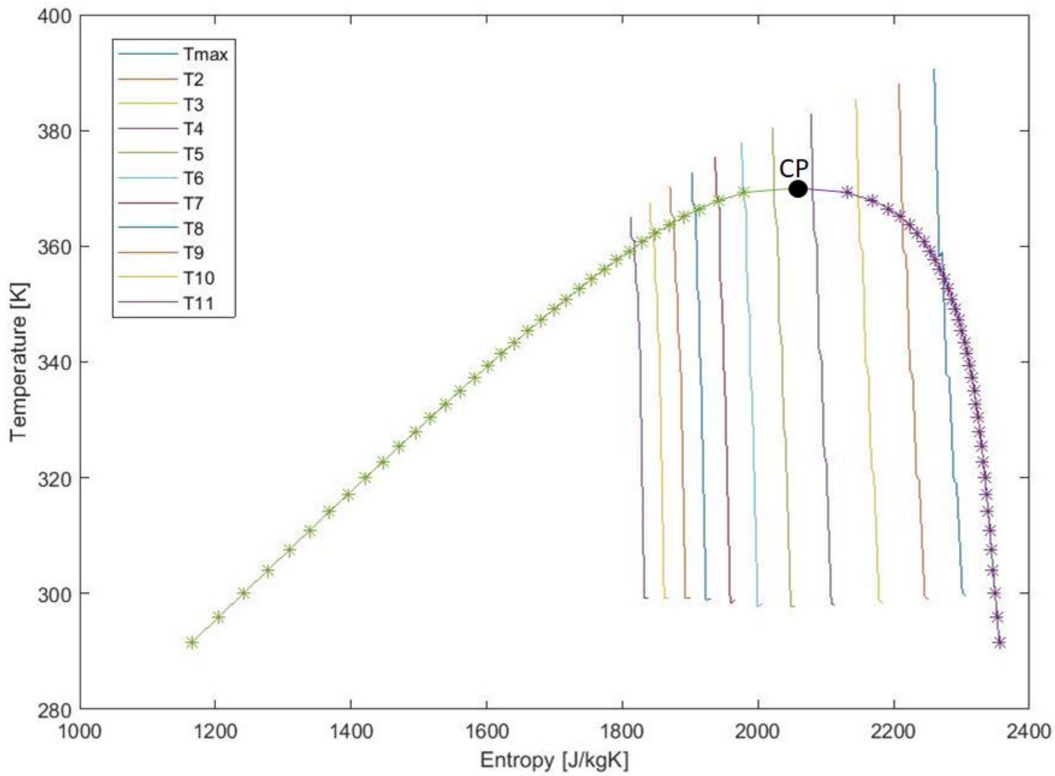


*Figure 8.9 - Diagram T-s from sensitivity analysis for inlet Temperature*

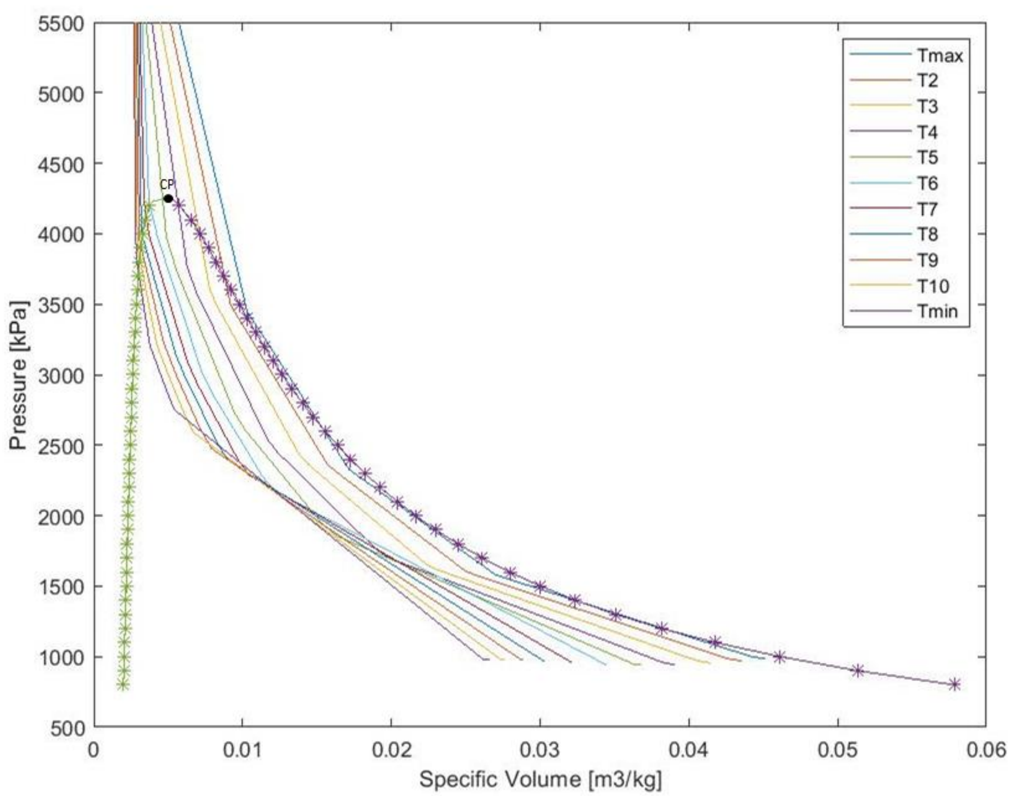


*Figure 8.10 - Diagram P-v from sensitivity analysis for inlet Temperature*

The high mass flow values are a result of the high pressure at the inlet, which increases the fluid density as temperature decreases, thereby causing an increase in mass flow, in contrast to changes in inlet pressure. However, this increased liquid content also results in a decrease in power output from the turbine as shown in the Figure 8.11, since the fluid expansion only occurs in the final stages of the turbine as in the Figures 8.8 and 8.9.

In the Figure 8.12 are presented the velocities for each cross section, it can be noticed that the fluid stays subsonic for all of the stages, having an increment in the velocity in the last stages, it can be explained because in the last stages, the content of liquid will be lower.

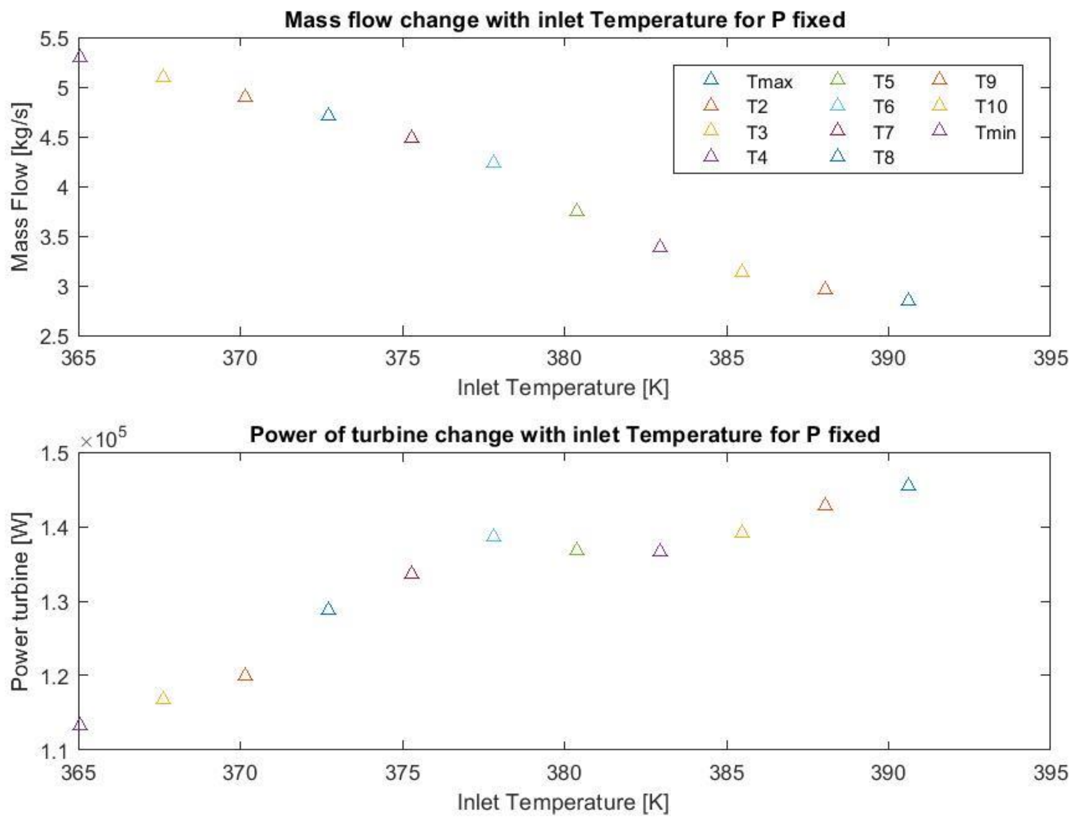


*Figure 8.11 - Power produced and mass flow from sensitivity analysis*

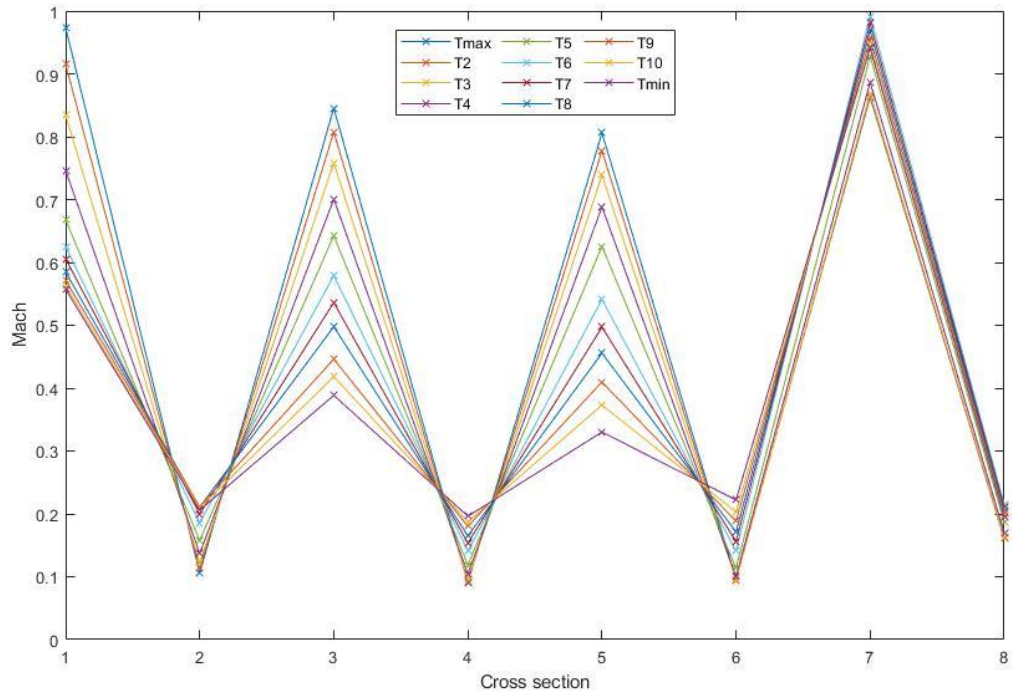


*Figure 8.12 - Mach number for the cross sections of the turbine for temperature sensitivity analysis*

Tables 11.24-11.34 in the appendix detail all the calculated values for each of the cross sections of the turbine for temperature sensitivity analysis.

# 9. Conclusions

The mean line analysis used to study the behavior of the ORC Turbine present in the MONIKA facility yielded various results considering geometric conditions, turbine inlet and outlet pressures, and inlet temperature as input data. The analysis involved iterating the calculated mass flow and feeding back the initial pressure distribution until this mass flow converged.

The process of verification for the method was made by comparing it with the design data provided by the manufacturer. The errors were approximately 1% for power produced and 2% for mass flow. These errors may have arisen due to the correlation used to calculate the labyrinth mass flow by the seals in the vane stages of the turbine, as well as the correlations considered to quantify the losses due to ventilation, filling and emptying losses, and the efficiency of the blades and vanes. Additionally, other types of losses were not considered in this analysis. Despite these factors, the error of only about 1% is considered acceptable.

The calculation method was also validated by comparison with measured data, and the difference between both of them was only in the range of 5% to 8% for power and mass flow rate. This difference may have been due to manufacturing inaccuracies, the precision of the geometrical characteristics, accuracy of the measuring instruments in the experimental data, and the nitrogen concentration present in the working fluid. The results obtained for different working conditions can be considered valid, considering the above factors.

The sensitivity analysis showed the turbine behavior if the input variables were modified. For superheated or supercritical fluid conditions, it was observed that the turbine power is proportional to the mass flow of it, maintaining a stable efficiency for these conditions. When entering the two-phase zone, this behavior is maintained when the fluid quality is greater than $X>0.8$.

When the quality of the fluid decreases, it was observed that although the mass flow increases, the power produced by the turbomachine decreases, a reason of it is that the expansion occurs in the last stages of the turbine in which the quality of the fluid increases. However, these results are not significant since being in qualities lower than $X<0.8$, the correlations of losses are no longer in their range of validity. These results only show that the calculation method is robust and can calculate various operating points. If it is wanted to validate the calculation under conditions where there are high amounts of liquid, it is necessary to replace the correlations used with others that contemplate the high presence of liquid in the working fluid.

During all the calculation stages, an important factor was the obtaining of the thermodynamic properties of the fluid, a good database can allow greater maneuverability when setting operating points.

To conclude, the approach used in the mean line analysis showed that it is possible to determine the properties of the fluid inside the existing turbine from its geometric characteristics and thermodynamic properties at the inlet and outlet of the turbomachine, being possible to verify and validate this method for the ORC Turbine of the MONIKA facility, and thus predict its operation under different load conditions.

A better approximation in the calculation can be made using a CFD analysis. The results of these calculations then replace the previously used loss correlations in the mean line analysis for each of the load cases.

# 10. References


[1] P. Colonna, E. Casati, C. Trapp, T. Mathijssen, J. Larjola, T. Turunen-Saaresti and A. Uusitalo, "Organic Rankine Cycle Power Systems: From the Concept to Current Technology, Application, and an Outlook to the Future," vol. 137, no. 10, pp. 100801-1-100801-19, 2015.

[2] H. Gao, C. Liu, C. He, X. Xu, S. Wu and Y. Li, "Performance Analysis and Working Fluid Selection of a Supercritical Organic Rankine Cycle for Low Grade Waste Heat Recovery ISSN 1996-1073," MDPI, Basel, 2012.

[3] Y. Chen, P. Lundqvist, A. Johansson and P. Platell, "A comparative study of the carbon dioxide transcritical power cycle compared with an organic Rankine cycle with R123 as working fluid in waste heat recovery.," *Applied Thermal Engineering,* vol. 26, no. 17-18, pp. 2142-2147, 2006.

[4] A. Schuster, S. Karellas and R. Aumann, "Efficiency optimization potential in supercritical Organic Rankine Cycles ISSN 0360-5442," Energy, Volume 35, Issue 2, Pages 1033-1039., 2010.

[5] D. Kuhn, "Modular Low Temperature Cycle Karlsruhe (MONIKA).," 14 November 2022. [Online]. Available: https://www.monika.kit.edu/english/.

[6] J. M. Perez, "Experimental examination of the MONIKA-ORC-Turbine and comparison of the results with thermodynamical calculation," Master Thesis, ITES, Karlsruhe Institut für Technologie, Karlsruhe, 2022.

[7] Edited By Ennio Macchi, Marco Astolfi, Organic Rankine Cycle (ORC) Power Systems Technologies and Applications ISBN: 978-0-08-100510-1, Elsevier, 2017.

[8] M. TURBINE-TECHNIK, "Turbinenanlage Propanexpander: Project 1 15 3514 0 2018.".

[9] E. Dick, Fundamentals of Turbomachines ISBN 978-94-017-9627-9, Dordrecht: Springer, 2015.

[10] S. L. Dixon, Fluid Mechanics, Thermodynamics of Turbomachinery ISBN 0 7506 7059 2, Oxford, UK: Butterworth-Heinemann, 1998.

[11] W. Traupel, Thermische Turbomaschinen Thermodynamisch-strömungstechnische Berechnung, ISBN : 978-3-642-62102-4, Verlag Berlin Heidelberg: Springer, 2001.

[12] W. Wagner, O. Kunz, R. Klimeck and M. Jaeschke, Wide-Range Equation of State for Natural Gases and Other Mixtures, ISBN 978-3-18-355706-6, Düsseldorf: GERG, 2007.

[13] H. Müller-Steinhagen and K. Heck, "A Simple Friction Pressure Drop Correlation for Two-Phase Flow in Pipes," Chemical Engineering and Processing: Process Intensification , 20, 297 - 308., 1986.

[14] T. Schulenberg, *Private conversations,* Karlsruhe, 2023.

[15] H. K. Müller and B. S. Nau, "www.fachwissen-dichtungstechnik.de," 2003. [Online]. Available: http://www.fachwissen-dichtungstechnik.de/Kapitelseiten/Kapitel17.html. [Accessed 12 January 2023].

[16] A.Berger, T. Polklas, O.Brunn and F. Joos, "Experimental investigation on performance of a control stage turbine under partial admission Paper ID ETC2019-135," Helmut Schmidt University, Hamburg, 2019.

[17] J. D. Hoffman, Numerical Methods for engineers and Scientists, Second Edition. ISBN: 0-8247-0443-6, New York: McGraw-Hill, 2001.

[18] S. a. d. Wiesche, L. Hake and P. Cinnella, EXPERIMENTAL AND NUMERICAL ASSESSMENT OF AN ASYMPTOTICALLY CORRECT CHOKING MACH NUMBER EXPRESSION FOR ORGANIC VAPOR FLOWS THROUGH TURBINE CASCADES, Paper ID: 83, Munich: 6th International Seminar on ORC Power Systems, 2021.

[19] L. J. Gardella, "Analysis and evaluation of MoNiKa’s first results in baypass configuration. Master Thesis," Master Thesis, ITES, Karlsruhe Institut für Technologie, Karlsruhe, 2019.

# 11. Appendix

## 11.1. Tables

| Day | Time | | Mass flow [kg/s] | | Temperature [K] | | | | Pressure [kPa] | | | |
|---|---|---|---|---|---|---|---|---|---|---|---|---|
| | | Min. of Running | 2 | 0p | Amb. Temp. | 2p | 1p | 0p | 2p | 1p | 0p | 4 |
| | | | Pumps | Turbine | | TS10-02 | TI10-03 | FI10-02 | PS10-02 | PI10-03 | PS10-03 | PI10-12 |
| 08.11.21 | 4th Running Steady State | Average | 2.20 | 2.20 | 283.25 | 381.31 | 369.73 | 369.43 | 5189.73 | 4321.12 | 4293.20 | 1035.19 |
| | 6th Running Steady State | Average | 1.90 | 1.90 | 283.62 | 383.07 | 364.56 | 364.29 | 5190.44 | 3916.59 | 3861.76 | 1039.66 |
| 09.11.21 | 3rd Running Steady State | Average | 2.60 | 2.60 | 282.67 | 383.56 | 375.30 | 374.88 | 5627.10 | 4818.46 | 4770.78 | 1115.65 |
| | 4th Running Steady State | Average | 2.60 | 2.60 | 283.01 | 382.50 | 375.41 | 375.08 | 5499.28 | 4824.35 | 4778.64 | 1117.04 |
| | 5th Running Steady State | Average | 2.60 | 2.60 | 283.32 | 382.07 | 375.67 | 375.38 | 5427.74 | 4837.38 | 4791.35 | 1120.02 |
| | 6th Running Steady State | Average | 2.60 | 2.60 | 283.66 | 380.77 | 375.58 | 375.31 | 5295.31 | 4830.88 | 4785.85 | 1121.49 |
| | 7th Running Steady State | Average | 2.60 | 2.60 | 283.80 | 379.93 | 375.91 | 375.64 | 5196.88 | 4851.64 | 4805.34 | 1123.68 |
| | 8th Running Steady State | Average | 2.60 | 2.60 | 283.74 | 379.15 | 375.84 | 375.60 | 5130.97 | 4849.48 | 4804.23 | 1124.41 |
| | 9th Running Steady State | Average | 2.68 | 2.68 | 283.77 | 379.89 | 376.72 | 376.47 | 5219.93 | 4935.01 | 4889.78 | 1128.61 |

*Table 11.1 – Measured data*

| Day | Time | | Valve | | Power [kW] | | Enthalpy [J/kg] | | | Entropy [J/kgK] | | Efficiency |
|---|---|---|---|---|---|---|---|---|---|---|---|---|
| | | Min. of Running | 3-3' | 3-3' | 0p-4 | 0p-4 | 2p | 1p | 4 | 0p | 4 | 0p-4 |
| | | | ByPass [%] | CV [%] | Power Grid | Power Turb. | H | H-Hloss | H | S | S | η |
| 08.11.21 | 4th Running Steady State | Average | 0.00 | 16.70 | 90.09 | 96.02 | 579683.27 | 579533.54 | 528966.53 | 2116.58 | 2116.58 | 0.86 |
| | 6th Running Steady State | Average | 0.00 | 14.60 | 78.49 | 83.66 | 601921.63 | 601744.88 | 549568.37 | 2184.44 | 2184.44 | 0.84 |
| 09.11.21 | 3rd Running Steady State | Average | 0.00 | 17.00 | 95.85 | 102.16 | 563768.65 | 566776.25 | 519431.38 | 2001.30 | 2001.30 | 0.83 |
| | 4th Running Steady State | Average | 0.00 | 18.30 | 96.29 | 102.63 | 561934.00 | 565111.21 | 518094.65 | 2005.58 | 2005.58 | 0.84 |
| | 5th Running Steady State | Average | 0.00 | 19.50 | 97.05 | 103.44 | 562537.75 | 565905.05 | 518787.12 | 2012.33 | 2012.33 | 0.84 |
| | 6th Running Steady State | Average | 0.00 | 22.20 | 96.70 | 103.07 | 559167.35 | 562724.62 | 516272.96 | 2011.46 | 2011.46 | 0.85 |
| | 7th Running Steady State | Average | 0.00 | 27.80 | 97.40 | 103.81 | 558031.25 | 561852.53 | 515567.89 | 2017.54 | 2017.54 | 0.86 |
| | 8th Running Steady State | Average | 0.00 | 71.94 | 97.22 | 103.62 | 555033.22 | 558908.88 | 513212.04 | 2016.20 | 2016.20 | 0.87 |
| | 9th Running Steady State | Average | 0.00 | 97.83 | 97.95 | 104.40 | 555982.27 | 559603.73 | 513619.04 | 2022.65 | 2022.65 | 0.85 |

*Table 11.2 – Measured data*

| Cross Section | Enthalpy $[J/kg]$ | Entropy $[J/kgK]$ | Pressure $[kPa]$ | Density $[kg/m^3]$ | Specific Volume $[m^3/kg]$ | Quality | Performance | Mass Flow $[kg/s]$ |
|---|---|---|---|---|---|---|---|---|
| 0 | 640520.18 | 2259.50 | 5500.00 | 175.01 | 0.01 | 1.00 | 0.00 | 0.00 |
| 1 | 627527.77 | 2267.04 | 3410.57 | 96.24 | 0.01 | 1.01 | 0.83 | 2.84 |
| 2 | 629496.32 | 2271.78 | 3436.48 | 96.28 | 0.01 | 1.03 | 0.74 | 2.84 |
| 3 | 616912.32 | 2277.52 | 2339.31 | 58.60 | 0.02 | 0.95 | 0.87 | 2.84 |
| 4 | 617880.04 | 2281.91 | 2309.43 | 57.39 | 0.02 | 0.95 | 0.74 | 2.84 |
| 5 | 604903.83 | 2288.11 | 1608.99 | 37.76 | 0.03 | 0.95 | 0.87 | 2.84 |
| 6 | 605642.95 | 2292.21 | 1587.50 | 37.05 | 0.03 | 0.95 | 0.74 | 2.84 |
| 7 | 591737.30 | 2298.83 | 1100.00 | 24.99 | 0.04 | 0.96 | 0.87 | 2.84 |
| 8 | 592048.88 | 2303.79 | 1070.65 | 24.19 | 0.04 | 0.96 | 0.74 | 2.84 |

*Table 11.3 – Results for calculation under design conditions*

| Cross Section | Enthalpy $[J/kg]$ | Entropy $[J/kgK]$ | Pressure $[kPa]$ | Density $[kg/m^3]$ | Specific Volume $[m^3/kg]$ | Quality | Performance | Mass Flow $[kg/s]$ | Temperature $[K]$ |
|---|---|---|---|---|---|---|---|---|---|
| 0 | 623159.90 | 2322.47 | 4288.47 | 126.85 | 0.01 | 0.00 | 0.00 | 0.00 | 369.22 |
| 1 | 606561.70 | 2332.65 | 2480.30 | 62.36 | 0.02 | 0.92 | 0.83 | 2.08 | 338.85 |
| 2 | 610185.07 | 2338.44 | 2585.74 | 65.07 | 0.02 | 0.93 | 0.74 | 2.08 | 340.92 |
| 3 | 597053.26 | 2345.20 | 1779.46 | 42.05 | 0.02 | 0.93 | 0.86 | 2.08 | 323.14 |
| 4 | 598162.53 | 2349.87 | 1762.88 | 41.41 | 0.02 | 0.93 | 0.74 | 2.08 | 322.73 |
| 5 | 587196.81 | 2355.41 | 1313.09 | 30.06 | 0.03 | 0.94 | 0.86 | 2.08 | 309.85 |
| 6 | 587448.31 | 2359.19 | 1285.84 | 29.30 | 0.03 | 0.94 | 0.74 | 2.08 | 308.97 |
| 7 | 579005.79 | 2362.87 | 1035.19 | 23.39 | 0.04 | 0.94 | 0.88 | 2.08 | 300.14 |
| 8 | 578276.55 | 2366.09 | 996.37 | 22.44 | 0.04 | 0.94 | 0.75 | 2.08 | 298.64 |

*Table 11.4 – Results calculation 08.11.2021 4th Running*

| Cross Section | Enthalpy $[J/kg]$ | Entropy $[J/kgK]$ | Pressure $[kPa]$ | Density $[kg/m^3]$ | Specific Volume $[m^3/kg]$ | Quality | Performance | Mass Flow $[kg/s]$ | Temperature $[K]$ |
|---|---|---|---|---|---|---|---|---|---|
| 0 | 634859.46 | 2364.15 | 3876.54 | 103.39 | 0.01 | 0.00 | 0.00 | 0.00 | 365.07 |
| 1 | 616411.73 | 2375.64 | 2218.16 | 52.04 | 0.02 | 0.97 | 0.83 | 1.83 | 333.52 |
| 2 | 620935.71 | 2381.85 | 2349.12 | 55.19 | 0.02 | 0.99 | 0.73 | 1.83 | 336.31 |
| 3 | 607705.23 | 2389.03 | 1644.19 | 36.88 | 0.03 | 0.98 | 0.85 | 1.83 | 319.66 |
| 4 | 608842.56 | 2393.76 | 1630.55 | 36.38 | 0.03 | 0.98 | 0.74 | 1.83 | 319.29 |
| 5 | 598841.81 | 2398.86 | 1261.67 | 27.69 | 0.04 | 0.98 | 0.86 | 1.83 | 308.24 |
| 6 | 598889.89 | 2402.43 | 1232.96 | 26.95 | 0.04 | 0.98 | 0.75 | 1.83 | 307.28 |
| 7 | 591947.33 | 2405.32 | 1039.66 | 22.63 | 0.04 | 0.98 | 0.89 | 1.83 | 300.37 |
| 8 | 591081.98 | 2408.03 | 1002.41 | 21.77 | 0.05 | 0.98 | 0.76 | 1.83 | 298.93 |

*Table 11.5– Results calculation 08.11.2021 6th Running*

| Cross Section | Enthalpy $[J/kg]$ | Entropy $[J/kgK]$ | Pressure $[kPa]$ | Density $[kg/m^3]$ | Specific Volume $[m^3/kg]$ | Quality | Performance | Mass Flow $[kg/s]$ | Temperature $[K]$ |
|---|---|---|---|---|---|---|---|---|---|
| 0 | 606420.84 | 2268.01 | 4793.05 | 162.98 | 0.01 | 0.00 | 0.00 | 0.00 | 374.31 |
| 1 | 592698.66 | 2276.26 | 2864.55 | 80.24 | 0.01 | 0.85 | 0.83 | 2.44 | 345.85 |
| 2 | 595003.28 | 2281.35 | 2908.52 | 81.23 | 0.01 | 0.85 | 0.74 | 2.44 | 346.64 |
| 3 | 583055.79 | 2287.03 | 2010.07 | 51.53 | 0.02 | 0.86 | 0.86 | 2.44 | 328.64 |
| 4 | 583872.20 | 2291.45 | 1977.87 | 50.31 | 0.02 | 0.87 | 0.74 | 2.44 | 327.89 |
| 5 | 573161.30 | 2296.50 | 1455.02 | 35.57 | 0.03 | 0.88 | 0.87 | 2.44 | 314.13 |
| 6 | 573355.89 | 2300.17 | 1421.46 | 34.55 | 0.03 | 0.88 | 0.74 | 2.44 | 313.13 |
| 7 | 564463.05 | 2303.96 | 1115.65 | 26.67 | 0.04 | 0.89 | 0.89 | 2.44 | 303.06 |
| 8 | 563790.86 | 2307.30 | 1071.74 | 25.50 | 0.04 | 0.89 | 0.75 | 2.44 | 301.45 |

*Table 11.6– Results calculation 09.11.2021 3rd Running*

| Cross Section | Enthalpy $[J/kg]$ | Entropy $[J/kgK]$ | Pressure $[kPa]$ | Density $[kg/m^3]$ | Specific Volume $[m^3/kg]$ | Quality | Performance | Mass Flow $[kg/s]$ | Temperature $[K]$ |
|---|---|---|---|---|---|---|---|---|---|
| 0 | 608484.08 | 2273.43 | 4798.66 | 161.22 | 0.01 | 0.00 | 0.00 | 0.00 | 374.60 |
| 1 | 594592.39 | 2281.79 | 2863.44 | 79.58 | 0.01 | 0.85 | 0.83 | 2.43 | 345.85 |
| 2 | 596970.29 | 2286.92 | 2911.51 | 80.70 | 0.01 | 0.86 | 0.74 | 2.43 | 346.71 |
| 3 | 584919.40 | 2292.67 | 2010.68 | 51.20 | 0.02 | 0.87 | 0.86 | 2.43 | 328.66 |
| 4 | 585760.31 | 2297.10 | 1979.64 | 50.03 | 0.02 | 0.87 | 0.74 | 2.43 | 327.95 |
| 5 | 574979.97 | 2302.21 | 1455.94 | 35.38 | 0.03 | 0.88 | 0.87 | 2.43 | 314.17 |
| 6 | 575189.67 | 2305.90 | 1422.91 | 34.38 | 0.03 | 0.89 | 0.74 | 2.43 | 313.19 |
| 7 | 566258.12 | 2309.71 | 1117.04 | 26.55 | 0.04 | 0.89 | 0.89 | 2.43 | 303.12 |
| 8 | 565591.10 | 2313.07 | 1073.35 | 25.40 | 0.04 | 0.90 | 0.75 | 2.43 | 301.52 |

*Table 11.7– Results calculation 09.11.2021 4th Running*

| Cross Section | Enthalpy $[J/kg]$ | Entropy $[J/kgK]$ | Pressure $[kPa]$ | Density $[kg/m^3]$ | Specific Volume $[m^3/kg]$ | Quality | Performance | Mass Flow $[kg/s]$ | Temperature $[K]$ |
|---|---|---|---|---|---|---|---|---|---|
| 0 | 611477.69 | 2281.20 | 4811.32 | 158.93 | 0.01 | 0.00 | 0.00 | 0.00 | 375.10 |
| 1 | 597339.56 | 2289.71 | 2863.88 | 78.72 | 0.01 | 0.87 | 0.83 | 2.42 | 345.89 |
| 2 | 599826.26 | 2294.89 | 2918.64 | 80.06 | 0.01 | 0.88 | 0.74 | 2.42 | 346.87 |
| 3 | 587630.40 | 2300.74 | 2013.56 | 50.80 | 0.02 | 0.88 | 0.86 | 2.42 | 328.75 |
| 4 | 588505.97 | 2305.19 | 1984.12 | 49.69 | 0.02 | 0.88 | 0.74 | 2.42 | 328.07 |
| 5 | 577626.61 | 2310.39 | 1458.66 | 35.15 | 0.03 | 0.89 | 0.87 | 2.42 | 314.26 |
| 6 | 577858.09 | 2314.10 | 1426.33 | 34.18 | 0.03 | 0.90 | 0.74 | 2.42 | 313.30 |
| 7 | 568869.32 | 2317.95 | 1120.02 | 26.42 | 0.04 | 0.90 | 0.88 | 2.42 | 303.24 |
| 8 | 568210.01 | 2321.33 | 1076.59 | 25.28 | 0.04 | 0.90 | 0.75 | 2.42 | 301.65 |

*Table 11.8– Results calculation 09.11.2021 5th Running*

| Cross Section | Enthalpy $[J/kg]$ | Entropy $[J/kgK]$ | Pressure $[kPa]$ | Density $[kg/m^3]$ | Specific Volume $[m^3/kg]$ | Quality | Performance | Mass Flow $[kg/s]$ | Temperature $[K]$ |
|---|---|---|---|---|---|---|---|---|---|
| 0 | 612920.59 | 2285.16 | 4804.55 | 157.29 | 0.01 | 0.00 | 0.00 | 0.00 | 375.17 |
| 1 | 598635.25 | 2293.76 | 2855.66 | 77.99 | 0.01 | 0.87 | 0.83 | 2.42 | 345.76 |
| 2 | 601187.16 | 2298.97 | 2914.22 | 79.45 | 0.01 | 0.88 | 0.74 | 2.42 | 346.80 |
| 3 | 588922.31 | 2304.88 | 2010.13 | 50.45 | 0.02 | 0.88 | 0.86 | 2.42 | 328.68 |
| 4 | 589814.54 | 2309.34 | 1981.55 | 49.37 | 0.02 | 0.89 | 0.74 | 2.42 | 328.02 |
| 5 | 578916.38 | 2314.56 | 1457.90 | 34.98 | 0.03 | 0.90 | 0.87 | 2.42 | 314.25 |
| 6 | 579152.04 | 2318.27 | 1425.83 | 34.02 | 0.03 | 0.90 | 0.74 | 2.42 | 313.30 |
| 7 | 570189.61 | 2322.12 | 1121.49 | 26.35 | 0.04 | 0.91 | 0.88 | 2.42 | 303.29 |
| 8 | 569526.71 | 2325.49 | 1078.15 | 25.22 | 0.04 | 0.91 | 0.75 | 2.42 | 301.72 |

***Table 11.9– Results calculation 09.11.2021 6$^{th}$ Running***

| Cross Section | Enthalpy $[J/kg]$ | Entropy $[J/kgK]$ | Pressure $[kPa]$ | Density $[kg/m^3]$ | Specific Volume $[m^3/kg]$ | Quality | Performance | Mass Flow $[kg/s]$ | Temperature $[K]$ |
|---|---|---|---|---|---|---|---|---|---|
| 0 | 615636.20 | 2292.04 | 4825.04 | 155.70 | 0.01 | 0.00 | 0.00 | 0.00 | 375.77 |
| 1 | 601146.60 | 2300.75 | 2862.71 | 77.49 | 0.01 | 0.88 | 0.83 | 2.42 | 345.91 |
| 2 | 603789.85 | 2306.01 | 2926.94 | 79.12 | 0.01 | 0.89 | 0.74 | 2.42 | 347.05 |
| 3 | 591391.26 | 2312.00 | 2016.47 | 50.21 | 0.02 | 0.89 | 0.86 | 2.42 | 328.85 |
| 4 | 592315.93 | 2316.49 | 1989.29 | 49.18 | 0.02 | 0.90 | 0.74 | 2.42 | 328.22 |
| 5 | 581299.50 | 2321.80 | 1461.66 | 34.81 | 0.03 | 0.90 | 0.87 | 2.42 | 314.37 |
| 6 | 581561.52 | 2325.54 | 1430.34 | 33.88 | 0.03 | 0.91 | 0.74 | 2.42 | 313.44 |
| 7 | 572496.38 | 2329.45 | 1123.68 | 26.22 | 0.04 | 0.91 | 0.88 | 2.42 | 303.38 |
| 8 | 571847.56 | 2332.85 | 1080.65 | 25.11 | 0.04 | 0.92 | 0.75 | 2.42 | 301.82 |

***Table 11.10– Results calculation 09.11.2021 7$^{th}$ Running***

| Cross Section | Enthalpy $[J/kg]$ | Entropy $[J/kgK]$ | Pressure $[kPa]$ | Density $[kg/m^3]$ | Specific Volume $[m^3/kg]$ | Quality | Performance | Mass Flow $[kg/s]$ | Temperature $[K]$ |
|---|---|---|---|---|---|---|---|---|---|
| 0 | 615677.55 | 2292.19 | 4822.86 | 155.57 | 0.01 | 0.00 | 0.00 | 0.00 | 375.74 |
| 1 | 601180.47 | 2300.91 | 2861.25 | 77.42 | 0.01 | 0.88 | 0.83 | 2.42 | 345.88 |
| 2 | 603827.02 | 2306.17 | 2925.64 | 79.06 | 0.01 | 0.89 | 0.74 | 2.42 | 347.03 |
| 3 | 591430.07 | 2312.16 | 2015.86 | 50.19 | 0.02 | 0.89 | 0.86 | 2.42 | 328.83 |
| 4 | 592354.35 | 2316.64 | 1988.68 | 49.16 | 0.02 | 0.90 | 0.74 | 2.42 | 328.21 |
| 5 | 581349.65 | 2321.95 | 1461.78 | 34.81 | 0.03 | 0.90 | 0.87 | 2.42 | 314.38 |
| 6 | 581609.04 | 2325.68 | 1430.41 | 33.88 | 0.03 | 0.91 | 0.74 | 2.42 | 313.45 |
| 7 | 572564.96 | 2329.58 | 1124.41 | 26.23 | 0.04 | 0.91 | 0.88 | 2.42 | 303.41 |
| 8 | 571913.21 | 2332.98 | 1081.34 | 25.12 | 0.04 | 0.92 | 0.75 | 2.42 | 301.84 |

*Table 11.11– Results calculation 09.11.2021 8th Running*

| Cross Section | Enthalpy $[J/kg]$ | Entropy $[J/kgK]$ | Pressure $[kPa]$ | Density $[kg/m^3]$ | Specific Volume $[m^3/kg]$ | Quality | Performance | Mass Flow $[kg/s]$ | Temperature $[K]$ |
|---|---|---|---|---|---|---|---|---|---|
| 0 | 612825.98 | 2283.16 | 4909.43 | 161.92 | 0.01 | 0.00 | 0.00 | 0.00 | 376.53 |
| 1 | 598798.53 | 2291.57 | 2928.76 | 80.79 | 0.01 | 0.87 | 0.83 | 2.48 | 347.03 |
| 2 | 601237.45 | 2296.71 | 2981.75 | 82.07 | 0.01 | 0.88 | 0.74 | 2.48 | 347.96 |
| 3 | 589009.68 | 2302.55 | 2053.87 | 51.86 | 0.02 | 0.88 | 0.86 | 2.48 | 329.69 |
| 4 | 589892.72 | 2306.99 | 2024.11 | 50.73 | 0.02 | 0.89 | 0.74 | 2.48 | 329.01 |
| 5 | 578840.73 | 2312.26 | 1480.74 | 35.65 | 0.03 | 0.89 | 0.87 | 2.48 | 314.92 |
| 6 | 579110.60 | 2316.00 | 1448.85 | 34.69 | 0.03 | 0.90 | 0.74 | 2.48 | 313.98 |
| 7 | 569820.76 | 2320.02 | 1128.61 | 26.57 | 0.04 | 0.90 | 0.88 | 2.48 | 303.55 |
| 8 | 569203.94 | 2323.49 | 1085.24 | 25.44 | 0.04 | 0.91 | 0.75 | 2.48 | 301.97 |

*Table 11.12– Results calculation 09.11.2021 9th Running*

| Cross Section | Enthalpy $[J/kg]$ | Entropy $[J/kgK]$ | Pressure $[kPa]$ | Density $[kg/m^3]$ | Specific Volume $[m^3/kg]$ | Quality | Performance | Mass Flow $[kg/s]$ | Temperature $[K]$ |
|---|---|---|---|---|---|---|---|---|---|
| 0 | 640520.18 | 2259.50 | 5500.00 | 175.01 | 0.01 | 0.00 | 0.00 | 0.00 | 390.60 |
| 1 | 627509.30 | 2267.05 | 3408.40 | 96.16 | 0.01 | 1.01 | 0.83 | 2.84 | 358.10 |
| 2 | 629484.43 | 2271.80 | 3434.75 | 96.22 | 0.01 | 1.03 | 0.74 | 2.84 | 358.94 |
| 3 | 616787.50 | 2277.60 | 2330.53 | 58.33 | 0.02 | 0.95 | 0.87 | 2.84 | 337.89 |
| 4 | 617782.97 | 2282.01 | 2302.05 | 57.17 | 0.02 | 0.95 | 0.74 | 2.84 | 337.27 |
| 5 | 604326.45 | 2288.48 | 1582.92 | 37.07 | 0.03 | 0.95 | 0.87 | 2.84 | 319.55 |
| 6 | 605192.91 | 2292.70 | 1565.27 | 36.46 | 0.03 | 0.95 | 0.74 | 2.84 | 319.04 |
| 7 | 588212.66 | 2301.08 | 1000.00 | 22.62 | 0.04 | 0.96 | 0.87 | 2.84 | 300.09 |
| 8 | 589346.92 | 2307.08 | 985.12 | 22.16 | 0.05 | 0.96 | 0.74 | 2.84 | 299.50 |

***Table 11.13 – Results for sensitivity analysis with inlet Pressure of 5500 kPa***

| Cross Section | Enthalpy $[J/kg]$ | Entropy $[J/kgK]$ | Pressure $[kPa]$ | Density $[kg/m^3]$ | Specific Volume $[m^3/kg]$ | Quality | Performance | Mass Flow $[kg/s]$ | Temperature $[K]$ |
|---|---|---|---|---|---|---|---|---|---|
| 0 | 652534.82 | 2292.75 | 5337.65 | 158.52 | 0.01 | 0.00 | 0.00 | 0.00 | 390.60 |
| 1 | 637320.30 | 2301.64 | 3182.29 | 82.76 | 0.01 | 1.05 | 0.83 | 2.65 | 356.00 |
| 2 | 640275.28 | 2306.89 | 3272.79 | 84.93 | 0.01 | 1.07 | 0.74 | 2.65 | 358.30 |
| 3 | 626553.63 | 2313.52 | 2202.35 | 52.25 | 0.02 | 0.99 | 0.86 | 2.65 | 335.09 |
| 4 | 627811.00 | 2318.11 | 2187.96 | 51.58 | 0.02 | 1.00 | 0.74 | 2.65 | 334.77 |
| 5 | 613701.95 | 2325.28 | 1500.31 | 33.70 | 0.03 | 0.99 | 0.86 | 2.65 | 317.15 |
| 6 | 614748.01 | 2329.66 | 1488.82 | 33.28 | 0.03 | 0.99 | 0.74 | 2.65 | 316.81 |
| 7 | 598582.83 | 2337.92 | 985.12 | 21.57 | 0.05 | 0.99 | 0.87 | 2.65 | 299.50 |
| 8 | 599489.69 | 2343.67 | 967.74 | 21.08 | 0.05 | 0.99 | 0.74 | 2.65 | 298.79 |

***Table 11.14 – Results for sensitivity analysis with inlet Pressure of 5337 kPa***

| Cross Section | Enthalpy $[J/kg]$ | Entropy $[J/kgK]$ | Pressure $[kPa]$ | Density $[kg/m^3]$ | Specific Volume $[m^3/kg]$ | Quality | Performance | Mass Flow $[kg/s]$ | Temperature $[K]$ |
|---|---|---|---|---|---|---|---|---|---|
| 0 | 663467.50 | 2323.49 | 5175.31 | 144.33 | 0.01 | 0.00 | 0.00 | 0.00 | 390.60 |
| 1 | 646270.15 | 2333.57 | 2995.87 | 73.01 | 0.01 | 1.08 | 0.83 | 2.48 | 355.08 |
| 2 | 650177.44 | 2339.18 | 3138.25 | 76.55 | 0.01 | 1.11 | 0.73 | 2.48 | 358.55 |
| 3 | 635473.29 | 2346.58 | 2094.96 | 47.36 | 0.02 | 1.03 | 0.86 | 2.48 | 335.67 |
| 4 | 636982.25 | 2351.23 | 2092.44 | 47.03 | 0.02 | 1.04 | 0.74 | 2.48 | 336.18 |
| 5 | 622335.93 | 2359.01 | 1433.62 | 31.02 | 0.03 | 1.02 | 0.86 | 2.48 | 318.00 |
| 6 | 623534.31 | 2363.48 | 1426.70 | 30.72 | 0.03 | 1.03 | 0.74 | 2.48 | 318.39 |
| 7 | 607880.66 | 2371.64 | 967.74 | 20.55 | 0.05 | 1.02 | 0.86 | 2.48 | 301.98 |
| 8 | 608649.47 | 2377.18 | 949.37 | 20.06 | 0.05 | 1.02 | 0.74 | 2.48 | 301.98 |

***Table 11.15 – Results for sensitivity analysis with inlet Pressure of 5175 kPa***

| Cross Section | Enthalpy $[J/kg]$ | Entropy $[J/kgK]$ | Pressure $[kPa]$ | Density $[kg/m^3]$ | Specific Volume $[m^3/kg]$ | Quality | Performance | Mass Flow $[kg/s]$ | Temperature $[K]$ |
|---|---|---|---|---|---|---|---|---|---|
| 0 | 673289.86 | 2351.65 | 5012.96 | 132.17 | 0.01 | 0.00 | 0.00 | 0.00 | 390.60 |
| 1 | 654308.54 | 2362.79 | 2834.75 | 65.54 | 0.02 | 1.11 | 0.83 | 2.34 | 354.82 |
| 2 | 659113.27 | 2368.69 | 3017.32 | 69.95 | 0.01 | 1.15 | 0.73 | 2.34 | 359.22 |
| 3 | 643601.27 | 2376.76 | 2003.23 | 43.49 | 0.02 | 1.07 | 0.85 | 2.34 | 337.15 |
| 4 | 645386.29 | 2381.62 | 2009.40 | 43.40 | 0.02 | 1.07 | 0.74 | 2.34 | 337.95 |
| 5 | 630441.92 | 2389.78 | 1381.38 | 28.95 | 0.03 | 1.05 | 0.85 | 2.34 | 320.66 |
| 6 | 631726.49 | 2394.27 | 1377.63 | 28.73 | 0.03 | 1.06 | 0.74 | 2.34 | 321.16 |
| 7 | 616290.40 | 2402.33 | 949.37 | 19.62 | 0.05 | 1.05 | 0.86 | 2.35 | 305.81 |
| 8 | 617002.68 | 2407.73 | 931.13 | 19.15 | 0.05 | 1.05 | 0.74 | 2.35 | 305.81 |

***Table 11.16 – Results for sensitivity analysis with inlet Pressure of 5012 kPa***

| Cross Section | Enthalpy $[J/kg]$ | Entropy $[J/kgK]$ | Pressure $[kPa]$ | Density $[kg/m^3]$ | Specific Volume $[m^3/kg]$ | Quality | Performance | Mass Flow $[kg/s]$ | Temperature $[K]$ |
|---|---|---|---|---|---|---|---|---|---|
| 0 | 682129.20 | 2377.56 | 4850.61 | 121.64 | 0.01 | 0.00 | 0.00 | 0.00 | 390.60 |
| 1 | 661623.48 | 2389.59 | 2697.36 | 59.73 | 0.02 | 1.14 | 0.83 | 2.22 | 355.06 |
| 2 | 667224.88 | 2395.72 | 2909.06 | 64.63 | 0.02 | 1.18 | 0.73 | 2.22 | 360.16 |
| 3 | 651379.44 | 2404.17 | 1940.43 | 40.77 | 0.02 | 1.10 | 0.85 | 2.22 | 339.21 |
| 4 | 653289.18 | 2409.12 | 1949.76 | 40.76 | 0.02 | 1.10 | 0.74 | 2.22 | 340.13 |
| 5 | 638183.20 | 2418.56 | 1339.25 | 27.28 | 0.04 | 1.08 | 0.83 | 2.22 | 323.44 |
| 6 | 639513.00 | 2423.03 | 1336.02 | 27.10 | 0.04 | 1.08 | 0.74 | 2.22 | 324.00 |
| 7 | 624529.86 | 2432.20 | 931.13 | 18.75 | 0.05 | 1.07 | 0.84 | 2.22 | 309.61 |
| 8 | 625120.69 | 2437.40 | 912.25 | 18.30 | 0.05 | 1.08 | 0.74 | 2.22 | 309.57 |

*Table 11.17 – Results for sensitivity analysis with inlet Pressure of 4850 kPa*

| Cross Section | Enthalpy $[J/kg]$ | Entropy $[J/kgK]$ | Pressure $[kPa]$ | Density $[kg/m^3]$ | Specific Volume $[m^3/kg]$ | Quality | Performance | Mass Flow $[kg/s]$ | Temperature $[K]$ |
|---|---|---|---|---|---|---|---|---|---|
| 0 | 690140.92 | 2401.63 | 4688.27 | 112.42 | 0.01 | 0.00 | 0.00 | 0.00 | 390.60 |
| 1 | 668019.23 | 2414.60 | 2555.51 | 54.50 | 0.02 | 1.16 | 0.83 | 2.10 | 355.17 |
| 2 | 674498.44 | 2420.97 | 2795.29 | 59.83 | 0.02 | 1.21 | 0.73 | 2.10 | 360.99 |
| 3 | 657838.59 | 2430.09 | 1848.37 | 37.68 | 0.03 | 1.12 | 0.84 | 2.10 | 340.42 |
| 4 | 660046.26 | 2435.28 | 1864.97 | 37.84 | 0.03 | 1.13 | 0.74 | 2.10 | 341.60 |
| 5 | 644631.77 | 2444.51 | 1287.14 | 25.59 | 0.04 | 1.10 | 0.84 | 2.10 | 325.57 |
| 6 | 646049.39 | 2448.99 | 1286.03 | 25.47 | 0.04 | 1.11 | 0.74 | 2.10 | 326.22 |
| 7 | 631438.57 | 2457.70 | 912.25 | 18.00 | 0.06 | 1.10 | 0.84 | 2.10 | 312.77 |
| 8 | 631934.39 | 2462.73 | 893.08 | 17.56 | 0.06 | 1.10 | 0.74 | 2.10 | 312.69 |

*Table 11.18 – Results for sensitivity analysis with inlet Pressure of 4688 kPa*

| Cross Section | Enthalpy $[J/kg]$ | Entropy $[J/kgK]$ | Pressure $[kPa]$ | Density $[kg/m^3]$ | Specific Volume $[m^3/kg]$ | Quality | Performance | Mass Flow $[kg/s]$ | Temperature $[K]$ |
|---|---|---|---|---|---|---|---|---|---|
| 0 | 697464.58 | 2424.22 | 4525.92 | 104.22 | 0.01 | 0.00 | 0.00 | 0.00 | 390.60 |
| 1 | 673820.88 | 2438.08 | 2422.93 | 50.03 | 0.02 | 1.18 | 0.83 | 1.99 | 355.40 |
| 2 | 681152.48 | 2444.66 | 2685.30 | 55.64 | 0.02 | 1.23 | 0.73 | 1.99 | 361.83 |
| 3 | 663789.05 | 2454.38 | 1763.59 | 35.02 | 0.03 | 1.15 | 0.84 | 1.99 | 341.66 |
| 4 | 666257.81 | 2459.76 | 1785.71 | 35.30 | 0.03 | 1.15 | 0.74 | 1.99 | 343.05 |
| 5 | 650628.99 | 2468.80 | 1239.04 | 24.11 | 0.04 | 1.13 | 0.84 | 1.99 | 327.63 |
| 6 | 652108.39 | 2473.28 | 1239.30 | 24.03 | 0.04 | 1.13 | 0.74 | 1.99 | 328.33 |
| 7 | 637862.61 | 2481.60 | 893.08 | 17.29 | 0.06 | 1.12 | 0.84 | 1.99 | 315.70 |
| 8 | 638266.79 | 2486.48 | 873.70 | 16.86 | 0.06 | 1.12 | 0.74 | 1.99 | 315.59 |

***Table 11.19 – Results for sensitivity analysis with inlet Pressure of 4525 kPa***

| Cross Section | Enthalpy $[J/kg]$ | Entropy $[J/kgK]$ | Pressure $[kPa]$ | Density $[kg/m^3]$ | Specific Volume $[m^3/kg]$ | Quality | Performance | Mass Flow $[kg/s]$ | Temperature $[K]$ |
|---|---|---|---|---|---|---|---|---|---|
| 0 | 704214.73 | 2445.64 | 4363.57 | 96.85 | 0.01 | 0.00 | 0.00 | 0.00 | 390.60 |
| 1 | 680446.33 | 2459.50 | 2373.66 | 47.80 | 0.02 | 1.21 | 0.83 | 1.91 | 357.27 |
| 2 | 687817.81 | 2466.09 | 2625.27 | 52.99 | 0.02 | 1.25 | 0.73 | 1.91 | 363.51 |
| 3 | 669821.50 | 2477.62 | 1698.17 | 32.95 | 0.03 | 1.17 | 0.82 | 1.91 | 343.33 |
| 4 | 672523.09 | 2483.15 | 1724.64 | 33.31 | 0.03 | 1.18 | 0.74 | 1.91 | 344.89 |
| 5 | 656616.51 | 2492.08 | 1199.93 | 22.90 | 0.04 | 1.15 | 0.84 | 1.91 | 329.88 |
| 6 | 658206.48 | 2496.65 | 1201.76 | 22.85 | 0.04 | 1.15 | 0.74 | 1.91 | 330.67 |
| 7 | 644055.21 | 2504.73 | 873.70 | 16.62 | 0.06 | 1.14 | 0.85 | 1.91 | 318.54 |
| 8 | 644437.17 | 2509.54 | 854.85 | 16.21 | 0.06 | 1.14 | 0.74 | 1.91 | 318.43 |

***Table 11.20 – Results for sensitivity analysis with inlet Pressure of 4363 kPa***

| Cross Section | Enthalpy $[J/kg]$ | Entropy $[J/kgK]$ | Pressure $[kPa]$ | Density $[kg/m^3]$ | Specific Volume $[m^3/kg]$ | Quality | Performance | Mass Flow $[kg/s]$ | Temperature $[K]$ |
|---|---|---|---|---|---|---|---|---|---|
| 0 | 710482.82 | 2466.14 | 4201.22 | 90.15 | 0.01 | 0.00 | 0.00 | 0.00 | 390.60 |
| 1 | 684868.26 | 2481.09 | 2223.58 | 43.59 | 0.02 | 1.22 | 0.83 | 1.81 | 356.99 |
| 2 | 693314.58 | 2487.92 | 2500.52 | 49.11 | 0.02 | 1.27 | 0.73 | 1.81 | 363.99 |
| 3 | 674800.11 | 2499.41 | 1618.17 | 30.75 | 0.03 | 1.19 | 0.82 | 1.81 | 344.40 |
| 4 | 677703.16 | 2505.07 | 1647.57 | 31.17 | 0.03 | 1.20 | 0.74 | 1.81 | 346.10 |
| 5 | 661788.57 | 2513.80 | 1155.10 | 21.67 | 0.05 | 1.17 | 0.85 | 1.81 | 331.69 |
| 6 | 663385.44 | 2518.35 | 1156.95 | 21.62 | 0.05 | 1.17 | 0.74 | 1.81 | 332.49 |
| 7 | 649727.99 | 2526.08 | 854.85 | 16.01 | 0.06 | 1.15 | 0.85 | 1.81 | 321.14 |
| 8 | 649988.40 | 2530.70 | 835.54 | 15.61 | 0.06 | 1.16 | 0.74 | 1.81 | 320.97 |

***Table 11.21 – Results for sensitivity analysis with inlet Pressure of 4201 kPa***

| Cross Section | Enthalpy $[J/kg]$ | Entropy $[J/kgK]$ | Pressure $[kPa]$ | Density $[kg/m^3]$ | Specific Volume $[m^3/kg]$ | Quality | Performance | Mass Flow $[kg/s]$ | Temperature $[K]$ |
|---|---|---|---|---|---|---|---|---|---|
| 0 | 716341.45 | 2485.92 | 4038.88 | 84.01 | 0.01 | 0.00 | 0.00 | 0.00 | 390.60 |
| 1 | 688871.79 | 2501.97 | 2080.06 | 39.80 | 0.03 | 1.24 | 0.83 | 1.71 | 356.73 |
| 2 | 698433.26 | 2509.03 | 2378.95 | 45.58 | 0.02 | 1.28 | 0.73 | 1.71 | 364.48 |
| 3 | 679489.30 | 2520.46 | 1541.71 | 28.75 | 0.03 | 1.21 | 0.83 | 1.71 | 345.46 |
| 4 | 682562.22 | 2526.22 | 1572.94 | 29.20 | 0.03 | 1.22 | 0.74 | 1.71 | 347.27 |
| 5 | 666715.62 | 2534.75 | 1112.06 | 20.53 | 0.05 | 1.19 | 0.85 | 1.71 | 333.46 |
| 6 | 668291.23 | 2539.25 | 1113.53 | 20.48 | 0.05 | 1.19 | 0.74 | 1.71 | 334.24 |
| 7 | 655135.12 | 2546.67 | 835.54 | 15.42 | 0.06 | 1.17 | 0.85 | 1.71 | 323.60 |
| 8 | 655275.79 | 2551.10 | 815.87 | 15.02 | 0.07 | 1.17 | 0.74 | 1.71 | 323.38 |

***Table 11.22 – Results for sensitivity analysis with inlet Pressure of 4038 kPa***

| Cross Section | Enthalpy $[J/kg]$ | Entropy $[J/kgK]$ | Pressure $[kPa]$ | Density $[kg/m^3]$ | Specific Volume $[m^3/kg]$ | Quality | Performance | Mass Flow $[kg/s]$ | Temperature $[K]$ |
|---|---|---|---|---|---|---|---|---|---|
| 0 | 721848.62 | 2505.14 | 3876.53 | 78.33 | 0.01 | 0.00 | 0.00 | 0.00 | 390.60 |
| 1 | 692496.98 | 2522.31 | 1942.01 | 36.36 | 0.03 | 1.25 | 0.83 | 1.61 | 356.48 |
| 2 | 703223.24 | 2529.60 | 2259.93 | 42.33 | 0.02 | 1.30 | 0.73 | 1.61 | 364.95 |
| 3 | 683937.31 | 2540.95 | 1468.26 | 26.91 | 0.04 | 1.22 | 0.83 | 1.61 | 346.51 |
| 4 | 687147.84 | 2546.79 | 1500.34 | 27.37 | 0.04 | 1.23 | 0.74 | 1.61 | 348.40 |
| 5 | 671442.46 | 2555.11 | 1070.47 | 19.47 | 0.05 | 1.20 | 0.85 | 1.61 | 335.17 |
| 6 | 672968.74 | 2559.54 | 1071.25 | 19.42 | 0.05 | 1.21 | 0.74 | 1.61 | 335.93 |
| 7 | 660327.16 | 2566.66 | 815.87 | 14.85 | 0.07 | 1.19 | 0.85 | 1.61 | 325.96 |
| 8 | 660349.13 | 2570.90 | 795.92 | 14.46 | 0.07 | 1.19 | 0.74 | 1.61 | 325.68 |

*Table 11.23 – Results for sensitivity analysis with inlet Pressure of 3876 kPa*

| Cross Section | Enthalpy $[J/kg]$ | Entropy $[J/kgK]$ | Pressure $[kPa]$ | Density $[kg/m^3]$ | Specific Volume $[m^3/kg]$ | Quality | Performance | Mass Flow $[kg/s]$ | Temperature $[K]$ |
|---|---|---|---|---|---|---|---|---|---|
| 0 | 640520.18 | 2259.50 | 5500.00 | 175.01 | 0.01 | 0.00 | 0.00 | 0.00 | 390.60 |
| 1 | 627509.29 | 2267.05 | 3408.40 | 96.16 | 0.01 | 1.01 | 0.83 | 2.84 | 358.10 |
| 2 | 629484.42 | 2271.80 | 3434.75 | 96.22 | 0.01 | 1.03 | 0.74 | 2.84 | 358.94 |
| 3 | 616787.50 | 2277.60 | 2330.53 | 58.33 | 0.02 | 0.95 | 0.87 | 2.84 | 337.89 |
| 4 | 617782.97 | 2282.01 | 2302.05 | 57.17 | 0.02 | 0.95 | 0.74 | 2.84 | 337.27 |
| 5 | 604326.44 | 2288.48 | 1582.92 | 37.07 | 0.03 | 0.95 | 0.87 | 2.84 | 319.55 |
| 6 | 605192.91 | 2292.70 | 1565.27 | 36.46 | 0.03 | 0.95 | 0.74 | 2.84 | 319.04 |
| 7 | 588212.67 | 2301.08 | 1000.00 | 22.62 | 0.04 | 0.96 | 0.87 | 2.84 | 300.09 |
| 8 | 589346.92 | 2307.08 | 985.12 | 22.16 | 0.05 | 0.96 | 0.74 | 2.84 | 299.50 |

*Table 11.24 – Results for sensitivity analysis with inlet Temperature 390 K*

| Cross Section | Enthalpy $[J/kg]$ | Entropy $[J/kgK]$ | Pressure $[kPa]$ | Density $[kg/m^3]$ | Specific Volume $[m^3/kg]$ | Quality | Performance | Mass Flow $[kg/s]$ | Temperature $[K]$ |
|---|---|---|---|---|---|---|---|---|---|
| 0 | 620337.70 | 2207.65 | 5500.00 | 194.96 | 0.01 | 0.00 | 0.00 | 0.00 | 388.05 |
| 1 | 609309.03 | 2214.03 | 3490.17 | 108.67 | 0.01 | 0.91 | 0.83 | 2.96 | 359.00 |
| 2 | 610629.07 | 2218.65 | 3454.08 | 106.20 | 0.01 | 0.92 | 0.74 | 2.96 | 358.43 |
| 3 | 599177.01 | 2223.66 | 2369.38 | 63.82 | 0.02 | 0.88 | 0.87 | 2.96 | 338.71 |
| 4 | 599877.15 | 2227.87 | 2323.74 | 61.96 | 0.02 | 0.88 | 0.74 | 2.96 | 337.74 |
| 5 | 587429.42 | 2233.53 | 1609.30 | 40.09 | 0.02 | 0.89 | 0.87 | 2.96 | 320.29 |
| 6 | 588032.29 | 2237.52 | 1582.57 | 39.17 | 0.03 | 0.89 | 0.74 | 2.96 | 319.54 |
| 7 | 570921.85 | 2245.56 | 985.12 | 23.45 | 0.04 | 0.91 | 0.88 | 2.96 | 299.50 |
| 8 | 572091.06 | 2251.61 | 970.22 | 22.96 | 0.04 | 0.91 | 0.74 | 2.96 | 298.89 |

***Table 11.25 – Results for sensitivity analysis with inlet Temperature 388.05 K***

| Cross Section | Enthalpy $[J/kg]$ | Entropy $[J/kgK]$ | Pressure $[kPa]$ | Density $[kg/m^3]$ | Specific Volume $[m^3/kg]$ | Quality | Performance | Mass Flow $[kg/s]$ | Temperature $[K]$ |
|---|---|---|---|---|---|---|---|---|---|
| 0 | 595893.20 | 2144.44 | 5500.00 | 223.35 | 0.00 | 0.00 | 0.00 | 0.00 | 385.49 |
| 1 | 587050.02 | 2149.54 | 3602.17 | 128.24 | 0.01 | 0.77 | 0.83 | 3.13 | 360.73 |
| 2 | 587837.35 | 2154.20 | 3491.00 | 121.01 | 0.01 | 0.78 | 0.75 | 3.13 | 359.01 |
| 3 | 577927.98 | 2158.36 | 2431.00 | 72.34 | 0.01 | 0.78 | 0.88 | 3.13 | 340.00 |
| 4 | 578308.44 | 2162.33 | 2362.73 | 69.32 | 0.01 | 0.79 | 0.74 | 3.13 | 338.57 |
| 5 | 567205.50 | 2167.05 | 1656.37 | 44.79 | 0.02 | 0.81 | 0.88 | 3.13 | 321.60 |
| 6 | 567487.77 | 2170.73 | 1616.66 | 43.36 | 0.02 | 0.82 | 0.74 | 3.13 | 320.50 |
| 7 | 550194.39 | 2178.35 | 970.22 | 24.64 | 0.04 | 0.85 | 0.88 | 3.13 | 298.89 |
| 8 | 551415.23 | 2184.48 | 955.37 | 24.10 | 0.04 | 0.85 | 0.74 | 3.13 | 298.29 |

***Table 11.26 – Results for sensitivity analysis with inlet Temperature 385.49 K***

| Cross Section | Enthalpy $[J/kg]$ | Entropy $[J/kgK]$ | Pressure $[kPa]$ | Density $[kg/m^3]$ | Specific Volume $[m^3/kg]$ | Quality | Performance | Mass Flow $[kg/s]$ | Temperature $[K]$ |
|---|---|---|---|---|---|---|---|---|---|
| 0 | 570391.63 | 2078.07 | 5500.00 | 256.55 | 0.00 | 0.00 | 0.00 | 0.00 | 382.94 |
| 1 | 563707.38 | 2081.90 | 3764.36 | 159.45 | 0.01 | 0.60 | 0.83 | 3.38 | 363.15 |
| 2 | 564146.53 | 2086.51 | 3577.58 | 144.56 | 0.01 | 0.62 | 0.75 | 3.38 | 360.35 |
| 3 | 555971.48 | 2089.82 | 2542.99 | 85.75 | 0.01 | 0.68 | 0.88 | 3.38 | 342.28 |
| 4 | 556072.19 | 2093.50 | 2447.04 | 80.84 | 0.01 | 0.69 | 0.75 | 3.38 | 340.33 |
| 5 | 546666.48 | 2097.25 | 1753.11 | 52.47 | 0.02 | 0.73 | 0.89 | 3.38 | 324.21 |
| 6 | 546604.98 | 2100.54 | 1695.44 | 50.17 | 0.02 | 0.74 | 0.75 | 3.38 | 322.67 |
| 7 | 528579.85 | 2107.93 | 955.37 | 26.08 | 0.04 | 0.78 | 0.89 | 3.38 | 298.29 |
| 8 | 530017.29 | 2114.31 | 943.38 | 25.56 | 0.04 | 0.79 | 0.74 | 3.38 | 297.79 |

***Table 11.27 – Results for sensitivity analysis with inlet Temperature 382.94 K***

| Cross Section | Enthalpy $[J/kg]$ | Entropy $[J/kgK]$ | Pressure $[kPa]$ | Density $[kg/m^3]$ | Specific Volume $[m^3/kg]$ | Quality | Performance | Mass Flow $[kg/s]$ | Temperature $[K]$ |
|---|---|---|---|---|---|---|---|---|---|
| 0 | 548843.16 | 2021.62 | 5500.00 | 285.14 | 0.00 | 0.00 | 0.00 | 0.00 | 380.38 |
| 1 | 543925.61 | 2024.41 | 3977.11 | 205.24 | 0.00 | 0.40 | 0.83 | 3.74 | 366.20 |
| 2 | 544313.33 | 2028.94 | 3735.29 | 179.36 | 0.01 | 0.46 | 0.77 | 3.74 | 362.73 |
| 3 | 537843.90 | 2031.48 | 2727.80 | 105.70 | 0.01 | 0.58 | 0.88 | 3.74 | 345.88 |
| 4 | 537779.19 | 2034.87 | 2602.46 | 97.92 | 0.01 | 0.59 | 0.76 | 3.74 | 343.46 |
| 5 | 530393.89 | 2037.67 | 1938.77 | 65.02 | 0.02 | 0.65 | 0.89 | 3.74 | 328.93 |
| 6 | 530034.92 | 2040.47 | 1858.19 | 61.30 | 0.02 | 0.66 | 0.75 | 3.74 | 326.92 |
| 7 | 510289.41 | 2048.06 | 943.38 | 27.49 | 0.04 | 0.73 | 0.90 | 3.74 | 297.79 |
| 8 | 512253.68 | 2054.98 | 940.76 | 27.20 | 0.04 | 0.74 | 0.74 | 3.74 | 297.68 |

***Table 11.28 – Results for sensitivity analysis with inlet Temperature 380.38 K***

| Cross Section | Enthalpy $[J/kg]$ | Entropy $[J/kgK]$ | Pressure $[kPa]$ | Density $[kg/m^3]$ | Specific Volume $[m^3/kg]$ | Quality | Performance | Mass Flow $[kg/s]$ | Temperature $[K]$ |
|---|---|---|---|---|---|---|---|---|---|
| 0 | 531463.51 | 1975.78 | 5500.00 | 307.02 | 0.00 | 0.00 | 0.00 | 0.00 | 377.83 |
| 1 | 527851.70 | 1977.81 | 4228.53 | 270.11 | 0.00 | -0.19 | 0.83 | 4.23 | 369.49 |
| 2 | 528456.21 | 1982.26 | 3969.49 | 232.44 | 0.00 | 0.26 | 0.82 | 4.23 | 366.09 |
| 3 | 523721.92 | 1984.07 | 3016.19 | 137.62 | 0.01 | 0.47 | 0.88 | 4.23 | 351.15 |
| 4 | 523646.14 | 1987.18 | 2863.48 | 125.38 | 0.01 | 0.49 | 0.77 | 4.23 | 348.41 |
| 5 | 518685.75 | 1988.98 | 2278.39 | 88.19 | 0.01 | 0.56 | 0.89 | 4.23 | 336.76 |
| 6 | 518197.47 | 1991.18 | 2173.78 | 82.16 | 0.01 | 0.57 | 0.77 | 4.23 | 334.45 |
| 7 | 495722.79 | 1999.45 | 940.76 | 29.02 | 0.03 | 0.69 | 0.90 | 4.23 | 297.68 |
| 8 | 498664.59 | 2007.47 | 956.81 | 29.28 | 0.03 | 0.69 | 0.74 | 4.23 | 298.34 |

***Table 11.29 – Results for sensitivity analysis with inlet Temperature 377.83 K***

| Cross Section | Enthalpy $[J/kg]$ | Entropy $[J/kgK]$ | Pressure $[kPa]$ | Density $[kg/m^3]$ | Specific Volume $[m^3/kg]$ | Quality | Performance | Mass Flow $[kg/s]$ | Temperature $[K]$ |
|---|---|---|---|---|---|---|---|---|---|
| 0 | 516775.35 | 1936.78 | 5500.00 | 324.19 | 0.00 | 0.00 | 0.00 | 0.00 | 375.28 |
| 1 | 513416.53 | 1938.67 | 4233.42 | 296.41 | 0.00 | -0.64 | 0.83 | 4.48 | 368.83 |
| 2 | 514249.67 | 1943.23 | 3990.99 | 269.62 | 0.00 | 0.11 | 0.83 | 4.48 | 366.39 |
| 3 | 510386.67 | 1944.70 | 3092.32 | 159.07 | 0.01 | 0.38 | 0.88 | 4.48 | 352.47 |
| 4 | 510388.27 | 1947.69 | 2933.84 | 143.75 | 0.01 | 0.42 | 0.79 | 4.48 | 349.68 |
| 5 | 506447.05 | 1949.10 | 2396.47 | 103.08 | 0.01 | 0.49 | 0.89 | 4.48 | 339.28 |
| 6 | 506011.27 | 1951.06 | 2287.28 | 95.66 | 0.01 | 0.51 | 0.79 | 4.48 | 336.95 |
| 7 | 484199.14 | 1958.99 | 956.81 | 31.10 | 0.03 | 0.65 | 0.90 | 4.48 | 298.34 |
| 8 | 486920.64 | 1966.78 | 969.08 | 31.24 | 0.03 | 0.66 | 0.74 | 4.48 | 298.85 |

***Table 11.30 – Results for sensitivity analysis with inlet Temperature 375.28 K***

| Cross Section | Enthalpy $[J/kg]$ | Entropy $[J/kgK]$ | Pressure $[kPa]$ | Density $[kg/m^3]$ | Specific Volume $[m^3/kg]$ | Quality | Performance | Mass Flow $[kg/s]$ | Temperature $[K]$ |
|---|---|---|---|---|---|---|---|---|---|
| 0 | 503780.83 | 1902.03 | 5500.00 | 338.30 | 0.00 | 0.00 | 0.00 | 0.00 | 372.72 |
| 1 | 500513.08 | 1903.88 | 4203.72 | 315.80 | 0.00 | -0.53 | 0.83 | 4.71 | 367.37 |
| 2 | 501549.44 | 1908.63 | 3984.14 | 307.35 | 0.00 | -0.01 | 0.84 | 4.71 | 366.25 |
| 3 | 498377.85 | 1909.83 | 3142.76 | 181.47 | 0.01 | 0.31 | 0.88 | 4.71 | 353.34 |
| 4 | 498494.98 | 1912.74 | 2986.76 | 163.30 | 0.01 | 0.35 | 0.82 | 4.71 | 350.63 |
| 5 | 495406.04 | 1913.83 | 2503.38 | 119.73 | 0.01 | 0.42 | 0.89 | 4.71 | 341.48 |
| 6 | 495083.25 | 1915.59 | 2397.23 | 111.17 | 0.01 | 0.44 | 0.82 | 4.71 | 339.30 |
| 7 | 473903.62 | 1923.23 | 969.08 | 33.07 | 0.03 | 0.62 | 0.90 | 4.71 | 298.85 |
| 8 | 476416.15 | 1930.80 | 977.22 | 33.05 | 0.03 | 0.62 | 0.74 | 4.71 | 299.18 |

*Table 11.31 – Results for sensitivity analysis with inlet Temperature 372.72 K*

| Cross Section | Enthalpy $[J/kg]$ | Entropy $[J/kgK]$ | Pressure $[kPa]$ | Density $[kg/m^3]$ | Specific Volume $[m^3/kg]$ | Quality | Performance | Mass Flow $[kg/s]$ | Temperature $[K]$ |
|---|---|---|---|---|---|---|---|---|---|
| 0 | 491919.94 | 1870.10 | 5500.00 | 350.35 | 0.00 | 0.00 | 0.00 | 0.00 | 370.17 |
| 1 | 488717.94 | 1871.92 | 4177.30 | 331.58 | 0.00 | -0.56 | 0.83 | 4.89 | 365.61 |
| 2 | 489793.47 | 1876.72 | 3954.88 | 324.84 | 0.00 | -0.09 | 0.84 | 4.89 | 364.82 |
| 3 | 487420.90 | 1877.62 | 3230.82 | 213.59 | 0.00 | 0.23 | 0.88 | 4.89 | 354.82 |
| 4 | 487807.99 | 1881.88 | 3010.88 | 182.16 | 0.01 | 0.29 | 0.54 | 4.89 | 351.05 |
| 5 | 485649.41 | 1882.63 | 2624.34 | 140.62 | 0.01 | 0.36 | 0.89 | 4.89 | 343.89 |
| 6 | 485546.12 | 1885.63 | 2474.23 | 126.00 | 0.01 | 0.39 | 0.54 | 4.89 | 340.89 |
| 7 | 465097.20 | 1892.97 | 977.22 | 34.82 | 0.03 | 0.59 | 0.90 | 4.89 | 299.18 |
| 8 | 467393.39 | 1900.32 | 980.63 | 34.60 | 0.03 | 0.60 | 0.74 | 4.89 | 299.32 |

*Table 11.32 – Results for sensitivity analysis with inlet Temperature 370.17 K*

| Cross Section | Enthalpy $[J/kg]$ | Entropy $[J/kgK]$ | Pressure $[kPa]$ | Density $[kg/m^3]$ | Specific Volume $[m^3/kg]$ | Quality | Performance | Mass Flow $[kg/s]$ | Temperature $[K]$ |
|---|---|---|---|---|---|---|---|---|---|
| 0 | 480867.02 | 1840.14 | 5500.00 | 360.93 | 0.00 | 0.00 | 0.00 | 0.00 | 367.61 |
| 1 | 477657.86 | 1841.98 | 4129.50 | 344.52 | 0.00 | -0.52 | 0.83 | 5.09 | 363.55 |
| 2 | 478739.66 | 1846.81 | 3899.26 | 338.76 | 0.00 | -0.14 | 0.84 | 5.09 | 362.96 |
| 3 | 476702.60 | 1847.58 | 3216.68 | 236.74 | 0.00 | 0.17 | 0.88 | 5.09 | 354.58 |
| 4 | 477223.41 | 1851.49 | 3028.13 | 204.26 | 0.00 | 0.23 | 0.59 | 5.09 | 351.36 |
| 5 | 475626.71 | 1852.04 | 2702.88 | 162.30 | 0.01 | 0.30 | 0.89 | 5.09 | 345.41 |
| 6 | 475718.92 | 1854.44 | 2588.79 | 148.65 | 0.01 | 0.32 | 0.61 | 5.09 | 343.19 |
| 7 | 455800.65 | 1861.59 | 980.63 | 36.58 | 0.03 | 0.56 | 0.90 | 5.09 | 299.32 |
| 8 | 457914.27 | 1868.75 | 979.47 | 36.14 | 0.03 | 0.57 | 0.74 | 5.09 | 299.27 |

*Table 11.33 – Results for sensitivity analysis with inlet Temperature 367.61 K*

| Cross Section | Enthalpy $[J/kg]$ | Entropy $[J/kgK]$ | Pressure $[kPa]$ | Density $[kg/m^3]$ | Specific Volume $[m^3/kg]$ | Quality | Performance | Mass Flow $[kg/s]$ | Temperature $[K]$ |
|---|---|---|---|---|---|---|---|---|---|
| 0 | 470420.18 | 1811.63 | 5500.00 | 370.42 | 0.00 | 0.00 | 0.00 | 0.00 | 365.06 |
| 1 | 467163.07 | 1813.50 | 4068.99 | 355.63 | 0.00 | -0.48 | 0.83 | 5.29 | 361.34 |
| 2 | 468234.22 | 1818.35 | 3828.16 | 350.52 | 0.00 | -0.16 | 0.84 | 5.29 | 360.88 |
| 3 | 466536.85 | 1819.00 | 3208.56 | 265.24 | 0.00 | 0.12 | 0.88 | 5.29 | 354.45 |
| 4 | 467232.06 | 1822.74 | 3053.24 | 232.02 | 0.00 | 0.17 | 0.63 | 5.29 | 351.80 |
| 5 | 466224.28 | 1823.09 | 2814.12 | 193.76 | 0.01 | 0.23 | 0.89 | 5.29 | 347.50 |
| 6 | 466610.02 | 1825.22 | 2747.63 | 183.02 | 0.01 | 0.25 | 0.65 | 5.29 | 346.26 |
| 7 | 446989.70 | 1832.25 | 979.47 | 38.18 | 0.03 | 0.54 | 0.90 | 5.29 | 299.27 |
| 8 | 449012.84 | 1839.41 | 974.96 | 37.55 | 0.03 | 0.54 | 0.74 | 5.29 | 299.09 |

*Table 11.34 – Results for sensitivity analysis with inlet Temperature 365.06 K*

## 11.2. Codes

### 11.2.1. Entrance of the Turbine

```
%% Turbine entrance
%% Cristian Leonardo Niño Avella - KIT - ITES
clc
clear all
%The turbine entrance has a pressure drop between the measure value in 2'
%and 0, this loss will change the behavior of the fluid before the first
%vane into the turbine.
%% Import table with properties

% As a first step it is necessary to import all the data related with
% geometry, measure data in the 2' and 1' points, the fluid concentration
% and therefore, the critical temperature and pressure of it.

% To calculate the inlet of the turbine it is necessary the files that
% include the pressure and temperature (Measured_data) and the geometry of
% the turbine (Geometry_stages)

run InletData.m

% Inlet variables
T_2p=MD(1,4); %[K]
P_2p=MD(1,7); %[kPa]
P_1p=MD(1,8); %[kPa]
T_1p_meassured=MD(1,5); %[K]
h_loss21p=(MD(1,15)-MD(1,16))/1000; % Enthalpy loss due to the Q losses in the pipe between 2p and 1p [kJ/kg]
N2_conc=(NCD(8,2)/100); % Concentration of nitrogen in mass fraction


%% Fluid properties

% Based on the nitrogen concentration the Critical pressure and Critical
% temperature must be determined.

Tcrit=refpropm('T','C',0,' ',0,'PROPANE','NITROGEN',[(1-N2_conc) (N2_conc)]); %[K]
Pcrit=refpropm('P','C',0,' ',0,'PROPANE','NITROGEN',[(1-N2_conc) (N2_conc)]); %[kPa]
```

```
%% Check fluid phase (Supercritical, superheated or two-phase fluid region in 2' (rho_2', h_2', s_2' using
T_2' and P_2') and find the fluid properties

% As a first step, it is necessary to determine the properties in the fluid
% we are, in order to do this, we must evaluate if the point is in the
% supercritical, superheated or two-phase zone.

if P_2p>=Pcrit
    fprintf('-2p Supercritical-')
    h_2p=(refpropm('H','T',T_2p,'P',P_2p,'PROPANE','NITROGEN',[(1-N2_conc) (N2_conc)]))/1000; %Enthalpy
[kJ/kg]
    rho_2p=refpropm('D','T',T_2p,'P',P_2p,'PROPANE','NITROGEN',[(1-N2_conc) (N2_conc)]); %Density [kg/m^3]
    s_2p=(refpropm('S','T',T_2p,'P',P_2p,'PROPANE','NITROGEN',[(1-N2_conc) (N2_conc)]))/1000; %Entropy [kJ/(kg
K)]

else
    if T_2p>refpropm('T','P',P_2p,'Q',1,'PROPANE','NITROGEN',[(1-(NCD(8,2)/100)) (NCD(8,2)/100)])
        fprintf('-2p superheated-')
        h_2p=(refpropm('H','T',T_2p,'P',P_2p,'PROPANE','NITROGEN',[(1-N2_conc) (N2_conc)]))/1000; %Enthalpy
[kJ/kg]
        rho_2p=refpropm('D','T',T_2p,'P',P_2p,'PROPANE','NITROGEN',[(1-N2_conc) (N2_conc)]); %Density [kg/m^3]
        s_2p=(refpropm('S','T',T_2p,'P',P_2p,'PROPANE','NITROGEN',[(1-N2_conc) (N2_conc)]))/1000; %Entropy
[kJ/(kg K)]
    else
        fprintf('-2p Two Phase Region, Enthalpy needed-')
    end
end

%% Calculate 1' using measure values of the enthalpy loss between 2' and 1'due to heat losses in the pipe

% Using the values found before, then we can proceed in finding the next
% point 1', in which we have also measure data for the pressure and the
% temperature.

 h_1p=h_2p-h_loss21p; %[kJ/kg]

if P_1p>=Pcrit
    fprintf('-1p Supercritical-')
    T_1p=(refpropm('T','H',h_1p*1000,'P',P_1p,'PROPANE','NITROGEN',[(1-N2_conc) (N2_conc)])); %Enthalpy
[kJ/kg]
```

```
    rho_1p=refpropm('D','H',h_1p*1000,'P',P_1p,'PROPANE','NITROGEN',[(1-N2_conc) (N2_conc)]); %Density
[kg/m^3]
    s_1p=(refpropm('S','H',h_1p*1000,'P',P_1p,'PROPANE','NITROGEN',[(1-N2_conc) (N2_conc)]))/1000; %Entropy
[kJ/(kg K)]

else
    if h_1p>(refpropm('H','P',P_1p,'Q',1,'PROPANE','NITROGEN',[(1-N2_conc) (N2_conc)]))/1000
        fprintf('-1p superheated-')
        T_1p=refpropm('T','H',h_1p*1000,'P',P_1p,'PROPANE','NITROGEN',[(1-N2_conc) (N2_conc)]); % Temperature
[K]
        rho_1p=refpropm('D','H',h_1p*1000,'P',P_1p,'PROPANE','NITROGEN',[(1-N2_conc) (N2_conc)]); %Density
[kg/m^3]
        s_1p=(refpropm('S','H',h_1p*1000,'P',P_1p,'PROPANE','NITROGEN',[(1-N2_conc) (N2_conc)]))/1000;
%Entropy [kJ/(kg K)]
    else
        fprintf('-1p Two Phase Region')
        X_1p=((h_1p*1000)-(refpropm('H','P',P_1p,'Q',0,'PROPANE','NITROGEN',[(1-N2_conc)
(N2_conc)])/1000))/((refpropm('H','P',MD(1,8),'Q',1,'PROPANE','NITROGEN',[(1-N2_conc) (N2_conc)])/1000)-
(refpropm('H','P',MD(1,8),'Q',0,'PROPANE','NITROGEN',[(1-N2_conc) (N2_conc)])/1000));
        s_1p=(X_1p*(refpropm('S','P',P_1p,'Q',1,'PROPANE','NITROGEN',[(1-N2_conc) (N2_conc)])/1000))+((1-
X_1p)*(refpropm('S','P',MD(1,8),'Q',0,'PROPANE','NITROGEN',[(1-N2_conc) (N2_conc)])/1000)); %Entropy [kJ/(kg
K)]
        rho_1p=(X_1p*(refpropm('D','P',P_1p,'Q',1,'PROPANE','NITROGEN',[(1-N2_conc) (N2_conc)])/1000))+((1-
X_1p)*(refpropm('D','P',MD(1,8),'Q',0,'PROPANE','NITROGEN',[(1-N2_conc) (N2_conc)])/1000));
        T_1p=refpropm('T','P',P_1p,'Q',1,'PROPANE','NITROGEN',[(1-N2_conc) (N2_conc)]);
    end
end

%% Velocity of flow

% Once we have got the properties for the fluid in 1', we proceed to
% calculate the pressure drop between 1' and 0', for this, it is necessary
% to determine the velocity, as a consideration, the density will remain
% constant in these two points, this value will be corrected by iteration.

d_0p=0.04; %diameter in 0' [m]
d_1p=0.05; %diameter in 1' [m]
A_0p=pi*(d_0p^2)/4; %Area in 0' [m2]
A_1p=pi*(d_1p^2)/4; %Area in 0' [m2]
rho_0p_iter=rho_1p; %density [kg/m3]
```

```
M=MD(1,2); % mass flow [kg/s]
error=0.00001;
rho_0p=rho_1p+5;

while abs(rho_0p_iter-rho_0p)>error

    rho_0p_iter=rho_0p;
    v_0p=M/(rho_0p_iter*A_0p); % velocity [m/s]
    v_1p=M/(rho_0p_iter*A_1p); % velocity [m/s]

%% Pressure drop for 0'

%In order to find the properties in 0', it is necessary to determine the
%pressure drop due to friction losses and the expansion at the entrance of
%the turbine, in order to do this, the function pressure_loss will be used.

%[Deltap_tpf]=pressure_loss(m,d,g_viscosity,l_viscosity,rho_g,rho_l,X,Pcrit,P,q,L)


    if P_1p>=Pcrit
        % Input parameters:

        d=d_1p;
        A=A_1p;
        m=M/A; % specific mass velocity [kg/m2*s]
        g_V=refpropm('V','T',T_1p,'P',P_1p,'PROPANE','NITROGEN',[(1-N2_conc) (N2_conc)]); % Dynamic viscosity
[Pa*s]
        l_V=0;                      % Dynamic viscosity [Pa*s]
        rho_g=rho_0p_iter;          % gas density [kg/m3]
        rho_l=0;                    %liquid density [kg/m3]
        g_viscosity=g_V/rho_g;      % viscosity of the gas [kg/m*s]
        l_viscosity=0;              % viscosity of the liquid [kg/m*s]
        X=1;                        % fluid quality
        P=P_1p;                     % fluid pressure
        q=0;                        % heat flux [W/m2]
        L=0.6;                      % length [m]
        dHv=0;                      % latent heat of evaporation [J/kg]
        v=v_1p;                     % velocity [m/s]
        ef=1;                       % ef expansion factor
```

```
        [Deltap_tpf]=pressure_loss(m,d,g_viscosity,l_viscosity,rho_g,rho_l,X,Pcrit,P,q,L,v,ef);

    else
        if T_1p>refpropm('T','P',P_1p,'Q',1,'PROPANE','NITROGEN',[(1-N2_conc) (N2_conc)])

            d=d_1p;
            A=A_1p;
            m=M/A;                  % specific mass velocity [kg/m2*s]
            g_V=refpropm('V','T',T_1p,'P',P_1p,'PROPANE','NITROGEN',[(1-N2_conc) (N2_conc)]); % Dynamic
viscosity [Pa*s]
            l_V=0;                  % Dynamic viscosity [Pa*s]
            rho_g=rho_0p_iter;      % gas density [kg/m3]
            rho_l=0;                %liquid density [kg/m3]
            g_viscosity=g_V/rho_g;  % viscosity of the gas [kg/m*s]
            l_viscosity=0;          % viscosity of the liquid [kg/m*s]
            X=1;                    % fluid quality
            P=P_1p;                 % fluid pressure
            q=0;                    % heat flux [W/m2]
            L=0.6;                  % length [m]
            dHv=0;                  % latent heat of evaporation [J/kg]
            v=v_1p;                 % velocity [m/s]
            ef=1;                   % ef expansion factor

            [Deltap_tpf]=pressure_loss(m,d,g_viscosity,l_viscosity,rho_g,rho_l,X,Pcrit,P,q,L,v,ef);


        else
            % Input parameters:

            d=d_1p; % diameter of the pipe [m]
            A=A_1p; %Cross section of the smaller pipe [m2]
            m=M/A; % specific mass velocity [kg/m2*s]
            g_V=refpropm('V','P',P_1p,'Q',1,'PROPANE','NITROGEN',[(1-N2_conc) (N2_conc)]); % Dynamic viscosity
[Pa*s]
            l_V=refpropm('V','P',P_1p,'Q',0,'PROPANE','NITROGEN',[(1-N2_conc) (N2_conc)]); % Dynamic viscosity
[Pa*s]
            rho_g=refpropm('D','P',P_1p,'Q',1,'PROPANE','NITROGEN',[(1-N2_conc) (N2_conc)]); % gas density
[kg/m3]
```

```
            rho_l=refpropm('D','P',P_1p,'Q',0,'PROPANE','NITROGEN',[(1-N2_conc) (N2_conc)]); %liquid density
[kg/m3]
            g_viscosity=g_V/rho_g;  % viscosity of the gas [kg/m*s]
            l_viscosity=l_V/rho_l;  % viscosity of the liquid [kg/m*s]
            X=X_1p;                 % fluid quality
            P=P_1p;                 % fluid pressure
            q=0                     % heat flux [W/m2] (It is considered that there is no heat loss in this
part of the pipe)
            L=0.6;                  % length [m]
            dHv=refpropm('H','P',P_1p,'Q',1,'PROPANE','NITROGEN',[(1-N2_conc) (N2_conc)])-
refpropm('H','P',P_1p,'Q',0,'PROPANE','NITROGEN',[(1-N2_conc) (N2_conc)]); % latent heat of evaporation [J/kg]
            v=v_1p;                 % velocity [m/s]
            ef=1;                   % ef expansion factor

            [Deltap_tpf]=pressure_loss(m,d,g_viscosity,l_viscosity,rho_g,rho_l,X,Pcrit,P,q,L,v,ef);

        end
    end
%% Isoenthalpic and find T_0', P_0', s_0', rho_0' and h_0'

% Once the pressure drop has been determined, it is possible to find the
% properties of the fluid in 0', for this we consider that the change of
% the state was made isoenthalpically.

    P_0p=P_1p-Deltap_tpf;           % [kPa]
    h_0p=h_1p;                      %Enthalpy [kJ/kg]
    if P_0p>=Pcrit
        fprintf('-0p Supercritical-')
        T_0p=(refpropm('T','H',h_0p*1000,'P',P_0p,'PROPANE','NITROGEN',[(1-N2_conc) (N2_conc)])); %Temperature
[K]
        rho_0p=refpropm('D','T',T_0p,'P',P_0p,'PROPANE','NITROGEN',[(1-N2_conc) (N2_conc)]);    %Density
[kg/m^3]
        s_0p=(refpropm('S','T',T_0p,'P',P_0p,'PROPANE','NITROGEN',[(1-N2_conc) (N2_conc)]))/1000; %Entropy
[kJ/(kg K)]
    else
        if h_0p>refpropm('H','P',P_0p,'Q',1,'PROPANE','NITROGEN',[(1-N2_conc) (N2_conc)])/1000  %[kJ/kg]
            fprintf('-0p superheated-')
            T_0p=(refpropm('T','H',h_0p*1000,'P',P_0p,'PROPANE','NITROGEN',[(1-N2_conc) (N2_conc)]));
%Temperature [K]
```

```
            rho_0p=refpropm('D','T',T_0p,'P',P_0p,'PROPANE','NITROGEN',[(1-N2_conc) (N2_conc)]); %Density
[kg/m^3]
            s_0p=(refpropm('S','T',T_0p,'P',P_0p,'PROPANE','NITROGEN',[(1-N2_conc) (N2_conc)]))/1000; %Entropy
[kJ/(kg K)]
        else
            fprintf('-0p Two Phase Region, Enthalpy is considered h_1p=h_0p-')
            X_0p=(h_0p-(refpropm('H','P',P_0p,'Q',0,'PROPANE','NITROGEN',[(1-N2_conc)
(N2_conc)])/1000))/((refpropm('H','P',P_0p,'Q',1,'PROPANE','NITROGEN',[(1-N2_conc) (N2_conc)])/1000)-
(refpropm('H','P',P_0p,'Q',0,'PROPANE','NITROGEN',[(1-N2_conc) (N2_conc)])/1000));
            s_0p=(X_0p*(refpropm('S','P',P_0p,'Q',1,'PROPANE','NITROGEN',[(1-N2_conc) (N2_conc)])/1000))+((1-
X_0p)*(refpropm('S','P',MD(1,8),'Q',0,'PROPANE','NITROGEN',[(1-N2_conc) (N2_conc)])/1000)); %Entropy [kJ/(kg
K)]
            rho_0p=(X_0p*(refpropm('D','P',P_0p,'Q',1,'PROPANE','NITROGEN',[(1-N2_conc)
(N2_conc)])/1000))+((1-X_0p)*(refpropm('D','P',MD(1,8),'Q',0,'PROPANE','NITROGEN',[(1-N2_conc)
(N2_conc)])/1000));
        end
    end

end

%% Velocity change

% Once we have determined the properties for the fluid at the entrance of
% the turbine, now we can find the velocity before the first vane stage.
% For this, we use the conservation of mass law (M), and we suppose that the
% density remains constant. rho_0p=rho_0.

rho_0=rho_0p; %[kg/m3]
Rm=(GD(1,5)+GD(1,6))*0.5;
width=GD(1,6)-GD(1,5);
A_0=width*Rm*GD(1,4)/1000000; %[m2]

v_0=M/(rho_0*A_0); %[m/s]

%% Inlet data for turbine calculations

% Once I have obtained the fluid properties at the entrance of the turbine,
% it is possible to proceed with the calculation of the different stages of
% it, for this, it is necessary to export the results obtained during this
% Analysis.
```

```
Enthalpy_Jkg=h_0p*1000;
Entropy_JkgK=s_0p*1000;
Pressure_kPa=P_0p;
Title=X;
Velocity_ms=v_0;
Density_kgm3=rho_0;
Temperature_K=T_0p;

Inlet_turbine=table(Enthalpy_Jkg,Entropy_JkgK,Pressure_kPa,Title,Velocity_ms,Density_kgm3,Temperature_K)
writetable(Inlet_turbine,'Inlet_turbine.xls')
```

### 11.2.2. Mean Line analysis for design properties

```
%% Turbine Mean line Analysis for design values and sensitivity analysis
% Cristian Leonardo Niño Avella

%% Inlet Data

% Stages, Pressure and Temperature
inlet_properties=readmatrix('Inlet_turbine.xls');
[GD,txt_GD,raw_GD]=xlsread('Geometry_stages.xlsx','Geometry','A1:T11');
stages=4;                                               % Number of stages
ncs=2*stages;                                           % Number of cross sections
P0=5500;                                                % Design Inlet pressure [kPa]
T0=117+273.6;                                           % Design Inlet temperature [K]
P(7)=1130;                                              %[kPa]
P(8)=1100;                                              %Design outlet pressure [kPa]

% Geometry

for n=1:ncs
    Re(n)=GD(n,6)*0.001;          %  Outer radius [m]
    Ri(n)=GD(n,5)*0.001;          % Inner radius [m]
    Rm(n)=sqrt((Re(n)^2+Ri(n)^2)/2);  % Mean radius [m]
    outlet_angle(n)=GD(n,14); %(n,14) for the method of Traupel for vanes and Measured outlet angle for blades
[rad]
    omega(n)=GD(n,4);             % Aperture angle of the cross sections [rad]
    F(n)=GD(n,4)/(2*pi);          % Fraction of aperture, partial admission
    An(n)=pi*(Re(n)^2-Ri(n)^2)*F(n); % Aperture Area in vanes [m2]bis
    ca(n)=GD(n,9)/1000;            % Chord length  [m]
    hb(n)=GD(n,10)/1000;           % Blade height  [m]
    DL(n)=GD(n,18)/1000;           % Diameter of Labyrinth tips [m]
    HL(n)=GD(n,19)/1000;           % Open clearance of Labyrinth tips [m]
    zl=3;                          % Number of Labyrinth tips
end

% Frequency and angular velocity

f=9960/60; % Rps
w=2*pi*f; %Angular velocity [rad/s]
```

```
%Inlet fluid conditions

% The inlet fluid conditions vary in order to evaluate the sensibility of
% the outlet of the turbine due to these properties.

% Substance definition

substance1='PROPANE';
substance2='NITROGEN';
N2_conc=0.0;                                    % Nitrogen concentration
mix_conc= [(1-N2_conc) (N2_conc)];              % Mixture concentration

%% Calculation of stages

% Parameters for decreasing temperature and Pressure
% In order to make a sensibility analysis, the inlet pressure and
% temperature will change from the theorical value to the measured value
% with losses, this value was gotten previously.


for m=1:1

    PR=P0/P(8);
    for n=1:stages
        if n==1
            P(2*n-1)=P0/(PR^(1/stages));
            P(2*n)=P(2*n-1);
        else
            P(2*n-1)=P(2*n-2)/(PR^(1/stages));
            P(2*n)=P(2*n-1);
        end
    end


    % Inlet properties

    % With the inlet pressure and temperature, we can now define the fluid
    % properties at the entrance of the turbine.
```

```
rho0=refpropm('D','T',T0,'P',P0,substance1,substance2,mix_conc);         %[kg/m3]
h0=refpropm('H','T',T0,'P',P0,substance1,substance2,mix_conc);           %[J/kg]
s0=refpropm('S','T',T0,'P',P0,substance1,substance2,mix_conc);           %[J/kgK]
v0=1/rho0;                                                               %[m3/kg]
alpha0=pi/2;                                                             % Inlet angle [rad]

% Critical properties

Tcrit=refpropm('T','C',0,' ',0,substance1,substance2,mix_conc);          % Critical temperature [K]
Pcrit=refpropm('P','C',0,' ',0,substance1,substance2,mix_conc);          % Critical pressure    [kPa]

% Iteration initiation

% In this method it will be used the mass flow to iterate, in order to use
% the inlet and outlet pressure of the turbine as an entrance data.

iterM=0;
iter_max=1000;
dM_min=0.00001;     % Min difference between Mass flow in iter
Merror=10;          % Error in Mass calculation

while Merror>dM_min && iterM<iter_max
        for n=1:ncs
            if n==1

                alpha(n)=outlet_angle(n);                            %[rad]
                U(n,1)=0;                                            %[m/s]
                U(n,2)=Rm(n)*w;                                      %[m/s]
                % Isoentropic Enthalpy calculation using the estimated pressure

                hs(n)=refpropm('H','P',P(n),'S',s0,substance1,substance2,mix_conc); %Isentropic enthalpy
[J/kg]

                % Soderberg loss correlation - Dixon Pg. 97

                epsrad(n)=alpha0-alpha(n);                           % Deflection angle [rad]
                eps(n)=epsrad(n)*180/pi;
```

```
zetas(n)=0.04+0.06*(eps(n)/100)^2;              % Eq. (4.12)
zeta1(n)=(1+zetas(n))*(0.993+0.021*ca(n)/hb(n))-1; % Eq. (4.13a) for nozzles
eta(n)=1-zeta1(n);                               % Efficiency (Leidtradwrikungsgrad Traupel
Pg. 164)


h(n)=h0-eta(n)*(h0-hs(n));                       % Real enthalpy [J/kg]

if P(n)>Pcrit
    warning('Supercritical Pressure');
    s(n)=refpropm('S','H',h(n),'P',P(n),substance1,substance2,mix_conc);    %[J/kgK]
    rho(n)=refpropm('D','H',h(n),'P',P(n),substance1,substance2,mix_conc);  %[kg/m3]
    T(n)=refpropm('T','H',h(n),'P',P(n),substance1,substance2,mix_conc);  %[K]
else
    hG(n)=refpropm('H','P',P(n),'Q',1,substance1,substance2,mix_conc);      %[J/kg]
    hL(n)=refpropm('H','P',P(n),'Q',0,substance1,substance2,mix_conc);      %[J/kg]
    x(n)=refpropm('Q','P',P(n),'H',h(n),substance1,substance2,mix_conc);    % Quality
    s(n)=refpropm('S','H',h(n),'P',P(n),substance1,substance2,mix_conc);    %[J/kgK]
    rho(n)=refpropm('D','H',h(n),'P',P(n),substance1,substance2,mix_conc);  %[kg/m3]
    T(n)=refpropm('T','H',h(n),'P',P(n),substance1,substance2,mix_conc);  %[K]
end

% Now it is possible to define an estimated mass flow
% based on the initial properties and in the estimated
% pressure in the outlet of the first vane, using these
% data Mv (Mass flow though the vane) is calculated as
% below:

Mv(n)=(2*(h0-h(n))*(-1/(rho0*An(n)*sin(alpha0))^2+1/(rho(n)*An(n)*sin(alpha(n)))^2)^-
1)^0.5; % Individual vane Mass flow [kg/s]

V(n,1)=Mv(n)/(An(n)*rho(n));                 % Vax [m/s]
V(n,2)=V(n,1)/tan(alpha(n));                 % Vu [m/s]
Vabs(n)=norm(V(n,:));                        %[m/s]

% Lybrynth losses

ML1(n)=0.8*pi*DL(n)*HL(n)*(rho0*1000*P0)^0.5;
ML(n)=ML1(n)*((1-(P(n)/P0)^2)/(zl+log(P0/P(n))))^0.5; %[kg/s]
```

```
        M(n)=Mv(n)+ML(n);                                %[kg/s]
        if x(n)>1
            SoS(n)=refpropm('A','T',T(n),'P',P(n),substance1,substance2,mix_conc); %Speed of sound
        else
            SoS(n)=refpropm('A','P',P(n),'Q',1,substance1,substance2,mix_conc); %Speed of sound
        end

    elseif rem(n,2)==0 %% For all the blades

        rho_prev(n)=rho(n-1);
        drho=100;
        iter=0;


        U(n,1)=0;                                        %[m/s]
        U(n,2)=Rm(n)*w;                                  %[m/s]
        W(n-1,:)=V(n-1,:)-U(n-1,:);                      %[m/s]
        beta(n-1)=atan(W(n-1,1)/W(n-1,2));               %[rad]
        beta(n)=outlet_angle(n);                         %[rad]

        % We consider the mass flow is the same for the blades
        % and the vanes

        M(n)=M(n-1);                                     %[kg/s]

        % Soderberg correlation

        epsrad(n)=beta(n)-beta(n-1);     % Deflection angle [rad]
        eps(n)=epsrad(n)*180/pi;         % Deflection angle [deg]
        zetas(n)=0.04+0.06*(eps(n)/100)^2;     % Eq. (4.12)
        zeta1(n)=(1+zetas(n))*(0.975+0.075*ca(n)/hb(n))-1; % Eq. (4.13b) for nozzles
        eta(n)=1-zeta1(n);               % Efficiency (Leidtradwrikungsgrad Traupel Pg. 164)

        while drho>0.1 & iter<10


            W(n,1)=M(n)*(An(n-1)*rho_prev(n))^-1;    %[m/s] assuming blade inlet cross section at
outlet
```

```
            W(n,2)=W(n,1)/tan(beta(n));             %[m/s]
            V(n,:)=W(n,:)+U(n,:);                   %[m/s]
            V(n,:)=V(n,:)*An(n-1)/An(n);            %[m/s] step diffuser to vane inlet cross
section

            Vabs(n)=norm(V(n,:));                   %[m/s]
            alpha(n)=atan(V(n,1)/V(n,2));           %[rad]
            Wabs(n-1)=norm(W(n-1,:));               %[m/s]
            Wabs(n)=norm(W(n,:));                   %[m/s]


            hs(n)=h(n-1)-((Wabs(n)^2)/(2*eta(n)))+(0.5*(Wabs(n-1)^2-U(n-1,2)^2+U(n,2)^2)); %[J/kg]

            % Ventilation losses  (Traupel, p. 420)
            C(n)=0.0095+0.55*(0.125-hb(n)/(2*Rm(n)))^2;                 % Eq. (8.4-33-3)
            PV=pi*C(n)*(1-F(n-1))*rho_prev(n)*2*Rm(n)*hb(n)*U(n,2)^3;    % Eq. (8.4-32) [W]
            qV(n)=PV/M(n);                                               %[J/kg]

            % Filling/emptying losses (Traupel, p. 421, Berger et al. Eq. (4))
            qFE(n)=0.21*ca(n)*U(n,2)*sqrt(abs(h(n-1)-hs(n)))/(F(n-1)*2*Rm(n));

            h(n)=h(n-1)-((Wabs(n)^2-Wabs(n-1)^2+U(n-1,2)^2-U(n,2)^2)*0.5);  %[J/kg]
            h(n)=h(n)+qV(n)+qFE(n);                                         %[J/kg]


            P(n)=nsecant_refprop(s(n-1),hs(n),P(n-1)-200,P(n),substance1,substance2,mix_conc); %
Secant method
            %P(n)=bisection_refprop(s(n-1),hs(n),P(1)+500,P(8)-
100,substance1,substance2,mix_conc);
            %Regula Falsi method


            if P(n)>Pcrit
                warning('Supercritical Pressure');
                s(n)=refpropm('S','H',h(n),'P',P(n),substance1,substance2,mix_conc);     %[J/kgK]
                rho(n)=refpropm('D','H',h(n),'P',P(n),substance1,substance2,mix_conc);   %[kg/m3]
                T(n)=refpropm('T','H',h(n),'P',P(n),substance1,substance2,mix_conc);   %[K]
            else
                hG(n)=refpropm('H','P',P(n),'Q',1,substance1,substance2,mix_conc);       %[J/kg]
```

```
                hL(n)=refpropm('H','P',P(n),'Q',0,substance1,substance2,mix_conc);      %[J/kg]
                x(n)=refpropm('Q','P',P(n),'H',h(n),substance1,substance2,mix_conc);    % Quality
                s(n)=refpropm('S','H',h(n),'P',P(n),substance1,substance2,mix_conc);    %[J/kgK]
                rho(n)=refpropm('D','H',h(n),'P',P(n),substance1,substance2,mix_conc);  %[kg/m3]
                T(n)=refpropm('T','H',h(n),'P',P(n),substance1,substance2,mix_conc);  %[K]
            end
            drho(n)=abs(rho(n)-rho_prev(n));
            rho_prev(n)=rho(n);
            iter=iter+1;

        end
        if x(n)>1
            SoS(n)=refpropm('A','T',T(n),'P',P(n),substance1,substance2,mix_conc); %Speed of sound
        else
            SoS(n)=refpropm('A','P',P(n),'Q',1,substance1,substance2,mix_conc); %Speed of sound
        end


    elseif n>2 && rem(n,2)==1         % For all the other vanes


        alpha(n)=outlet_angle(n);       %[rad]
        U(n,1)=0;                       %[m/s]
        U(n,2)=Rm(n)*w;                 %[m/s]

        % Isoentropic Enthalpy calculation using the estimated pressure

        hs(n)=refpropm('H','P',P(n),'S',s(n-1),substance1,substance2,mix_conc); %Isentropic
enthalpy [J/kg]

        % Soderberg loss correlation - Dixon Pg. 97

        epsrad(n)=alpha(n-1)-alpha(n);                          % Deflection angle [rad]
        eps(n)=epsrad(n)*180/pi;                                % Deflection angle [deg]
        zetas(n)=0.04+0.06*(eps(n)/100)^2;                      % Eq. (4.12)
        zeta1(n)=(1+zetas(n))*(0.993+0.021*ca(n)/hb(n))-1;      % Eq. (4.13a) for nozzles
        eta(n)=1-zeta1(n);                                      % Efficiency (Leidtradwrikungsgrad
Traupel Pg. 164)
```

```
h(n)=h(n-1)-eta(n)*(h(n-1)-hs(n));                    % Real enthalpy [J/kg]

if P(n)>Pcrit
    warning('Supercritical Pressure');
    s(n)=refpropm('S','H',h(n),'P',P(n),substance1,substance2,mix_conc);    %[J/kgK]
    rho(n)=refpropm('D','H',h(n),'P',P(n),substance1,substance2,mix_conc);  %[kg/m3]
    T(n)=refpropm('T','H',h(n),'P',P(n),substance1,substance2,mix_conc);  %[K]
else
    hG(n)=refpropm('H','P',P(n),'Q',1,substance1,substance2,mix_conc);      %[J/kg]
    hL(n)=refpropm('H','P',P(n),'Q',0,substance1,substance2,mix_conc);      %[J/kg]
    x(n)=refpropm('Q','P',P(n),'H',h(n),substance1,substance2,mix_conc);    % Quality
    s(n)=refpropm('S','H',h(n),'P',P(n),substance1,substance2,mix_conc);    %[J/kgK]
    rho(n)=refpropm('D','H',h(n),'P',P(n),substance1,substance2,mix_conc);  %[kg/m3]
    T(n)=refpropm('T','H',h(n),'P',P(n),substance1,substance2,mix_conc);  %[K]
end

% Now it is possible to define an estimated mass flow
% based on the initial properties and in the estimated
% pressure in the outlet of the first vane, using these
% data Mv (Mass flow though the vane) is calculated as
% below:

Mv(n)=(2*(abs(h(n-1)-h(n)))*(-1/(rho(n-1)*An(n)*sin(alpha(n-
1)))^2+1/(rho(n)*An(n)*sin(alpha(n)))^2)^-1)^0.5; % Individual vane Mass flow [kg/s]

V(n,1)=Mv(n)/(An(n)*rho(n));                    % Vax [m/s]
V(n,2)=V(n,1)/tan(alpha(n));                    % Vu [m/s]
Vabs(n)=norm(V(n,:));                           %[m/s]

% Labrynth losses

ML1(n)=0.8*pi   *DL(n)*HL(n)*(rho(n-1)*1000*P(n-1))^0.5;        %[kg/s]
ML(n)=ML1(n)*((1-(P(n)/P(n-1))^2)/(zl+log(P(n-1)/P(n))))^0.5;   %[kg/s]

M(n)=Mv(n)+ML(n);                               %[kg/s]
if x(n)>1
    SoS(n)=refpropm('A','T',T(n),'P',P(n),substance1,substance2,mix_conc); %Speed of sound
else
```

```
                    SoS(n)=refpropm('A','P',P(n),'Q',1,substance1,substance2,mix_conc); %Speed of sound
                end

            end

            end

    for i=1:ncs
        v(i)=1/rho(i);              % Specific volume [m3/kg]
    end

    M0=M(1);
    for n=1:ncs
        dM(n)=M(n)/M0-1;            % Relative mass flow differences
    end
    for n=1:2:ncs-3
        dP(n)=-P(n)*dM(n+2);        % Pressure correction
        P(n)=P(n)+dP(n)*0.1;        % New pressure
    end
    Merror=max(abs(dM));
    iterM=iterM+1;
end

alphadeg=alpha*180/pi;
betadeg=beta*180/pi;
Pturb=M0*(h0-h(ncs));
houtis=refpropm('H','P',P(8),'S',s0,substance1,substance2,mix_conc);
etaturb=(h0-h(ncs))/(h0-houtis);


%Results

h_res(1,m)=h0;
P_res(1,m)=P0;
s_res(1,m)=s0;
v_res(1,m)=v0;
rho_res(1,m)=rho0;
T_res(1,m)=T0;
```

```
for i=1:ncs
    h_res(i+1,m)=h(i);
    P_res(i+1,m)=P(i);
    s_res(i+1,m)=s(i);
    v_res(i+1,m)=v(i);
    x_res(i+1,m)=x(i);
    rho_res(i+1,m)=rho(i);
    Mstage_res(i+1,m)=M(i);
    eta_res(i+1,m)=eta(i);
    T_res(i+1,m)=T(i);
    Mach(i,m)=Vabs(i)/SoS(i);
end

Pturb_res(1,m)=Pturb;
M_res(1,m)=M0;

% Graphics

figure(1)
subplot(2,2,1),plot(s_res(:,m),h_res(:,m))
title('h-s diagram for design condiitions')
xlabel('Entropy [J/kg*K]')
ylabel('Enthalpy [J/kg]')
hold on

figure(1)
subplot(2,2,2),plot(s_res(:,m),T_res(:,m))
title('T-s diagram for design condiitions')
xlabel('Entropy [J/kg*K]')
ylabel('Temperature [K]')
hold on

figure(2)
subplot(2,1,1),plot(P_res(1,m),M_res(1,m),'^')
title('Mass flow change for design condiitions')
xlabel('Inlet Pressure [kPa]')
ylabel('Mass Flow [kg/s]')
hold on
```

```
    figure(2)
    subplot(2,1,2),plot(P_res(1,m),Pturb_res(1,m),'^')
    title('Power of turbine change for design condiitions')
    xlabel('Inlet Pressure [kPa]')
    ylabel('Power turbine [W]')
    hold on

    figure(1)
    subplot(2,2,3),plot(v_res(:,m),P_res(:,m))
    title('P-v diagram for design condiitions')
    xlabel('Specific Volume [m3/kg]')
    ylabel('Pressure [kPa]')
    hold on


    figure(3)
    plot(Mach(:,m),'x-')
    xlabel('Cross section')
    ylabel('Mach')
    hold on

end

%% Saturation Line

% In order to get a better understanding, the lines of saturation will be
% added to the graphs.

P_line=800:100:4200;

for j=1:size(P_line,2)
    hG_res(j,1)=refpropm('H','P',P_line(j),'Q',1,substance1,substance2,mix_conc);       %[J/kg]
    hL_res(j,1)=refpropm('H','P',P_line(j),'Q',0,substance1,substance2,mix_conc);       %[J/kg]
    sL_res(j,1)=refpropm('S','P',P_line(j),'Q',0,substance1,substance2,mix_conc);       %[J/kgK]
    sG_res(j,1)=refpropm('S','P',P_line(j),'Q',1,substance1,substance2,mix_conc);       %[J/kgK]
    vG_res(j,1)=1/(refpropm('D','P',P_line(j),'Q',1,substance1,substance2,mix_conc));   %[m3/kg]
    TG_res(j,1)=refpropm('T','P',P_line(j),'Q',1,substance1,substance2,mix_conc);       %[K]
end
```

```
figure(1)
subplot(2,2,1),plot(sG_res(:,1,1),hG_res(:,1,1))
hold on

figure(1)
subplot(2,2,2),plot(sG_res(:,1,1),TG_res(:,1,1))
hold on

figure(1)
subplot(2,2,3),plot(vG_res(:,1,1),P_line(1,:,1))
hold on

%% Table of Results

CrossSection(2:2*stages+1,1)=[1:2*stages].';
Enthalpy_Jkg=h_res;
Entropy_JkgK=s_res;
Pressure_kPa=P_res;
Quality=x_res;
SpecificVolume_m3kg=v_res;
Performance=eta_res;
Density_kgm3=rho_res;
MassFlow_kgs=Mstage_res;
Temperature_K=T_res;


Results=table(CrossSection,Enthalpy_Jkg,Entropy_JkgK,Pressure_kPa,Density_kgm3,SpecificVolume_m3kg,Quality,Per
formance,MassFlow_kgs,Temperature_K)
writetable(Results,'Results_for_design_conditions.xls')
```

### 11.2.3. Mean line analysis for measured data

```
%% Turbine Mean line Analysis
% Cristian Leonardo Niño Avella

%% Inlet Data

run Entrance_of_turbine.m

%% Stages, Pressure and Temperature

inlet_properties=readmatrix('Inlet_turbine.xls');
[GD,txt_GD,raw_GD]=xlsread('Geometry_stages.xlsx','Geometry','A1:T11');
stages=4;                               % Number of stages
ncs=2*stages;                           % Number of cross sections

% Geometry

for n=1:ncs
    Re(n)=GD(n,6)*0.001;                % Outer radius [m]
    Ri(n)=GD(n,5)*0.001;                % Inner radius [m]
    Rm(n)=sqrt((Re(n)^2+Ri(n)^2)/2);    % Mean radius [m]
    outlet_angle(n)=GD(n,14);           %(n,14) for the method of Traupel for vanes and Measured outlet angle
for blades [rad]
    omega(n)=GD(n,4);                   % Aperture angle of the cross sections [rad]
    F(n)=GD(n,4)/(2*pi);                % Fraction of aperture, partial admission
    An(n)=pi*(Re(n)^2-Ri(n)^2)*F(n);    % Aperture Area in vanes [m2]bis
    ca(n)=GD(n,9)/1000;                 % Chord length  [m]
    hb(n)=GD(n,10)/1000;                % Blade height  [m]
    DL(n)=GD(n,18)/1000;                % Diameter of Labyrinth tips [m]
    HL(n)=GD(n,19)/1000;                % Open clearance of Labyrinth tips [m]
    zl=3;                               % Number of Labyrinth tips
end

% Frequency and angular velocity

f=9960/60;                              % RPS
w=2*pi*f;                               % Angular velocity [rad/s]
```

```
%% Calculation with different inlet fluid confitions

% The inlet fluid conditions vary in order to evaluate the sensibility of
% the outlet of the turbine due to these properties.

for j=1:size(inlet_properties,1)

    P0=inlet_properties(j,3);            % Inlet pressure [kPa]
    T0=inlet_properties(j,7);            % Inlet temperature [K]
    P(7)=MD(j,10)+20;
    P(8)=MD(j,10);


    % Substance definition

    substance1='PROPANE';
    substance2='NITROGEN';
    N2_conc=0.016;                        % Nitrogen concentration
    mix_conc= [(1-N2_conc) (N2_conc)];    % Mixture concentration

    % Calculation of stages

    for b=1:1

        for m=1:1

            PR=P0/P(8);
            for n=1:stages
                if n==1
                    P(2*n-1)=P0/(PR^(1/stages));                 %[kPa]
                    P(2*n)=P(2*n-1);                             %[kPa]
                else
                    P(2*n-1)=P(2*n-2)/(PR^(1/stages));           %[kPa]
                    P(2*n)=P(2*n-1);                             %[kPa]
                end
            end
```

```
% Inlet properties

% With the inlet pressure and temperature, we can now define the fluid
% properties at the entrance of the turbine.

rho0=inlet_properties(j,6);                          %[kg/m3]
h0=inlet_properties(j,1);                            %[J/kg]
s0=inlet_properties(j,2);                            %[J/kgK]
v0=1/rho0;                                           %[m3/kg]
alpha0=pi/2;                                         %Inlet angle [rad]

% Critical properties

Tcrit=refpropm('T','C',0,' ',0,substance1,substance2,mix_conc); % Critical temperature [K]
Pcrit=refpropm('P','C',0,' ',0,substance1,substance2,mix_conc); % Critical pressure    [kPa]

% Iteration initiation

% In this method it will be used the mass flow to iterate, in order to use
% the inlet and oulet pressure of the turbine as an entrance data.

iterM=0;
iter_max=1000;
dM_min=0.00001;     % Min difference between Mass flow in iter
Merror=10;          % Error in Mass calculation

while Merror>dM_min && iterM<iter_max
        for n=1:ncs
            if n==1

                alpha(n)=outlet_angle(n);            %[rad]
                U(n,1)=0;                            %[m/s]
                U(n,2)=Rm(n)*w;                      %[m/s]
                % Isoentropic Enthalpy calculation using the estimated pressure

                hs(n)=refpropm('H','P',P(n),'S',s0,substance1,substance2,mix_conc); %Isentropic 
enthalpy [J/kg]
```

```
% Soderberg loss correlation - Dixon Pg. 97

epsrad(n)=alpha0-alpha(n);           % Deflection angle [rad]
eps(n)=epsrad(n)*180/pi;             % Deflection angle [deg]
zetas(n)=0.04+0.06*(eps(n)/100)^2;   % Eq. (4.12)
zeta1(n)=(1+zetas(n))*(0.993+0.021*ca(n)/hb(n))-1; % Eq. (4.13a) for nozzles
eta(n)=1-zeta1(n);                   % Efficiency (Leidtradwrikungsgrad Traupel Pg. 164)


h(n)=h0-eta(n)*(h0-hs(n));           % Real enthalpy [J/kg]

if P(n)>Pcrit
    warning('Supercritical Pressure');
    s(n)=refpropm('S','H',h(n),'P',P(n),substance1,substance2,mix_conc); %[J/kgK]

    rho(n)=refpropm('D','H',h(n),'P',P(n),substance1,substance2,mix_conc); %[kg/m3]

    T(n)=refpropm('T','H',h(n),'P',P(n),substance1,substance2,mix_conc);  %[K]
else
    hG(n)=refpropm('H','P',P(n),'Q',1,substance1,substance2,mix_conc); %[J/kg]

    hL(n)=refpropm('H','P',P(n),'Q',0,substance1,substance2,mix_conc); %[J/kg]

    x(n)=refpropm('Q','P',P(n),'H',h(n),substance1,substance2,mix_conc);    % Quality

    s(n)=refpropm('S','H',h(n),'P',P(n),substance1,substance2,mix_conc); %[J/kgK]

    rho(n)=refpropm('D','H',h(n),'P',P(n),substance1,substance2,mix_conc); %[kg/m3]

    T(n)=refpropm('T','H',h(n),'P',P(n),substance1,substance2,mix_conc);  %[K]

end

% Now it is possible to define an estimated mass flow
% based on the initial properties and in the estimated
% pressure in the outlet of the first vane, using these
% data Mv (Mass flow though the vane) is calculated as
% below:
```

```
            Mv(n)=(2*(h0-h(n))*(-
1/(rho0*An(n)*sin(alpha0))^2+1/(rho(n)*An(n)*sin(alpha(n)))^2)^-1)^0.5; % Individual vane Mass flow [kg/s]

            V(n,1)=Mv(n)/(An(n)*rho(n));     % Vax [m/s]
            V(n,2)=V(n,1)/tan(alpha(n));     % Vu [m/s]
            Vabs(n)=norm(V(n,:));            %[m/s]

            % Labyrinth losses

            ML1(n)=0.8*pi*DL(n)*HL(n)*(rho0*1000*P0)^0.5;
            ML(n)=ML1(n)*((1-(P(n)/P0)^2)/(zl+log(P0/P(n))))^0.5; %[kg/s]

            M(n)=Mv(n)+ML(n);                %[kg/s]

            if x(n)>1
                SoS(n)=refpropm('A','T',T(n),'P',P(n),substance1,substance2,mix_conc); %Speed
of sound
            else
                SoS(n)=refpropm('A','P',P(n),'Q',1,substance1,substance2,mix_conc); %Speed of
sound
            end


        elseif rem(n,2)==0 %% For all the blades

            rho_prev(n)=rho(n-1);
            drho=100;
            iter=0;


            U(n,1)=0;                            %[m/s]
            U(n,2)=Rm(n)*w;                      %[m/s]
            W(n-1,:)=V(n-1,:)-U(n-1,:);          %[m/s]
            beta(n-1)=atan(W(n-1,1)/W(n-1,2));   %[rad]
            beta(n)=outlet_angle(n);             %[rad]

            % We consider the mass flow is the same for the blades
            % and the vanes
```

```
M(n)=M(n-1);                          %[kg/s]

% Soderberg correlation

epsrad(n)=beta(n)-beta(n-1);              % Deflection angle [rad]
eps(n)=epsrad(n)*180/pi;                  % Deflection angle [deg]
zetas(n)=0.04+0.06*(eps(n)/100)^2;        % Eq. (4.12)
zeta1(n)=(1+zetas(n))*(0.975+0.075*ca(n)/hb(n))-1; % Eq. (4.13b) for nozzles
eta(n)=1-zeta1(n);                        % Efficiency (Leidtradwrikungsgrad Traupel
Pg. 164)

while drho>0.1 & iter<10

    W(n,1)=M(n)*(An(n-1)*rho_prev(n))^-1;    %[m/s] assuming blade inlet cross
section at outlet
    W(n,2)=W(n,1)/tan(beta(n));              %[m/s]
    V(n,:)=W(n,:)+U(n,:);                    %[m/s]
    V(n,:)=V(n,:)*An(n-1)/An(n);             %[m/s] step diffuser to vane inlet
cross section

    Vabs(n)=norm(V(n,:));                    %[m/s]
    alpha(n)=atan(V(n,1)/V(n,2));            %[rad]
    Wabs(n-1)=norm(W(n-1,:));                %[m/s]
    Wabs(n)=norm(W(n,:));                    %[m/s]

    hs(n)=h(n-1)-((Wabs(n)^2)/(2*eta(n)))+(0.5*(Wabs(n-1)^2-U(n-1,2)^2+U(n,2)^2));
%[J/kg] Traupel pag 165

    % Ventilation losses  (Traupel, p. 420)
    C(n)=0.0095+0.55*(0.125-hb(n)/(2*Rm(n)))^2;                 % Eq. (8.4-33-
3)
    PV=pi*C(n)*(1-F(n-1))*rho_prev(n)*2*Rm(n)*hb(n)*U(n,2)^3;   % Eq. (8.4-32)
[W]
    qV(n)=PV/M(n);                                              % [J/kg]

    % Filling/emptying losses (Traupel, p. 421, Berger et al. Eq. (4))
    qFE(n)=0.21*ca(n)*U(n,2)*sqrt(abs(h(n-1)-hs(n)))/(F(n-1)*2*Rm(n)); %[J/kg]
```

```
                                h(n)=h(n-1)-((Wabs(n)^2-Wabs(n-1)^2+U(n-1,2)^2-U(n,2)^2)*0.5);  %[J/kg]
                                h(n)=h(n)+qV(n)+qFE(n);                                        %[J/kg]


                                P(n)=nsecant_refprop(s(n-1),hs(n),P(n-1)-
200,P(n),substance1,substance2,mix_conc); % Secant method
                                %P(n)=bisection_refprop(s(n-1),hs(n),P(1)+500,P(8)-
100,substance1,substance2,mix_conc);
                                %Regula Falsi method


                                if P(n)>Pcrit
                                    warning('Supercritical Pressure');
                                    s(n)=refpropm('S','H',h(n),'P',P(n),substance1,substance2,mix_conc);
%[J/kgK]
                                    rho(n)=refpropm('D','H',h(n),'P',P(n),substance1,substance2,mix_conc);
%[kg/m3]
                                    T(n)=refpropm('T','H',h(n),'P',P(n),substance1,substance2,mix_conc);  %[K]
                                else
                                    hG(n)=refpropm('H','P',P(n),'Q',1,substance1,substance2,mix_conc);
%[J/kg]
                                    hL(n)=refpropm('H','P',P(n),'Q',0,substance1,substance2,mix_conc);
%[J/kg]
                                    x(n)=refpropm('Q','P',P(n),'H',h(n),substance1,substance2,mix_conc);    %
Quality of the substance
                                    s(n)=refpropm('S','H',h(n),'P',P(n),substance1,substance2,mix_conc);
%[J/kgK]
                                    rho(n)=refpropm('D','H',h(n),'P',P(n),substance1,substance2,mix_conc);
%[kg/m3]
                                    T(n)=refpropm('T','H',h(n),'P',P(n),substance1,substance2,mix_conc);  %[K]
                                end
                                drho(n)=abs(rho(n)-rho_prev(n));
                                rho_prev(n)=rho(n);
                                iter=iter+1;

                            end
                            if x(n)>1
                                SoS(n)=refpropm('A','T',T(n),'P',P(n),substance1,substance2,mix_conc); %Speed
of sound
```

```
                            else
                                SoS(n)=refpropm('A','P',P(n),'Q',1,substance1,substance2,mix_conc); %Speed of
sound
                            end



                        elseif n>2 && rem(n,2)==1         % For all the other vanes


                            alpha(n)=outlet_angle(n);        %[rad]
                            U(n,1)=0;                        %[m/s]
                            U(n,2)=Rm(n)*w;                  %[m/s]

                            % Isentropic Enthalpy calculation using the estimated pressure

                            hs(n)=refpropm('H','P',P(n),'S',s(n-1),substance1,substance2,mix_conc);
%Isentropic enthalpy [J/kg]

                            % Soderberg loss correlation - Dixon Pg. 97

                            epsrad(n)=alpha(n-1)-alpha(n);           % Deflection angle [rad]
                            eps(n)=epsrad(n)*180/pi;                 % Deflection angle [deg]
                            zetas(n)=0.04+0.06*(eps(n)/100)^2;       % Eq. (4.12)
                            zeta1(n)=(1+zetas(n))*(0.993+0.021*ca(n)/hb(n))-1; % Eq. (4.13a) for nozzles
                            eta(n)=1-zeta1(n);                       % Efficiency (Leidtradwrikungsgrad Traupel
Pg. 164)


                            h(n)=h(n-1)-eta(n)*(h(n-1)-hs(n));       % Real enthalpy [J/kg]

                            if P(n)>Pcrit
                                warning('Supercritical Pressure');
                                s(n)=refpropm('S','H',h(n),'P',P(n),substance1,substance2,mix_conc);
%[J/kgK]

                                rho(n)=refpropm('D','H',h(n),'P',P(n),substance1,substance2,mix_conc);
%[kg/m3]

                                T(n)=refpropm('T','H',h(n),'P',P(n),substance1,substance2,mix_conc);  %[K]
                            else
```

```
        hG(n)=refpropm('H','P',P(n),'Q',1,substance1,substance2,mix_conc);
%[J/kg]
        hL(n)=refpropm('H','P',P(n),'Q',0,substance1,substance2,mix_conc);
%[J/kg]
        x(n)=refpropm('Q','P',P(n),'H',h(n),substance1,substance2,mix_conc);     %
Quality
        s(n)=refpropm('S','H',h(n),'P',P(n),substance1,substance2,mix_conc);
%[J/kgK]
        rho(n)=refpropm('D','H',h(n),'P',P(n),substance1,substance2,mix_conc);
%[kg/m3]
        T(n)=refpropm('T','H',h(n),'P',P(n),substance1,substance2,mix_conc);  %[K]
    end

    % Now it is possible to define an estimated mass flow
    % based on the initial properties and in the estimated
    % pressure in the outlet of the first vane, using these
    % data Mv (Mass flow though the vane) is calculated as
    % below:

    Mv(n)=(2*(abs(h(n-1)-h(n)))*(-1/(rho(n-1)*An(n)*sin(alpha(n-
1)))^2+1/(rho(n)*An(n)*sin(alpha(n)))^2)^-1)^0.5; % Individual vane Mass flow [kg/s]

    V(n,1)=Mv(n)/(An(n)*rho(n));     % Vax [m/s]
    V(n,2)=V(n,1)/tan(alpha(n));     % Vu [m/s]
    Vabs(n)=norm(V(n,:));            %[m/s]

    % Lybrynth losses

    ML1(n)=0.8*pi   *DL(n)*HL(n)*(rho(n-1)*1000*P(n-1))^0.5;         %[kg/s]
    ML(n)=ML1(n)*((1-(P(n)/P(n-1))^2)/(zl+log(P(n-1)/P(n))))^0.5;    %[kg/s]

    M(n)=Mv(n)+ML(n);                                                %[kg/s]
    if x(n)>1
        SoS(n)=refpropm('A','T',T(n),'P',P(n),substance1,substance2,mix_conc); %Speed
of sound
    else
        SoS(n)=refpropm('A','P',P(n),'Q',1,substance1,substance2,mix_conc); %Speed of
sound
    end
```

```
        end

        end

    for i=1:ncs
        v(i)=1/rho(i);                                      % Specific volume [m3/kg]
    end

    M0=M(1);
    for n=1:ncs
        dM(n)=M(n)/M0-1;                                    % Relative mass flow differences
    end
    for n=1:2:ncs-3
        dP(n)=-P(n)*dM(n+2);                                % Pressure correction
        P(n)=P(n)+dP(n)*0.5;                                % New pressure
    end
    Merror=max(dM);
    iterM=iterM+1;
end

alphadeg=alpha*180/pi;
betadeg=beta*180/pi;
Pturb=M0*(h0-h(ncs));
houtis=refpropm('H','P',P(8),'S',s0,substance1,substance2,mix_conc);
etaturb=(h0-h(ncs))/(h0-houtis);


%Results

h_res(1,j,m,b)=h0;
P_res(1,j,m,b)=P0;
s_res(1,j,m,b)=s0;
v_res(1,j,m,b)=v0;
rho_res(1,j,m,b)=rho0;
T_res(1,j,m,b)=T0;

for i=1:ncs
    h_res(i+1,j,m,b)=h(i);
```

```
        P_res(i+1,j,m,b)=P(i);
        s_res(i+1,j,m,b)=s(i);
        v_res(i+1,j,m,b)=v(i);
        x_res(i+1,j,m,b)=x(i);
        rho_res(i+1,j,m,b)=rho(i);
        Mstage_res(i+1,j,m,b)=M(i);
        eta_res(i+1,j,m,b)=eta(i);
        T_res(i+1,j,m,b)=T(i);
        Mach(i,j,m,b)=Vabs(i)/SoS(i);
    end


    Pturb_res(j,b,m)=Pturb;
    etaturb_res(j,b,m)=etaturb;
    M_res(j,b,m)=M0;

    % Graphics

    figure(1)
    subplot(2,2,1),plot(s_res(:,j,m,b),h_res(:,j,m,b))
    title('h-s diagram for measured data')
    xlabel('Entropy [J/kg*K]')
    ylabel('Enthalpy [J/kg]')
    hold on

    figure(2)
    subplot(2,1,1),plot(P_res(1,j,m),M_res(j,1,m),'^')
    title('Mass flow for measured data')
    xlabel('Inlet Pressure [kPa]')
    ylabel('Mass Flow [kg/s]')
    hold on

    figure(2)
    subplot(2,1,2),plot(P_res(1,j,m),Pturb_res(j,1,m),'^')
    title('Power of turbine for measured data')
    xlabel('Inlet Pressure [kPa]')
    ylabel('Power turbine [W]')
    hold on

    figure(1)
```

```
            subplot(2,2,2),plot(v_res(:,j,m,b),P_res(:,j,m,b))
            title('P-v diagram for measured data')
            xlabel('Specific Volume [m3/kg]')
            ylabel('Pressure [kPa]')
            hold on

            figure(1)
            subplot(2,2,3),plot(s_res(:,j,m,b),T_res(:,j,m,b))
            title('T-s diagram for measured data')
            xlabel('Entropy [J/kg*K]')
            ylabel('Temperature [K]')
            hold on

            figure(3)
            plot(Mach(:,j,m,b),'x-')
            xlabel('Cross section')
            ylabel('Mach')
            hold on



        end
    end
end
%% Saturation Line

% In order to get a better understanding, the lines of saturation will be
% added to the graphs.

P_line=800:100:4700;

for j=1:size(P_line,2)
    hG_res(j,1)=refpropm('H','P',P_line(j),'Q',1,substance1,substance2,mix_conc);       %[J/kg]
    sG_res(j,1)=refpropm('S','P',P_line(j),'Q',1,substance1,substance2,mix_conc);       %[J/kgK]
    vG_res(j,1)=1/(refpropm('D','P',P_line(j),'Q',1,substance1,substance2,mix_conc));   %[m3/kg]
    TG_res(j,1)=refpropm('T','P',P_line(j),'Q',1,substance1,substance2,mix_conc);       %[K]
end

figure(1)
```

```
subplot(2,2,1),plot(sG_res(:,1,1),hG_res(:,1,1))
xlabel('Entropy [J/kg*K]')
ylabel('Enthalpy [J/kg]')
hold on

figure(1)
subplot(2,2,2),plot(vG_res(:,1,1),P_line(1,:,1))
xlabel('Specific Volume [m3/kg]')
ylabel('Pressure [kPa]')
hold on

figure(1)
subplot(2,2,3),plot(sG_res(:,1,1),TG_res(:,1,1))
xlabel('Entropy [J/kg*K]')
ylabel('Temperature [K]')
hold on




%% Table of Results

CrossSection(2:2*stages+1,1)=[1:2*stages].';
Enthalpy_Jkg=h_res;
Entropy_JkgK=s_res;
Pressure_kPa=P_res;
Quality=x_res;
SpecificVolume_m3kg=v_res;
Performance=eta_res;
Density_kgm3=rho_res;
MassFlow_kgs=Mstage_res;
Temperature_K=T_res;

for m=1:9
      Results=table(CrossSection,Enthalpy_Jkg(:,m),Entropy_JkgK(:,m),Pressure_kPa(:,m),Density_kgm3(:,m),Speci
      ficVolume_m3kg(:,m),Quality(:,m),Performance(:,m),MassFlow_kgs(:,m),Temperature_K(:,m))
      writetable(Results,'Results.xls','sheet',m)
end
```

### 11.2.4. Sensitivity analysis for Inlet Pressure

The code used to calculate the sensitivity analysis is the same as in design conditions, the only variation made was when it was set the inlet pressure instead of using only one value, it was used an array of pressures, using the command presented below.

```
% Parameters for decreasing Pressure
% In order to make a sensibility analysis, the inlet pressure
% will change from the theorical value to the measured value
% with losses, this value was gotten previously.


P0p=3876.53;                                % Lowest Inlet measured pressure with losses [kPa]

Pt=P0;                                      %[kPa]


for m=1:11
    sP=(Pt-P0p)/10;                         %[kPa]
    P0=Pt-(sP*(m-1));                       %[kPa]

    PR=P0/P(8);
    for n=1:stages
        if n==1
            P(2*n-1)=P0/(PR^(1/stages));
            P(2*n)=P(2*n-1);
        else
            P(2*n-1)=P(2*n-2)/(PR^(1/stages));
            P(2*n)=P(2*n-1);
        end
    end
```

### 11.2.5. Sensitivity analysis for inlet Temperature

The code used to calculate the sensitivity analysis is the same as in design conditions, the only variation made was when it was set the inlet pressure instead of using only one value, it was used an array of temperature, using the command presented below.

```
%% Calculation of stages

% Parameters for decreasing temperature
% In order to make a sensibility analysis, the inlet
% temperature will change from the theorical value to the measured value
% with losses, this value was gotten previously.

T0p=365.06;                   % Lowest Inlet measured Temperature with losses [K]

Tt=T0;




    for m=1:11
        sT=(Tt-T0p)/10;      %[kPa]
        T0=Tt-(sT*(m-1));    %[kPa]

        PR=P0/P(8);
        for n=1:stages
            if n==1
                P(2*n-1)=P0/(PR^(1/stages));
                P(2*n)=P(2*n-1);
            else
                P(2*n-1)=P(2*n-2)/(PR^(1/stages));
                P(2*n)=P(2*n-1);
            end
```

### 11.2.6. Secant method applied to REFPROP

```
%% Newton secant method applied to REFPROP
% Cristian Leonardo Nino Avella

% The objective of this method is to find the entropy of a given mixture
% using an input, the enthalpy and pressure. REFPROP is the data program
% that is used for this purpose.

function [Pout]=nsecant_refprop(s_given,h_given,P_1,P_2,substance1,substance2,mix_conc)

Nmax=100;
error=1e-3;
s1=s_given;
h=h_given;
X(1)=P_1;
X(2)=P_2;
Nmax=100;
n=1;

while n<Nmax

    f(n)=s1-refpropm('S','P',X(n),'H',h,substance1,substance2,mix_conc);
    f(n+1)=s1-refpropm('S','P',X(n+1),'H',h,substance1,substance2,mix_conc);

    g(n+1)=(f(n+1)-f(n))/(X(n+1)-X(n));

    X(n+2)=X(n+1)-(f(n+1)/g(n+1));
    n=n+1;
    if abs(f(n))<error
        break
    end
end

Pout=X(n+1);
end
```

### 11.2.7. Pressure drop

```
%% Functions Pressure Drop
% Supercritical fluid and Two-phase flow pressure drop

function [Deltap_tpf]=pressure_loss(m,d,g_viscosity,l_viscosity,rho_g,rho_l,X,Pcrit,P,q,L,v,ef,dHv)

% Input parameters:
% m is specific mass velocity [kg/m2*s]
% d is diameter of the pipe [m]
% g_viscosity of the gas [kg/m*s]
% l_viscosity of the liquid [kg/m*s]
% rho_g gas density [kg/m3]
% tho_l liquid density [kg/m3]
% X is fluid quality
% P fluid pressure
% Pcrit pressure of the fluid in the critical point
% q heat flux [W/m2]
% L length [m]
% dHv latent heat of evaporation [J/kg]
% v velocity [m/s]
% ef expansion factor


A=(pi*d^2)/4;
dH=d; % Hydraulic diameter [m]
rough=1; % Where Can I find these values????

% Single phase friction factor

if X<=0 || X>=1 || P>=Pcrit
    Re=abs(m*d/(A*g_viscosity));
    if Re<2000
        f=64/Re;
    else
        fturb=0.309/(log10(Re/7))^2;            % Dubbel
        frough=1/(2*log10(3.71*dH/rough))^2;    % Nikuradse
        f=max(fturb,frough);                    %friction factor
    end;
```

```
   % In order to calculate the pressure loss, it is apllied the Bernoulli
   % Equiation, using the friction coefficient gotten previously.

   Deltap_tpf=(0.5*rho_g*(v^2)*((f*L/d)+ef))/1000; % pressure drop[kPa]


else
    % Muller-Steinhagen and Heck (1986)
    % Reynolds for both states of the fluid

    Re_g=(m*d)/(A*g_viscosity);
    Re_l=(m*d)/(A*l_viscosity);

    if Re_g<=1187
        f_g=64/Re_g;
    else
        f_g=0.3164/(Re_g^0.25);
    end
    if Re_l<=1187
        f_l=64/Re_l;
    else
        f_l=0.3164/(Re_l^0.25);
    end

    % Now we calculate de parameters A and B that represents the pressure
    % drop of each phase of the flow

    A=f_l*(m^2)/(2*rho_l*d);
    B=f_g*(m^2)/(2*rho_g*d);

    % Having A and B, it is possible now to calculate a G(A,B) that
    % represent the linear increase of the pressure drop for increasing
    % quality of X<0.7

    G=A+(2*X*(B-A));

    % In order to solve the pressure drop, it is necessary to find the
    % quality at the end of the pressure drop, to find it, it is used the
```

```
    % energy balance. (dX/dL)=(4*q)/(m*d*dHv)

    Xout=X+(4*q*L/(m*d*dHv));

    % To cover the full range of quality 0<X<1 it is used:

    %(dP/dL)=(G(1-X)^(1/C))+(B*X^C)

    dPdL=((((-1/3)*(1-Xout)^(4/3))*(A+2*(B-A)*Xout))+(0.25*B*Xout^4)-((9/14)*(B-A)*(1-Xout)^(7/3)))-((((-
1/3)*(1-X)^(4/3))*(A+2*(B-A)*X))+(0.25*B*X^4)-((9/14)*(B-A)*(1-X)^(7/3)));

    Deltap_tpf=dPdL*L/1000; % pressure drop [kPa]
end
```